ACTA UNIVERSITATIS SZEGEDIENSIS

ACTA MINERALOGICA—PETROGRAPHICA

TOMUS XVIII. FASC. 2.

1967—68

TWENTY FIFTH ANNIVERSARY VOLUME (1943—1968)

SZEGED, HUNGARIA
1968

ACTA UNIVERSITATIS SZEGEDIENSIS

ACTA MINERALOGICA—PETROGRAPHICA

TOMUS XVIII. FASC. 2.

TWENTY FIFTH
ANNIVERSARY VOLUME (1943—1968)

SZEGED, HUNGARIA
1968

Redigit
GYULA GRASSELLY

Edit
Institutum Mineralogicum, Geochimicum et Petrographicum
Universitatis Szegediensis de Attila József nominatae
(Szeged, Táncsics Mihály u. 2.)

Nota
Acta Miner. Petr., Szeged

Szerkeszti
GRASSELLY GYULA

Kiadja
a József Attila Tudományegyetem Ásványtani, Geokémiai és Kőzettani Intézete
(Szeged, Táncsics Mihály u. 2.)

Kiadványunk címének rövidítése
Acta Miner. Petr., Szeged

INVESTIGATIONS ON THE ELECTRODE POTENTIAL OF SULFIDE ORES

MRS. M. AGÓCS

Institute of Mineralogy, Geochemistry and Petrography,
Attila József University, Szeged

INTRODUCTION

The main territory of weathering and sedimentation is the border between lithosphere and atmosphere characterized by the greatest change of the redox potential observed in nature. In the course of weathering mostly minerals containing elements with altering valency undergo changes, when their valency has not yet reached the highest one possible at redox values available in the nature [E. SZÁDECZKY-KARDOSS, 1952]. The weathering of sulfide ore deposits is especially remarkable, since the S^{2-} anion at the redox-potential-change observed on the surface changes into the central S^{6+} cation of the $(SO_4)^{2-}$ complex anion. That is, sulfide ion on the surface changes into a sulfate with lower free energy, thus sulfide minerals change into sulfates of lower compound potentials. The ionic potential of sulfide ion is 1,16, that of the sulfate ion 0,68. This important fact is moreover supported by the role of cations with altering valence. The oxidation of sulfides containing cations with altering valency takes place in several steps. E.g. in the case of iron(II)-sulfide:

$$FeS \rightarrow FeSO_4 \rightarrow Fe_2(SO_4)_3 \rightarrow Fe(OH)_3.$$

In the last step besides ferri hydroxide sulfuric acid is formed, what serves as a source for further reactions.

The rate of oxidation is influenced by other sulfides present since minerals with different chemical composition, different potentials, occuring simultaneously, after having got into contact with circulating mine water as electrolyte, form micro- and macro- galvanic elements, respectively. In consequence of this the weathering is not only a physical and chemical, but also an electrochemical process. Of two simultaneously precipitated sulfide ores the one having lower potential behaves like anode, i.e. oxygen separates on it, what accelerates the oxidation. E.g. in the case when marcasite and sphalerite get into contact, the electrode potential of which as related to copper is given by V. H. GOTTSCHALK and H. A. BUEHLER [1910] as 0,37 and —0,30, V., resp., shpalerite is oxidized 10—14 times more rapidly marcasite 4—6 times slower than alone.

Similar data for ores have been determined by H. RECHENBERG [1951] recalculating the obtained electrode potential values for normal hydrogen scale, to

compare them with the electrode potentials of the metals. On the basis of the obtained values RECHENBERG arranged the sulfide minerals into an electromotive force series, similar to that of the metals.

However, it was pointed out by GY. GRASSELLY [1954] that these two series cannot be considered as identical since in the case of ores it is impossible to suppose a uniform basis for comparison in respect to all of the deposits, thus it is impossible to write up a generally valid potential series, similar to metals. Namely in the case of ores it is not always solutions containing own ions that play the role of electrolytes and the ores cannot be regarded as reversible electrodes. On the other hand, the circulating mine water as electrolyte is not a solution with unit activity, thus the values measured are different from the normal redox potential value of metals in this respect, too. In view of these causes, it is impossible to give for the ores generally valid values of the normal redox potential, but the results obtained from a detailed study of the given mines and mineral associations, respectively, may be characteristic of the expected processes.

According to E. SZÁDECZKY-KARDOSS [1952] the oxidation of ores starts at a certain redox potential value as determined by the redox value necessary for sulfide sulfur to change into atomic sulfur. This redox value in 10^{-2} mole dilution, at pH=0, is about +0,2 Volt; at pH = 7 −0,2 Volt. This supposition seems to be proved by GARRELS calculations as well [1954].

The weathering and sedimentation of sulfide ore deposits is a process having importance for geochemistry, since on the one hand it results in concentration of some important metallic elements in the oxidation zone itself, and in the underlying cementation zone on the other. Namely through an interaction of the unchanged sulfide ores with sulfate and sulfuric acid solutions, moving downwards, sulfides of relatively more noble metals and native metals respectively, may be precipitated and enriched.

THEORETICAL PART

Electrochemical processes resulting in weathering of sulfide ore deposits are essentially such oxidation-reduction processes in which both electron migration and changes in the hydrogen ion concentration play an important part. In the case of metals POURBAIX has dealt with the generally possible processes. He first used the redox potential — pH equilibrium diagrams (nowadays named after him), to characterize metal — water systems, to illustrate their dissolution and stability relations, respectively.

It was R. M. GARRELS [1954] who applied the POURBAIX-diagrams for the stability relations of natural systems in order to interpret processes taking place in the nature.

The superposition of POURBAIX-diagrams and the explanation of the behaviour of multicomponent systems was carried out the first time by J. HORVÁTH and M. NOVÁK [1964] drawn the diagrams of several metal-sulfur-water ternary systems from corresponding thermochemical data.

In order to secure a systematic method of interpretation the following conventions are assumed: any reaction in which substance A is converted into substance B can be written in a form where the equation, besides substances A and B merely contains water molecules, hydrogen ions and electrons. The equation is always written in the direction of reduction, then it is reduced to 0:

$$aA + bB + cH_2O + mM^+ + ne^- = 0.$$

In case of given compounds the equation practically contains two independent variables, namely the potential which is connected with the electron transition and the pH, i.e. the hydrogen ion concentration. The above equation written in a similar form

$$\sum_{\gamma} v_{\gamma} M_{\gamma} + ne^{-} = 0$$

where M_{γ} represents components taking part in the reaction (activity, fugacity).

Using the chemical potential of thhe components:

$$-\sum_{\gamma} v_{\gamma}\mu_{\gamma} + 23{,}060\, nE = 0,$$

where μ_{γ} = chemical potential and E the electrode potential.

This equation fulfills the condition that an equilibrium state between two different states of the system may occur only if the maximum useful work of the reversible state equals to zero. Since in the present case metal passes from the electrode into the solution, the work is done not only owing to the different chemical potentials of the metal and the dissolved ions, but to the different electric potentials prevailing in the double layer formed at the phase border. Multiplying factor 23,960 is, however, necessary for the common nominator since chemical potentials usually are given in Kcal/mole. (1 eV = 23,060 Kcal/M).

$$\mu_{\gamma} = \mu_{\gamma}^{\circ} + RT \ln M$$

where μ_{γ}° is the chemical normal potential.

Substituting into the former equation

$$RT \sum_{\gamma} v_{\gamma} \ln M_{\gamma} = -\sum_{\gamma} v_{\gamma}\mu_{\gamma}^{\circ} + 23{,}060\, nE.$$

When the temperature is 25 °C (R = 1,987 cal/degree)

$$592{,}5 \sum_{\gamma} v_{\gamma} \ln M_{\gamma} = -\sum_{\gamma} v_{\gamma}\mu_{\gamma}^{\circ} + 23{,}060\, nE.$$

On applying decimal logarithm:

$$1363 \sum_{\gamma} v_{\gamma} \log M_{\gamma} = -\sum_{\gamma} v_{\gamma}\mu_{\gamma}^{\circ} + 23{,}060\, nE$$

$$\sum_{\gamma} v_{\gamma} \log M_{\gamma} = \frac{-\sum_{\gamma} v_{\gamma}\mu_{\gamma}^{\circ}}{1363} + \frac{nE}{0{,}0591}$$

$$\frac{0{,}0591}{n} \sum_{\gamma} v_{\gamma} \log M_{\gamma} = -\frac{\sum_{\gamma} v_{\gamma}\mu_{\gamma}^{\circ}}{23{,}060\, n} + E$$

Written in other form:

$$\sum_{\gamma} v_{\gamma} \log M_{\gamma} = \log K + \frac{nE}{0{,}0591}$$

and

$$E = E^{\circ} + \frac{0{,}0591}{n} \sum_{\gamma} v_{\gamma} \log M_{\gamma}$$

where K = equilibrium constant, E° = electrochemical normal potential.

Therefore

$$\log K = -\frac{\sum_{\gamma} \nu_\gamma \mu_\gamma^\circ}{1363} \quad \text{and} \quad E^\circ = \frac{\sum_{\gamma} \nu_\gamma \mu_\gamma^\circ}{23{,}060\, n}$$

In a fuller form

$$\log K = -\frac{a\mu_A^\circ + b\mu_B^\circ + c\mu_{H_2O}^\circ + m\mu_{H^+}^\circ}{1363}$$

and

$$E^\circ = \frac{a\mu_A^\circ + b\mu_B^\circ + c\mu_{H_2O}^\circ + m\mu_{H^+}}{23{,}060\, n}$$

From these formulas the equilibrium conditions of any chemical or electrochemical reaction can be calculated if the standard chemical potential of the components, μ°, or the value of K or E° are known, determined from the chemical potentials. Below POURBAIX-diagrams of some sulfide ores investigated are demonstrated. Thermodynamic data required for the construction of the diagrams are taken from V. M. LATIMER's book [1950].

The Eh—pH diagrams of the metal-sulfur-water ternary systems were constructed relying upon the following reactions: dissolution of metals, formation of metal sulfides in the course of the reaction of the metal and hydrogen sulfide, dissolution of metal sulfides, their oxidation to metallic oxides and metal hydroxides, resp., when elementary sulfur was precipitated.

POURBAIX-*diagram of the system Fe-S-H_2O*

Reactions, on the basis of which the diagram was constructed, are:

1. $Fe^{2+} + 2e^- = Fe$
   $E = -0{,}441 + 0{,}0295 \log a_{Fe^{2+}}$
2. $FeS + 2\,H^+ + 2e^- = Fe + H_2S$
   $E = -0{,}334 - 0{,}0591\ pH - 0{,}0295 \log p_{H_2S}$
3. $FeS + H^+ + 2e^- = Fe + HS^-$
   $E = -0{,}564 - 0{,}0295\ pH - 0{,}0295 \log a_{HS}$
4. $FeS + 2e^- = Fe + S^{2-}$
   $E = -0{,}970 - 0{,}0295 \log a_{S^{2-}}$
5. $Fe^{2+} + H_2S = FeS + 2\,H^+$
   $\log K = -3{,}7$
   $\log a_{Fe^{2+}} = 3{,}7 - 2\,pH - \log p_{H_2S}$
6. $FeS_2 + 2\,H^+ + 2e^- = FeS + H_2S$
   $E = -0{,}187 - 0{,}0591\ pH - 0{,}0295 \log p_{H_2S}$
7. $FeS_2 + H^+ + 2e^- = FeS + HS^-$
   $E = -0{,}423 - 0{,}0295\ pH - 0{,}0295 \log a_{HS}$
8. $FeS_2 + 2e^- = FeS + S^{2-}$
   $E = -0{,}837 - 0{,}0295 \log a_{S^{2-}}$
9. $Fe^{2+} + H_2S = FeS_2 + 4\,H^+ + 2e^-$
   $E = -0{,}140 - 0{,}118\ pH - 0{,}0295 \log a_{Fe^{2+}}$
10. $Fe_2O_3 + 4\,SO_4^{2-} + 38\,H^+ + 30e^- = 2\,FeS_2 + 19\,H_2O$
    $E = 0{,}390 - 0{,}048\ pH.$

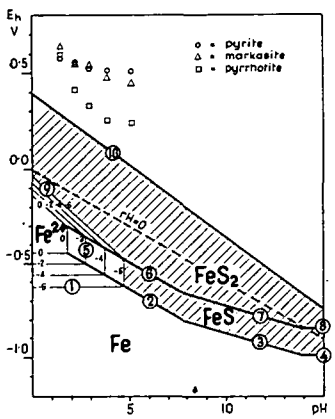

Fig. 1. Eh-pH diagram of the system Fe-S-H_2O

Numbers on the diagram represent the reaction with corresponding order No, by which the given straights could be determined. Points marked with o are measurement data.

POURBAIX-*diagram of the system Zn-S-H_2O*

1. $Zn^{2+} + 2e^- = Zn$
   $E = -0{,}763 + 0{,}0295 \log a_{Zn^{2+}}$
2. $ZnS + 2\,H^+ + 2e^- = Zn + H_2S$
   $E = -0{,}775 - 0{,}0591\ pH - 0{,}0295 \log p_{H_2S}$
3. $ZnS + H^+ + 2e^- = Zn + HS^-$
   $E = -1{,}00 - 0{,}0295\ pH - 0{,}0295 \log a_{HS^-}$
4. $ZnS + 2e^- = Zn + S^{2-}$
   $E = -1{,}415 - 0{,}0295 \log a_{S^{2-}}$
5. $Zn^{2+} + H_2S = ZnS + 2\,H^+$
   $\log K = 0{,}132$
   $\log a_{Zn^{2+}} = -0{,}132 - 2\,pH - \log p_{H_2S}$
6. $Zn^{2+} + S + 2e^- = ZnS$
   $E = 0{,}174 + 0{,}0295 \log a_{Zn^{2+}}$
7. $Zn(OH)_2 + S + 2\,H^+ + 2e^- = ZnS + 2\,H_2O$
   $E = 0{,}519 - 0{,}591\ pH.$

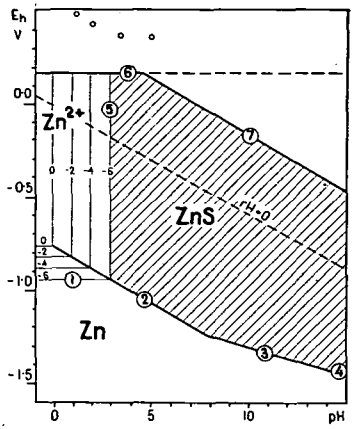

Fig. 2. Eh-pH diagram of the system Zn-S-H_2O

POURBAIX-*diagram of the system Pb-S-H_2O*

1. $Pb^{2+} + 2e^- = Pb$
   $E = -0{,}125 - 0{,}0295 \log a_{Pb^{2+}}$
2. $PbS + 2\,H^+ + 2e^- = Pb + H_2S$
   $E = -0{,}310 - 0{,}591\ pH - 0{,}0295 \log p_{H_2S}$
3. $PbS + H^+ + 2e^- = Pb + HS^-$
   $E = -0{,}545 - 0{,}0295\ pH - 0{,}0295 \log a_{HS^-}$
4. $PbS + 2e^- = Pb + S^{2-}$
   $E = -0{,}96 - 0{,}0295 \log a_{S^{2-}}$
5. $Pb^{2+} + H_2S = PbS + 2\,H^+$
   $\log K = 6{,}23$
   $\log a_{Pb^{2+}} = -6{,}23 - 2\,pH - \log p_{H_2S}$
6. $Pb^{2+} + S + 2e^- = PbS$
   $E = 0{,}354 + 0{,}0295 \log a_{Pb^{2+}}$
7. $PbO + S + 2\,H^+ + 2e^- = PbS + H_2O$
   $E = 0{,}825 - 0{,}0591\ pH.$

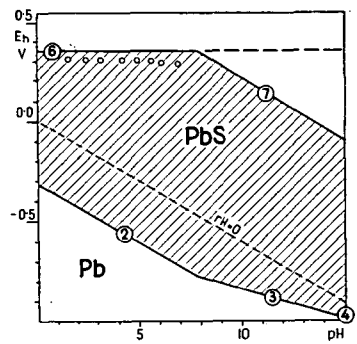

Fig. 3. Eh-pH diagram of the system Pb-S-H_2O

POURBAIX-*diagram of the system Cu-S-H_2O*

1. $Cu_2S + 2\,H^+ + 2e^- = 2\,Cu + H_2S$
   $E = -0{,}270 - 0{,}0591\ pH - 0{,}0295 \log p_{H_2S}$
2. $Cu_2S + H^+ + 2e^- = 2\,Cu + HS^-$
   $E = -0{,}499 - 0{,}0295\ pH - 0{,}0295 \log a_{HS^-}$
3. $Cu_2S + 2e^- = 2\,Cu + S^{2-}$
   $E = -0{,}900 - 0{,}0295 \log a_{S^{2-}}$
4. $CuS + 2\,H^+ + 2e^- = Cu + H_2S$
   $E = -0{,}084 - 0{,}0591\ pH - 0{,}0295 \log p_{H_2S}$
5. $CuS + H^+ + 2e^- = Cu + HS^-$
   $E = -0{,}340 - 0{,}0295\ pH - 0{,}0295 \log a_{HS^-}$
6. $CuS + 2e^- = Cu + S^{2-}$
   $E = -0{,}730 - 0{,}0295 \log a_{S^{2-}}$

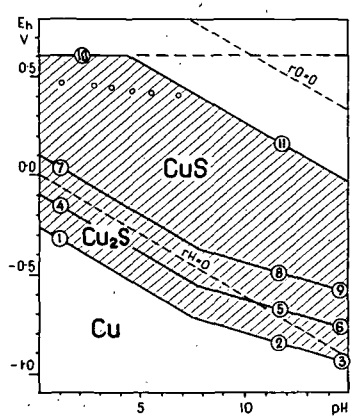

Fig. 4. Eh-pH diagram of the system Cu-S-H_2O

7. $CuS + 2H^+ + 2e^- = Cu_2S + H_2S$
   $E = 0{,}100 - 0{,}0591\ ph - 0{,}0295 \log p_{H_2S}$
8. $2CuS + H^+ + 2e^- = Cu_2S + HS^-$
   $E = -0{,}126 - 0{,}0295\ pH - 0{,}0295 \log a_{HS} -$
9. $2CuS + 2e^- = Cu_2S + S^{2-}$
   $E = -0{,}539 - 0{,}0295 \log a_{S^2} -$
10. $Cu^{2+} + S + 2e^- = CuS$
    $E = 0{,}600 + 0{,}0295 \log a_{Cu^{2+}}$
11. $Cu(OH)_2 + S + 2e^- + 2H^+ = CuS + 2H_2O$
    $E = 0{,}862 - 0{,}0591\ pH.$

These diagrams, constructed and calculated from thermodynamical data, are of theoretical character. It is an important problem to find suitable experimental methods to prove them. Methods for controlling the correctness of the calculated values have been elaborated by NAGEL, K. E. LANGE and R. OHSE [1957], then by J. HORVÁTH and L. HACKL [1965]. They have recognized the fact that when a voltage of constant intensity is applied from an outer source on a cell consisting of an electrode and a counter-electrode dipped into an electrolyte, and this current is stopped after some time, a potential value characteristic for the electrode to be investigated can be measured on the effect of the given impulse. The process which takes place can be interpreted in the following manner: the ohmic resistance caused by the electrolyte and the cover-layer on the metal exerts its effect in a few μsec after switching on the current, and there is a sudden change of the potential. After certain time an electric double layer is formed on the border surface of the metal and the electrolyte, resulting in a nearly constant electrode potential in consequence of the electrode processes taking place very rapidly. When the potential changes again, that is the concentration polarisation gets dominating, the current must be stopped. Then the reverse of the former process takes place. When on the effect of the outer voltage a new potential-determining process starts on the surface of the electrode, the potential measured after the stop of the current corresponds to the equilibrium potential of the electrode reaction. With corresponding technical devices J. HORVÁTH and L. HACKL [1965] succeeded in measuring for metals values agreeing with potentials calculated from thermodynamical data.

For a special study of the oxidation relations of rocks, methods have been developed by Soviet researchers, referred to by M. BOD and GY. BÁRDOSSY [1959]. Its essence is that extremely finely grained rock powder is saturated up to normal moisture content with distilled water via capillary absorption. Into the moistened rock powder platinum and calomel electrodes are placed, measuring the potential differences as well as the pH. The obtained equilibria values are regarded as the „redox potential" of the questioned rock. The above mentioned authors, considering that the pH of the rocks is about 6—8, at which value most of the elements with altering ionization state dissolve hardly or not at all, treated the samples with strong oxidizing agents so that processes leading to the change of the potential, occur. Sulfuric acid-potassium dichromate solution had been applied as oxidizing agent. Essentially this is an indirect method, since it is not the redox potential of the rock which is observed, but the change in the redox potential of the potassium dichromate system. In our opinion the values thus obtained do not agree with the redox potential of the rock, being a value of theoretical character, practically unattainable.

The above mentioned measurement methods applied after the required modifications, may largely contribute to a more detailed knowledge of processes occuring in the weathering of sulfide ore deposits.

In the course of the present study we were looking for an answer of the potential values of electrodes prepared from the sulfides to be investigated against saturated calomel electrodes, on the one hand in solutions with concentrations corresponding to natural mine water in neighbourhood of sulfide ore deposits, containing own and foreign ions, respectively, and in solutions having different pH. The question may also arrisen whether the potential values thus obtained can be reproduced and are characteristic of the given sulfide mineral, and whether they can be correlated with the redox potential values of given systems, with data obtained through calculations.

EXPERIMENTAL PART

For the experiments carefully selected ore samples, free of contaminations and inclusions, have been chosen, embedded into polymethyl-metacrylate, one side ground and polished. In order to secure an electric contact, a hole was drilled down to the ore through the acrylate sample-holder, a glass tube inserted and fastened with piceine into the hole. The tube was filled with distilled mercury which kept a wire the other end of which was connected with the measuring apparatus. The polishing of the surface was repeated prior to each experiment, in order to secure largely the same experimental conditions. The ore-electrode thus prepared was put into closed cell together with the connection tube of the saturated calomel electrode as well as the inlet and the outlet gas tubes. Thus the investigated galvanic cell is:

(+) metal sulfide | metal salt solution | saturated KCl | saturated calomel (−).

The concentration of the applied solutions was 10^{-4}, 10^{-3}, 10^{-2} and in some cases 10^{-1}, the pH was adjusted by sulfuric acid or nitric acid and sodium hydroxide, resp. The potentials were measured with a (Radelkisz) titrimeter supplied by a stabilized electrical source. Before starting measurements, that is prior to inserting the sulfide electrode, N_2 was bubbled through the solution in the cell for ten minutes in order to expel air.

Relationship of the potential and ionic concentration

Potentials of electrodes inserted into solutions with ions same as the cations of the ores investigated (pH = 2) measured *versus* saturated calomel electrodes are given in Table 1.

Table 1

	concentration (mole/l)			
	10^{-4}	10^{-3}	10^{-2}	10^{-1}
	potential (mV)			
pyrite	383	426	482	515
marcasite	392	443	498	533
pyrrhotite	293	312	370	428
covellite	229	232	235	245
sphalerite	195	215	218	232
galena	29	40	60	75

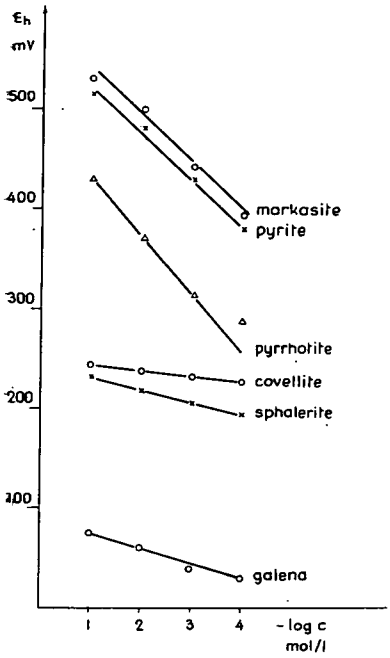

Fig. 5. Relationship of the potential and ionic concentration

Data in Table 1 are means of repeated measurements. In one measurement the readings were done in the first, third and fifth minutes inserting the electrodes. Of these values only one, obtained in the fifth minute was considered in the mean value.

Inserting different sulfide ores into solutions of different concentration, containing own ions, the first thing to be stated is that they follow the NERNST-equation what means that the measured potential and the concentration of the solutions are in linear connection as shown in *Fig. 5.* Since in each case the anion of the solution is SO_4^{2-}, representing the more oxidized form in the system, the decrease of the concentration of SO_4^{2-} brings about the lowering of the potential in every case, of course in a rate depending on the system. It can also be stated that of the iron sulfides pyrrhotite shows the most rapid changes as it has the lowest potential. This is also indicated by the fact that in strongly acidic solutions (pH = 1 – 3) it is very difficult to obtain reproducible values for pyrrhotite since in acidic solutions it easily decomposes yielding H_2S and Fe^{2+} ions. In the case of pyrite and marcasite the values differ, what indicates that the value of the electrode potential is also influenced by differences in the lattice structure.

Connection between the potential and the pH

This connection has also been studied in the case of the previous ores in solutions containing own ions with a concentration of 10^{-2} mole/l *versus* saturated calomel electrodes. Measurement data are enlisted in Table 2.

Values measured for the study of the connection between the potential and the pH were recalculated for normal hydrogen scale and are drawn on the corresponding POURBAIX-diagrams obtained by calculations (marked with circles). In the case of natural sulfides it appears that by this method (which for ores from the same deposit renders a tolerably well reproducible determination of the potential values, thus it is possible to make conclusions on the weathering processes of a given mine) is impossible to measure potential values which would agree with those calculated from thermodynamical data and thus regarded as absolute ones. In some cases the same tendencies can be observed in the run of the straights connecting the measured and calculated points, but a numerical identity cannot be experienced. Literature contains several references concerning the fact that minerals primarily formed in great depth and at high temperatures getting into contact with the atmosphere undergo errosion, the latter being a process analogous to the corrosion of metals. Since we are in lack of corresponding methods this analogy experimentally has not been so far justified, although the intermittent galvanostatic polarisation method suggested by J. HORVÁTH and L. HACKL appears to be applicable even in case of sulfides, thus it serves as a basis for further investigations.

Table 2

pyrite	pH	1,42	2,15	2,92	3,85	5,07		
	mV	325	302	283	269	259		
marcasite	pH	1,42	2,15	2,92	3,85	5,07		
	mV	378	298	284	222	200		
pyrrhotite	pH	1,42	2,15	2,92	3,85	5,07		
	mV	340	155	70	2	—5		
covellite	pH	1,01	2,70	3,57	4,66	5,67	6,86	
	mV	218	206	193	172	165	151	
sphalerite	pH	1,15	2,00	3,45	5,00			
	mV	230	190	121	103			
galena	pH	1,67	2,50	3,11	4,15	4,98	5,62	6,10	6,91
	mV	65	62	61	58	58	49	43	40

Connection between the potential and the foreign ion concentration in changing atmosphere

For a better approach of natural conditions experiments have been done with solutions of different cations (Zn^{2+}, Ni^{2+}, Fe^{3+}, Co^{2+}, Cu^{2+}) in the same concentration ($10^{-2}-10^{-6}$ mole/l) and in solutions containing all these cations as well (pH = 2). Measurement data are shown in Table 3. Measurements A, B and C are values obtained in air, without mixing, then on introducing nitrogen and air, respectively.

Of data in Table 3 values obtained in air without mixing (unbroken line) and those obtained when introducing air (broken line) were plotted in *Fig. 6* as functions of concentration (pyrite x; marcasite o; pyrrhotite △ and sphalerite □.)

Table 3

		concentration (mole/l)				
		10^{-6}	10^{-5}	10^{-4}	10^{-3}	10^{-2}
		potential (mV)				
pyrite	A	300	359	382	400	425
	B	375	385	387	392	412
	C	354	385	395	428	488
marcasite	A	365	382	395	425	482
	B	405	428	438	442	515
	C	405	415	430	464	493
pyrrhotite	A	240	462	300	345	381
	B	322	325	330	347	400
	C	310	328	337	354	390
sphalerite	A	110	140	170	208	275
	B	150	160	180	220	260
	C	174	198	223	273	309

As the run of curves shows, the measured potentials do not follow the NERNST-function when the solutions applied as electrolytes contain simultaneously more cations in the same concentration. Moreover, the measured potential values do not show a numerical agreement with those obtained for a sulfide electrode dipped into a solution with own ions, *versus* saturated calomel electrode. Since in natural mine water, being in contact with the ores, the simultaneous presence of several ions must be considered, the earlier observations have got experimental proof, namely that in the case of natural sulfides a generally valid potential series, similar to that of metals, cannot be compiled. This is further proved by the difference of the list according to increasing electrode potentials given by the results of the two former set of measurements, although here always a simplified form of the natural conditions is considered, since the solutions contain only SO_4^{2-} anions.

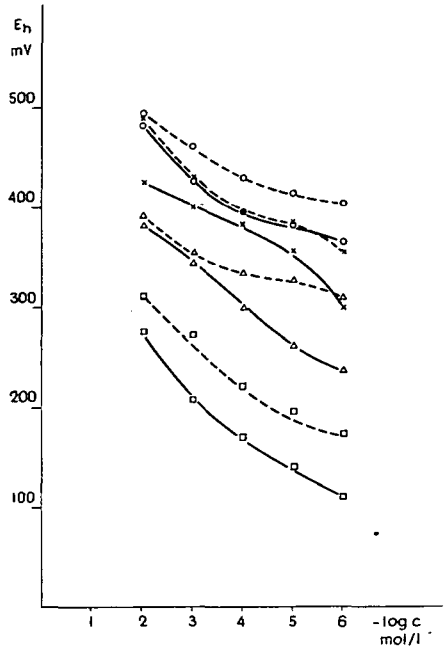

Fig. 6. Electrode potentials as functions of the concentration (in air without mixing: unbroken line; with introducing air: broken line)

The fact that when introducing air the measured potential values are always higher, gives an answer of the question, what part does the airing of the ore deposits play in the weathering. Obviously the more expressed weathering of the minerals in the upper part of the mine can be of the air. Moreover, the process of weathering is accelerated by the difference of potentials owing to the atmospheric conditions existing between ores in the lower layers having no contact with air and those in the upper layers, when they get into ascribed to a wider contact with the oxygen contact through the downwards leaking mine water.

Potentials measured in the nitrogen stream numerically differ from the previous ones and they are not suitable for setting up a generally valid potential series.

Study of „mixed electrodes"

Experiments were also carried out to study what potential values can be measured *versus* saturated calomel electrode in the case of coupling several metal sulfide electrodes, namely of a „mixed electrode".

As it is known the potential of the mixed electrode is the same as that of a one-component electrode made up of the less noble (i.e. having more negative potential) constituents in the same solution. The more noble part practically does not influence the potential supposed that the normal potentials of the metals are not too near each other — there is a difference of at least 50—100 mV.

First of all the potentials of the single electrodes have been measured — using culfuric acid solutions of different concentration as electrolytes — *versus* saturated salomel electrode. These results are summarized in Table 4.

Table 4

	H_2SO_4 concentration (N)			
	10^{-4}	10^{-3}	10^{-2}	10^{-1}
	potential (mV)			
pyrite ①	323	330	340	350
marcasite ②	348	357	365	375
pyrrhotite ③	275	277	290	320
sphalerite ④	110	120	135	155

As a second step the potential of the „mixed electrode" composed of two-two sulfides was also measured *versus* saturated calomel electrode, too, in sulfuric acid solutions with changing concentrations. Values thus obtained are given in Table 5.

Table 5

	H_2SO_4 concentration (N)			
	10^{-4}	10^{-3}	10^{-2}	10^{-1}
	potential (mV)			
pyrite-marcasite ⑤	305	310	325	345
pyrrhotite-marcasite ⑥	306	310	333	376
pyrrhotite-sphalerite ⑦	195	206	242	320

In the measurement special care was taken that the connection tube of the calomel electrode was at the same distance from all the components of the „mixed electrode". Connection between the measured potential values and sulfuric acid concentration are illustrated by *Fig.* 7.

Figure 7 indicates electrode potentials thus measured do not correspond to potentials of mixed electrodes taken according to the definition. In the case when two ores of different composition are coupled in the above described manner, in sulfuric acid solution with higher concentration a value equal to the potential of the two ores being the more noble, can be measured, i.e. which has a more positive electrode potential. Moving towards lower concentrations the measured potentials more and more approach the average value of the potential of the two coupled electrodes. This shows that changes taking place on the surface of both of the electrodes play a part in the determination of the potential.

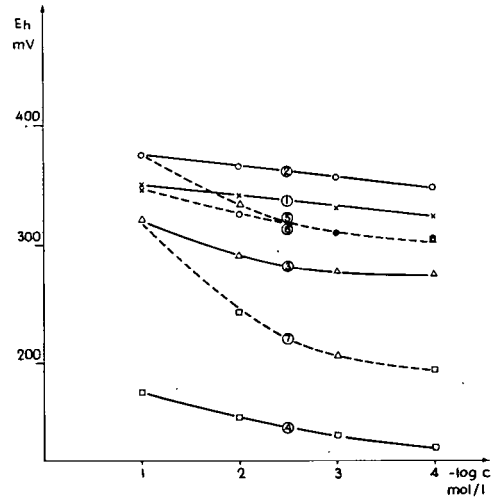

Fig. 7. Relationship of the potential of „mixed electrodes" and sulfuric acid concentration

If the pointed end of the connection tube of the reference electrode is placed near to any of the metal sul-

fides, different potential values are obtained, which do not agree with, but are quite near those of the single electrodes.

Experiments to compose a „mixed electrode" have also been carried out in a way that plates cut off the different sulfides were bedded together. The embedding happened in Wood-metal, the contacting borders of the plates as well as the whole of the Wood-metal were covered with wax. „Mixed electrodes" thus prepared behaved similar as described previously.

These measurements likely prove the fact that to carry out processes taking place in nature, to control theoretical values in an experimental way is by far a complex problem even the conditions having been simplified to a very marked extent.

SUMMARY

1. The connection between the potential and ion concentration in a solution with own cations likely follows the NERNST-equation, while it is not valid for solutions containing simultaneously several cations.

2. The study of the connection between the potential and the hydrogen ion concentration can be done only by special methods so that data, in agreement with the potential values calculated from thermodynamical data, be obtained.

3. Values received when applying different atmospheres yield information concerning the role of airing, influencing weathering.

4. It is not probable that formation of mixed electrodes play a part in weathering, merely galvanic elements could be formed, on the effect of which ores with more negative potentials suffer a more marked dissolution.

REFERENCES

BOD, M. and GY. BÁRDOSSY [1959]: Új módszer az üledékes kőzetek redox viszonyainak meghatározására. (New Method for Determination of the Redox Relations of Sedimentary Rocks) — Geofizikai Közlemények *VIII*, 1—2.

GARRELS, R. M. [1954]: Mineral Species as Functions of pH and Oxidation-Reduction Potentials, with Special Reference to the Zone of Oxidation and Secondary Enrichment of Sulphide Ore Deposits. — Geochim. Cosmochim. Acta *5*, 153—168.

GRASSELLY, GY. [1953—54]: Electrochemical Examination of the Oxidation Processes of Sulfide Ores. — Acta Miner.—Petr., *VII*, 47—64.

HORVÁTH, J. and L. HACKL [1965]: Check of the Potential pH Equilibrium Diagrams of Different Metal-Sulphur-Water Ternary Systems by Intermittent Galvanostatic Polarisation Method. — Corrosion Sci. *5*, 525—538.

HORVÁTH, J., M. NOVÁK [1964]: Potential-pH Equilibrium Diagrams of Some Me-S-H_2O Ternary Systems and Their Interpretation from the Point of View of Metallic Corrosion. — Corrosion Sci. *4*, 159—178.

LATIMER, V. M. [1950]: The Oxidation States of the Elements and Their Potentials in Aqueous Solutions. — Prentice-Hall, Inc., Englewood Cliffs, N. J.

POURBAIX, M. J. N. [1949]: Thermodynamics of Dilute Aqueous Solutions. — Edward Arnold, London.

RECHENBERG, H. [1951]: The Electrochemical Potential Series of Ore Minerals. — Neues Jahrb. Monatsh. 88—91.

SZÁDECZKY-KARDOSS, E. [1955]: Geokémia. — Akadémiai Kiadó, Budapest.

MRS MARGIT AGÓCS
Institute of Mineralogy, Geochemistry
and Petrography
Attila József University at Szeged
Táncsics M. u. 2.
Szeged, Hungary

ON THE PHOSPHORUS-BEARING MINERAL OF THE MANGANESE OXIDE ORE DEPOSITS OF EPLÉNY AND URKUT

GY. GRASSELLY

Institute of Mineralogy, Geochemistry and Petrography,
Attila József University, Szeged

INTRODUCTION

The mean P content of the manganese oxide ore deposits of Eplény and Urkut is generally less than 1,00 per cent. The P frequency distribution of the two deposits is illustrated by *Figs. 1* and *2*. It is very likely to suppose that a mineral belonging to the apatite-group must be the phosphorus-bearing one. However, in consequence of the generally low P content, the small grain size of the phosphorus-bearing mineral, of its fine distribution and difficulties of its separation and enrichment, instead of correct identification merely suppositions are to be found in the literature.

K. NAGY [1953], in his investigations on the mineral association of the manganese carbonate ores of Urkut, on the basis of X-ray and D.T.A. investigations, did not succeed in identifying the phosphorus mineral.

M. SZABÓ—DRUBINA [1957], reports that in some places in the upper part of the grey carbonate deposit of Urkut the phosphorus content is quite considerable: 14—22% P_2O_5 and that according to X-ray investigations these layers with considerable phosphate content contain very fine-grained fluorapatite. Unfortunately this work does not contain X-ray data.

E. NEMECZ [1960], also in connection with the Urkut manganese carbonate ores dealt with the problem of phosphorus-bearing minerals. However, the mineral could not be identified owing to its small grain size, fine distribution and relatively small amount. Lines, belonging to the phosphate mineral could not be detected on the X-ray patterns either. The enrichment by oleine flotation of the carbonate mineral similarly did not bring any results.

GY. GRASSELLY and E. KLIVÉNYI [1960a,b], dealing with the phosphorus content distribution of Urkut oxide ore deposits stated that in the Urkut manganese oxide ore deposit the P content as a rule ranges between 0,08—0,30%, and that the phosphorus-bearing is an extremely finely distributed secondary apatite-mineral, in the formation of which the role of organic life might had been quite considerable. The fact that the P content of the area shows quite a wide range can be interpreted by the sedimentary origin of the deposit, the reaccumulation processes which had taken place in the deposit and the mostly organic origin of phosphate. In regard

of the chemical analysis of a sample having relatively larger phosphate content the presence of fluorapatite has been supposed as well.

As a final result, relying upon an X-ray pattern and an data of chemical analysis, the phosphorus-bearing mineral present in manganese carbonate and oxide ores of Eplény and Urkut had so far been regarded as fluorapatite. This is scarcely enough, however, for a final decision.

Therefore it promised some interesting findings to investigate from different viewpoints samples with considerable phosphate content thus making an attempt to clear up the nature of the phosphorus-bearing mineral of the Urkut and Eplény manganese ore deposits.

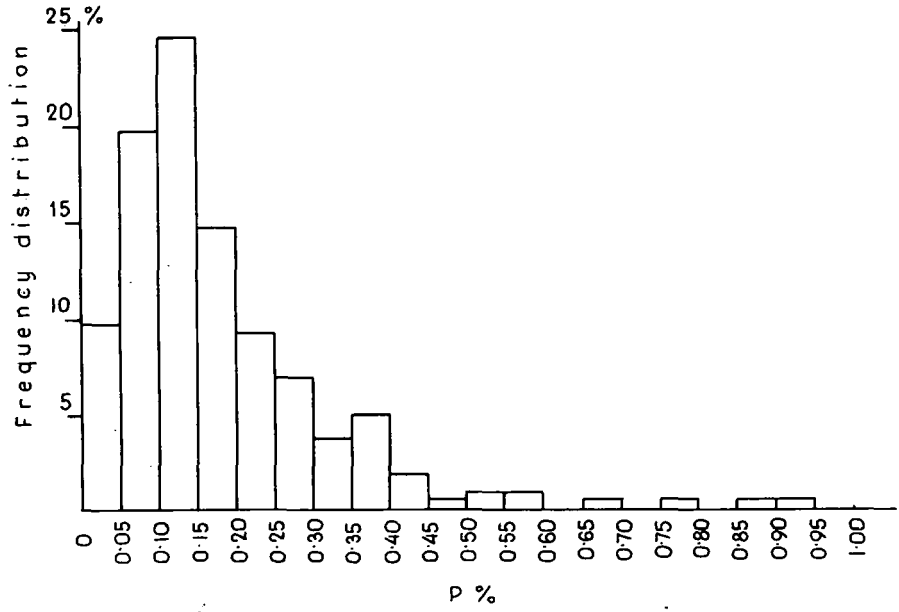

Fig. 1. Frequency distribution of P in 218 samples from Eplény manganese oxide ore deposit

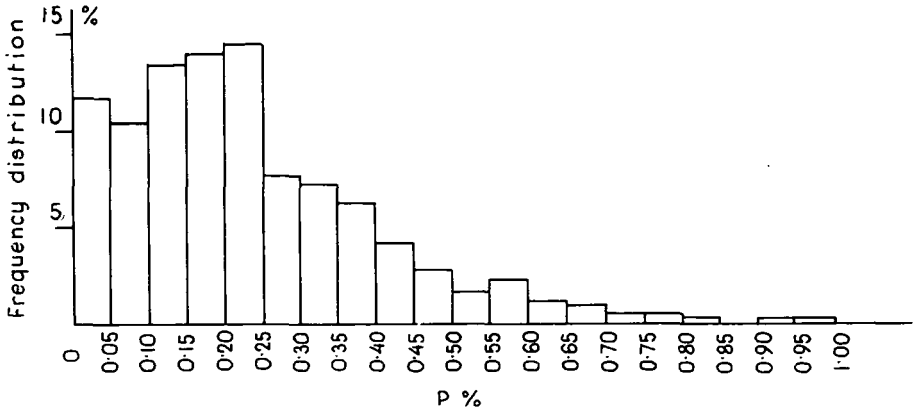

Fig. 2. Frequency distribution of *P* in 599 samples from Úrkút manganese oxide ore deposit

RESULTS OF CHEMICAL ANALYSIS

To give an approximate proof of the supposition that an apatite mineral must be the phosphorus-bearing, the correlation of CaO and P_2O_5, as determined in 30 samples of the Urkut oxide deposit [GRASSELLY, 1960a] could be used. There is a positive correlation between the two values *(Fig. 3)* and although the correlation is not a strict one (the empiric correlation coefficient is 0,45), the connection between the two amounts can be regarded a relyable one. The correlation is weakened by the fact even if phosphorus is supposed completely belonging to apatite, calcium is surely a constituent not only of apatite but of other minerals without phosphorus content as well.

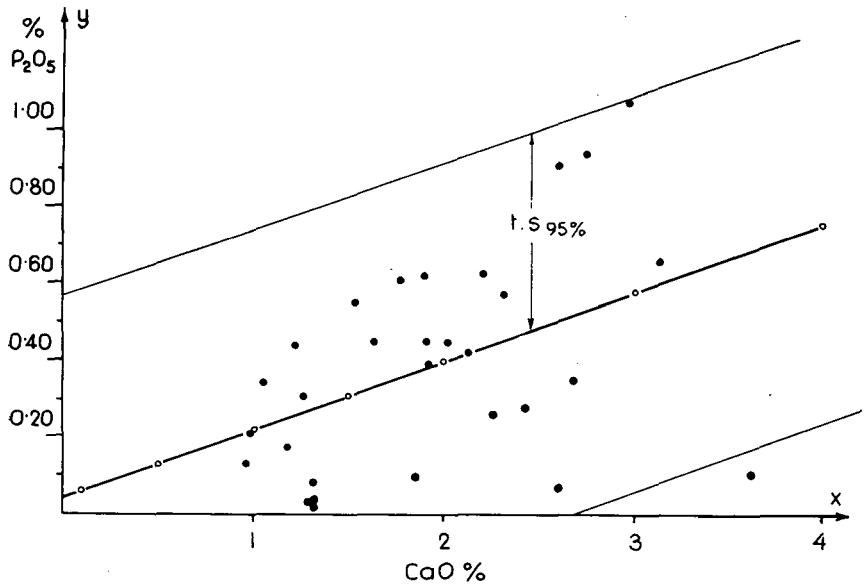

Fig. 3. Correlation between the CaO and P_2O_5 content of manganese oxide ore samples from Úrkút

Data of analysis of a 1,5—2 cm thick phosphate-containing lens from the Upper—Liassic dark grey radiolarian clay-marl in Eplény as well as of a sample from the immediate underlying rock of the manganese oxide deposit of Urkut (shaft No II) are summarized in Table 1.

Unfortunately this analysis — owing to the nature of the samples themselves — is not suitable for calculating the composition of the phosphate mineral present. Although the phosphate content of the samples is considerable, the phosphate component cannot be separated from other minerals present. Thus data of the analysis cannot be used for calculating the formula of the apatite mineral. The P_2O_5, F, Cl content can completely be regarded as belonging to apatite, but the same cannot be said of the other components. At most approximate calculations can be carried out, taking as a basis for calculation the P_2O_5 content determined, and the following general formula: $9CaO \cdot 3P_2O_5 \cdot CaX_2$. A part of the CaO content belongs to apatite, the other to the calcite present. Therefore a part of CO_2 also belongs to calcite, the other — although it is not proved that all what remain besides the part

necessary for calcite — belongs to apatite. The case is similar with the determination of the H_2O^+ content: the sample also contains limonite as well as manganese(IV)-oxyhydrate and opal was observable, too. Thus a part of the water content does not belong to apatite, but its amount cannot be exactly given. The same can be told of the alkali content: silicates were also found in the samples, thus a part of the alkalies may belong to them, but it is not out of question that a part of them belongs to apatite.

Table 1

	Sample from Eplény (No 13)			Sample from Úrkút		
	a	b	c	a	b	c
Insoluble	25,13%			17,86%		
CaO	27,48	25,10	55,16	37,06	31,92	54,82
P_2O_5	19,12	19,12	42,01	24,32	24,32	41,81
Fe_2O_3	6,82			1,71		
Al_2O_3	5,48			4,39		
MnO_2	0,88			2,13		
K_2O	1,12			0,51		
Na_2O	0,62			0,55		
CO_2	2,48	0,62	1,36	5,36	1,33	2,28
Organic C	0,99			0,18		
H_2O^+	2,87	0,46	1,01	2,19	0,38	0,65
H_2O^-	3,57			3,55		
S	4,22			0,18		
F	0,21	0,21	0,46	0,19	0,20	0,34
Cl	—			0,02	0,02	0,03
	100,99%	45,17%	100,00%	100,20%	58,17%	100,00
Less O	1,14			0,13		
	99,85%			100,07%		

We could therefore restrict ourselves to an approximate calculation of the amount of CO_2 (the quantity remaining after calculating the part belonging to $CaCO_3$) and H_2O^+, respectively, which likely belongs to apatite, besides the slight amount of F and Cl. Data of analyses are summarized in column *a* of Table 1, percentage amounts belonging to the phosphate component in column *b*, while column *c* contains the same amounts recalculated to 100 per cent.

Partial analytical data of another Upper—Liassic grey, fine striped nodule (Nr. 11) also from Eplény, together with analytical data of dahllite as published by D. McConnell [1960] are summarized in Table 2. From the analysis of dahllite only those data were considered, which components have also been used in our own analysis as constituents of apatite.

Although the calculations must be considered as approximate and whatever is the uncertainity concerning them, it appears at least that in the apatite mineral of the Urkut and Eplény manganese ore deposit besides the slight amount of F and Cl, CO_3^{2-} and OH^- must also be present, thus in the light of chemical analysis it must be regarded as hydroxy-carbonate apatite with fluorine content.

This statement is supported by L. L. Ames [1959] declaring that if the CO_3 content is less than 10 per cent, it completely may enter the apatite lattice. Carbonate groups, as stated by D. McConnell [1960] substitute the phosphate groups and not the (F, OH) groups.

Table 2

	Sample (No 11.) Eplény			Dahllite D. McConnell, [1960]		
	a	b	c	a	b	c
CaO	47,94%	46,00%	54,57%	51,44%	51,10%	53,67%
P_2O_5	34,98	34,98	41,50	39,92	39,92	41,93
CO_2	4,33	2,81	3,33	2,72	2,72	2,85
H_2O^+	1,90	0,21	0,24	2,83	1,03	1,08
F	0,20	0,20	0,24	0,03	0,03	0,03
Cl	0,10	0,10	0,12	0,42	0,42	0,44
		84,30%	100,00%		95,22%	100,00%

RESULTS OF INFRARED ABSORPTION INVESTIGATIONS

A study of the infrared absorption spectra also renders an excellent possibility for the identification of phosphate minerals.

The free PO_3^{4-} ion has a T_d symmetry and accordingly in the ideal symmetry four fundamental vibrations are possible, of which, however, only two are infrared active ones, namely in the range 950—1200 cm^{-1} the $[\nu(\alpha)PO_4]$ or ν_3 stretching vibrations, and under 650 cm^{-1} $[\delta(\alpha)PO_4]$ or ν_4 bending vibration. Both are triply degenerated vibrations. Thus of the fundamental bands only the absorption corresponding to ν_3 and ν_4 can be observed, the other two vibrations, ν_2 and ν_1 merely in the case when the ion configuration is modified by point groups of a lower symmetry [Herzberg, 1945; H. Moenke, 1962; H. H. Adler, 1964].

All the phosphate minerals show a strong absorption between 950—1200 cm^{-1} that is 10,5—8,3 μ, while a less expressed absorption occurs under 650 cm^{-1}, that is in the range of longer wavelengths.

In his publication referred to, H. Moenke [1962] published the infrared spectra of an apatite (Kragerö, Norway) and a phosphorite (Florida, U.S.A.). The characteristic absorption bands of PO_3^{4-} of the apatite recordings appear at the following wave length:

1095, 1050, 965 cm^{-1}, and 605, 579, 574 cm^{-1},

9,13, 9,52, 10,36 μ, and 16,52, 17,27, 17,42 μ,

while at the Florida phosphorite:

1105, 1050, 970 cm^{-1}, and 610, 580, 572 cm^{-1},

9,04, 9,52, 10,30 μ, and 16,33, 17,24, 17,48 μ.

There are other two bands in the Florida phosphorite, namely at 1435 cm^{-1} and 1460 cm^{-1}, which are not contained in the spectrum of the Kragerö apatite. These two bands appear quite strongly in spectra of the Urkut and Eplény samples as well. In this range the CO_3 group shows strong absorption. The sometimes appearing double band likely can be ascribed to the fact that a well defined carbonate (calcite, manganocalcite or perhaps rodochrozite) may appear in the sample, but the CO_3 group is present partly as a constituent of „phosphorite".

Infrared spectra of the Eplény and Urkut samples are represented in *Fig. 4*. The spectrum of a Florida phosphorite is also included for sake of comparison.

The places of absorption bands observed in the spectra and characteristic for PO_4^{3-} are summarized in Table 3. Absorption bands appearing between 1425—1450 cm^{-1}, characteristic for the CO_3 group are also included.

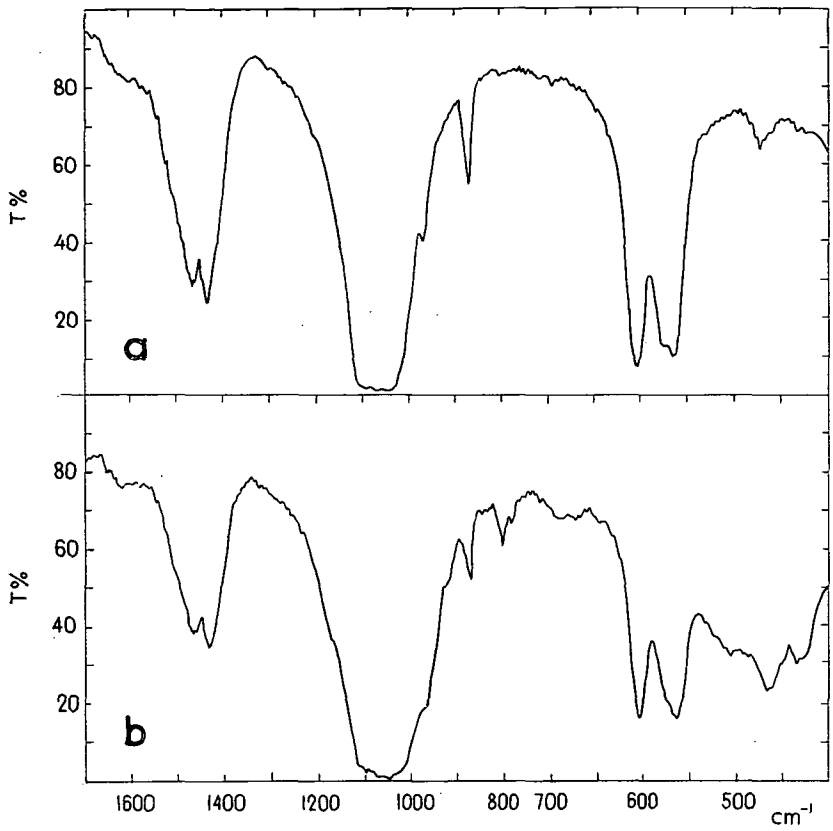

Fig. 4/1 Infrared spectra of the samples investigated
a) Sample No. 11 from Eplény deposit
b) Sample No. 13 from Eplény deposit

The infrared spectra shown in *Fig. 4*, and the absorption bands summarized in Table 3, respectively, are in good agreement with HERZBERG's statement [1945], namely that vibrations ν_3 and ν_1 for the PO_4^{3-} ion are at 1082 cm^{-1} (9,2 μ) and 980 cm^{-1} (10,2 μ), respectively. These frequencies, depending on the crystal structure, may alter to a certain extent.

H. H. ADLER [1964], dealing with the symmetry and substitution effect of the pyromorphite series, refers to the apatite-series as well, and remarks that vibration ν_3 consists of two infrared active modes, namely bands appearing at 9,16 μ (1080 cm^{-1}) and 9,62 μ (1040 cm^{-1}) correspond to this vibration, while the band appearing at 10,35 μ (960 cm^{-1}) corresponds to vibration ν_1. These bands — with but a slight difference — have also been found in the spectra of samples from Eplény and Urkut.

R. B. FISCHER and CH. E. RING [1957] stated that when investigating fluorapatite and hydroxyapatite mixtures from a quantitative viewpoint, first of ay the study of bands between 15—24 μ was fruitful. According to ADLER [1964] thell

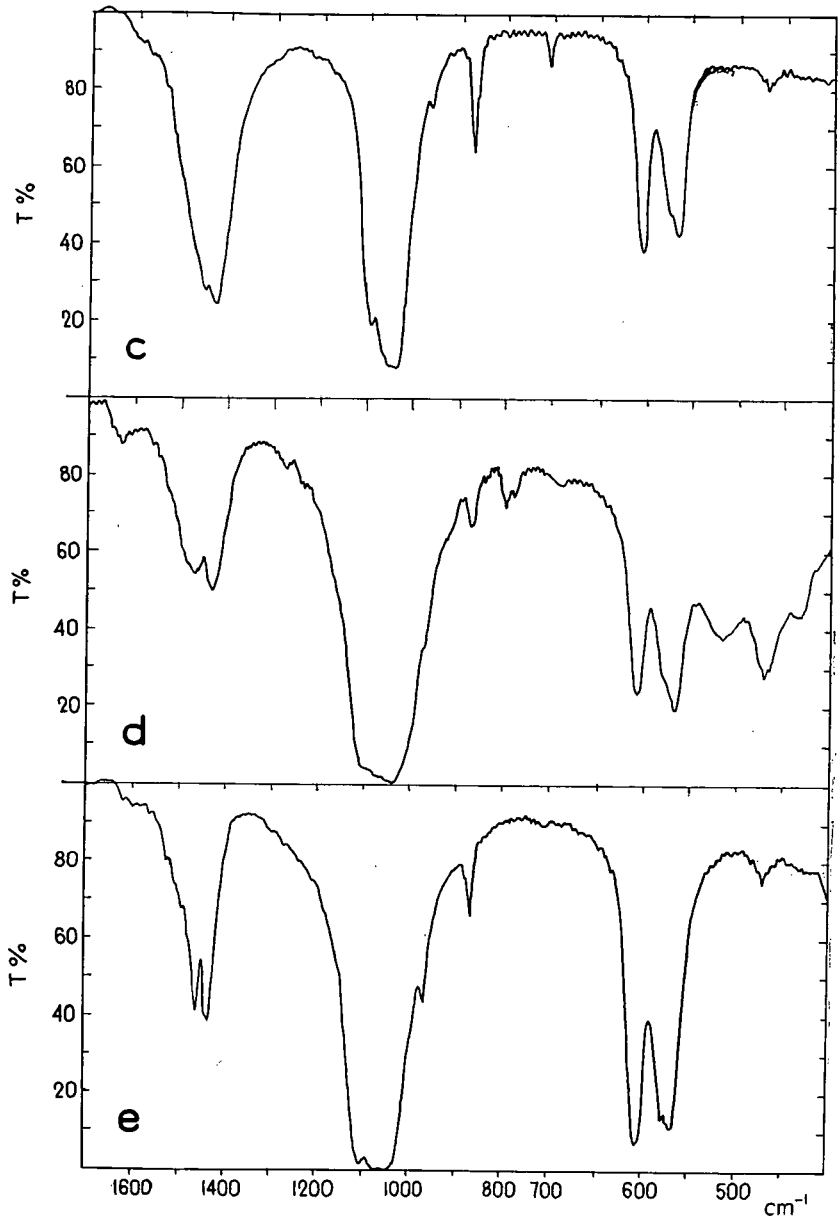

Fig. 4/2 Infrared spectra of the samples investigated
c) Sample from the manganese oxide deposit of Úrkút
d) Sample from the immediate underlying rock of the manganese oxide deposit of Úrkút
e) „Phosphorite", Florida

Table 3

PO_4 infrared absorption bands of samples from the Eplény and Urkut manganese ore deposite, with large phosphate content, in the range 16—18 μ and 9—10,5μ

	a		b		c		d		e	
	Eplény, Sample No. 11		Eplény, Sample No. 13		Úrkút, Shaft No. II. from oxide deposit		Úrkút, Shaft No. II. from underlaying rock of oxide deposit		Phosphorite, Florida	
	cm^{-1}	μ	cm^{-1}	μ	cm^{-1}	μ	cm^{-1}	μ	cm^{-1}	μ
PO_4^{3-}	565	17,69	565	17,69	565	17,69	565	17,69	567	17,63
	575	17,3	575	17,3	575	17,3	575	17,3	577	17,33
	604	16,55	603	16,58	604	16,55	605	16,5	603	16,58
	969	10,31	970	10,30	969	10,31	970	10,3	969	10,31
	1070	9,34	1040	9,61	1050	9,52	1040	9,61	1060	9,43
	1090	9,17	1090	9,17	1090	9,17	1080	9,25	1085	9,21
CO_3^{2-}	1432	6,98	1431	6,99	1430	6,99	1430	6,99	1430	6,99
	1458	6,86	1465	6,82	1460	6,85	1458	6,86	1460	6,85
	1469	6,81					1472	6,79		

correspond to ν_4 fundamental vibration. According to R. B. FISCHER and CH. E. RING if fluorapatite is dominant in the sample, the band appears at 17,5 μ, and on the contrary, the more considerable the amount of hydroxyapatite, this band is more and more displaced towards 17,8 μ. In connection with the change fluorapatite: hydroxyapatite ratio this displacement of the band from 17,5 μ towards 17,8 μ is accompained by a change of the form of bands appearing between 16,6—17,8 μ.

In the samples investigated at present the characteristic band mentioned by R. B. FISCHER and CH. E. RING is at 17,69 μ as seen in the Table 3, thus it is nearer 17,8 μ, characteristic for hydroxyapatite, than to 17,5 μ characteristic for fluorapatite. The considerable carbonate and OH-content of the samples — although they cannot be in their complete amount ordered to the phosphate component — is in accordance with the infrared spectra, what indicates that we have a carbonate hydroxyapatite with F-content.

RESULTS OF X-RAY STUDIES

Although the inhomogeneity of the samples made possible only some informatory records, the X-ray diffraction pattern of the samples had been taken by Cu/Ni radiation. Table 4 shows *d* values as obtained for the Eplény No. 11 and No. 13 samples and for the Urkut one. The Table 4 contains only diffraction lines which likely come from the apatite component. We have omitted from the Table a number of lines of fairly slight intensity, coming from other minerals present. The X-ray diffraction pattern has been taken in the range 2Θ 25—55°. For sake of comparison some *d* values of francolite by GRUNER and MCCONNELL [1937] of dahllite by MCCONNELL [1960] and for fluorapatite (also by MCCONNELL) of the A.S.T.M. card are also enlisted.

The *d* values as obtained for the samples studied are quite similar to those taken for comparison, perhaps most of all to those of francolite. Although the diffraction

Table 4

X-ray diffraction data of the samples; Cu/Ni radiation

Sample Nr. 11 from Eplény		Sample Nr. 13 from Eplény		Sample from Úrkút		Francolite [GRUNER, MCCONNELL, 1937]			Dahllite [MCCONNELL, 1960]		Fluorapatite [A. S. T. M.]	
d	I	d	I	d	I	hkl	d	I	d	I	d	I
						200			4,094	1		
						111			3,899	2		
3,443	m	3,451	m	3,442	w	002	3,437	1	3,446	3	3,44	20
3,174	vw	3,172	w	3,165	w	102	3,160	0,5				
3,086	m	3,093	w	3,098	vw							
3,067	w					120	3,050	3	3,095	3	3,07	30
2,794	vs	2,800	vs	2,797	vs	121	2,789	10	2,823	10	2,81	100
2,787	vs	2,797	vs	2,791	s				2,785		2,78	40
2,693	m	2,704	m	2,700	m	300	2,694	6	2,729	8	2,71	60
2,622	w	2,624	w	2,617	w	202	2,622	3	2,636	2	2,63	30
2,505	vw	2,497	w			301	2,507	0,5	2,537	1	2,53	5
				2,277	vw	122	2,289	0,5			2,30	5
2,245	w					130	2,242	2	2,271	3	2,26	20
2,137	w			2,144	vw	131	2,131	1	2,135	1	2,14	10
2,060	vw					113			2,066	1	2,06	10
						132β	2,067	0,5				
				2,033	vw	123β	2,026	0,5				
1,934	w	1,938	w	1,942	vw	222	1,931	3	1,950	3	1,94	40
1,883	vw	1,883	vw	1,876	vw	132	1,880	1	1,896	1	1,89	10
						230			1,878	1		
1,839	m	1,839	vw	1,836	vw	120	1,836	3			1,84	60
1,796	vw					231	1,795	2	1,812	1	1,80	30
1,768	vw	1,770	vw			140	1,764	2	1,787	1	1,77	30
1,750	vw	1,750	vw			402	1,745	2	1,760	1	1,75	30
						303			1,758			
1,722	w	1,720	w	1,718	vw	004	1,721	2	1,723	1	1,72	30

vw: very weak; w: weak; m: middle; s: strong; vs: very strong

pattern of francolite and fluorapatite is very similar, according to MCCONNELL [1952] reflexion *300* of francolite is of greater intensity than reflexion *121*, however, the same is reversely valid for fluorapatite. The diffraction patterns of the Eplény and Urkut samples have as the most intensive — in an order of decreasing intensity — diffraction lines corresponding to reflexions *121*, *300* and *202*. Accordingly fluorapatite would have been supposed if the slight fluor content of the sample and the place of characteristic bands in the infrared spectra did not contradict this. It must be noted that in the comparative data in Table 4, reflexion *121* is the most intensive for all the three apatite minerals and reflexion *300* is somewhat weaker.

X-ray data of the Urkut and Eplény phosphate mineral have good agreement in respect to several lines with X-ray data of an U-containing phosphate (Pécsely) investigated by J. KISS and K. VIRÁGH [1959]. The authors referred to regard the phosphate studied by them as a carbonate apatite with fluor content. The present studies are in good accordance with this view.

The analytical and X-ray data of the Urkut and Eplény phosphate mineral are quite similar to those given by R. ORTMANN [1960] for the phosphate mineral in Dukaj, Albany. The author, considering chemical composition, regards the phosphate component a carbonate hydroxyapatite, near to dahllite.

CONCLUSIONS

On comparing results of chemical analysis, infrared absorption and X-ray diffraction, in spite of the uncertainities coming from the inhomogeneity of the material, we have come to the conclusion that it is not reasonable to maintain the general designation „fluorapatite" for the phosphate mineral of the Urkut and Eplény manganese ore deposit, since it would only be justified to use, if — as pointed out by McConnell [1958] — the amount of CO_2 and H_2O content were less than 1 per cent and the F content exceeded 3 per cent. By approximative calculations — only considering components belonging to apatite — and calculating the results for 100 per cent, the CO_2 and H_2O content of the samples of Urkut and Eplény phosphate mineral is over 2 and even 3 per cent, and the F content in each sample is below 1%. On the basis of chemical analysis hydroxy-carbonate-apatite with fluor content can be considered. The place of bands between 17,5—17,8 μ in the infrared absorption spectra, more correctly, their displacement towards 17,8 μ similarly indicates that hydroxy-carbonate-apatite with some fluor content must be considered. X-ray diffraction data of samples are nearest to those of francolite. Francolite is essentially carbonate apatite. However, as the F content is low, and in the lattice of the phosphate component the presence of CO_3^{2-} and OH^- groups is obvious, as proved by infrared investigations, by all probability, the phosphorus-bearing mineral of the Urkut and Eplény manganese ore deposit is dahllite, what designation according to McConnell [1958] is correct for hydroxy-carbonate apatite of phosphate sediments, with low F content.

ACKNOWLEDGEMENT

The writer expresses his distinguished thanks to Mrs. Ilona Kispéter for the chemical analyses, to Mr. Ákos Bertalan for obtaining the X-ray patterns and to Mr. József Mezősi for his kind comments as well as to Mr. Nándor Marek for the infrared spectra.

REFERENCES

Adler, Hans H. [1964]: Infrared Spectra of Phosphates. — The Amer. Miner. *49*, 1002—1015.
Ames, L. L. [1959]: The Genesis of Carbonate Apatites. — Econ. Geol. *54*, 829—841.
Fischer, R. B., C. E. Ring [1957]: Quantitative Infrared Analysis of Apatite Minerals. — Anal. Chem. *29*, 431—434.
Grasselly, Gy., E. Klivényi [1960a]: Data on the Phosphorous Content and Organic Remains of Manganese Oxide Ores from Urkut. — Acta Miner. Petr. Univ. Szegediensis *13*, 3—8.
Grasselly, Gy. [1960b]: Report on the Investigations of Phosphorous Content of Mangenese Oxide Ores from Urkut. — Manuscript, Only in Hungarian.
Gruner, John W., Duncan McConnell [1937]: The Problem of the Carbonate-Apatites. The Structure of Francolite. — Z. f. Kristallogr. (A) *97*, 208—215.
Herzberg, G. [1945]: Molecular Spectra and Molecular Structure. II. Infrared and Raman Spectra of Polyatomic Molecules. — D. Van Nostrand Co., Inc., New York.
Kiss, J., K. Virágh [1959]: An Uranium-bearing Phosphatic Rock in the Triassic of the Balaton Uplands around Pécsely. — Földtani Közlöny *59*, 85—97. In Hungarian with an English summary.
McConnell, Duncan [1952]: The Problem of the Carbonate Apatites. IV. Structural Substitutions Involving CO_3 and (OH). — Bull, Soç. Franç. Minér. Crist. *75*, 428—445.
McConnell, Duncan [1958]: The Apatite-like Mineral of Sediments. — Econ. Geol. *53*, 110—111.
McConnell, Duncan [1960]: The Crystal Chemistry of Dahllite. — The Amer. Miner. *45*, 209—216.
Moenke, H. [1962]: Mineralspektren. — Akademie Verlag, Berlin.

NAGY, K. [1955]: Mineralogical Characteristics of the Manganese Ore Deposit of Urkut, Bakony Mountains, Hungary. — Földtani Közlöny *85*, 145—152. In Hungarian with an English summary.

NEMECZ, E. [1960]: Report on the Investigations of Manganese Carbonate Ores from Úrkút. — Manuscript, only in Hungarian.

ORTMAN, RENATE [1960]: Mineralogische Untersuchungen des Phosphatkalks von Dukaj bei Tepelene (Albanien). — Z. f. angew. Geol. *6*, 259—262.

SZABÓ—DRUBINA, MRS. M. [1957]: Caractére géologique et minéralogique sédimentaire des minerais de manganese de la Hongrie. — Földtani Közlöny *87*, 261—273. In Hungarian with a French summary.

PROF. DR. GYULA GRASSELLY
Institute of Mineralogy, Geochemistry and Petrography
Attila József University at Szeged
Táncsics M. u. 2.
Szeged, Hungary

ADSORPTION PROPERTIES OF SOME MANGANESE OXIDES

Preliminary report

GY. GRASSELLY and MISS M. HETÉNYI

Institute of Mineralogy, Geochemistry and Petrography,
Attila József University, Szeged

INTRODUCTION

Taken into consideration the fairly considerable number of works dealing with the general properties of natural and artificial manganese oxides as well as that of the mineralogical and geological studies on manganese ore deposits, it can be stated that the manganese oxides and oxyhydrates, respectively, belong to the minerals investigated the most frequently, from the most different viewpoints and in detail.

However, the consideration may also be arisen that presumably a problem is manysidedly investigated and discussed just when there are still several open questions, problems to be solved and hypotheses to be proved.

Although it is well known that among other factors the sorption processes play an important role in the migration and enrichment of the elements, in the literature relatively few data can be found concerning the adsorption properties of manganese oxides and oxyhydrates, respectively, based on model-experiments.

In the literature there are numerous data as regards the minor elements determined in the manganese minerals of different origin and the probability of enrichment of certain elements in oxidative environments like the manganese oxide deposits, is also known. Even the enrichment of certain minor elements in some formations and the lack of others, respectively, is assumed to be in correlation with the presence of certain MnO_2 modifications [K. H. WEDEPOHL, 1961].

Some data on the ion exchange properties of manganese oxides can also be found. According to A. D. WADSLEY [1950] the Na^+ ion of the manganese oxyhydrate $(Na, Mn)Mn_3O_7 \cdot nH_2O$ prepared by oxidation of $Mn(OH)_2$ in aqueous alkaline solution may be exchanged by other metal-ions.

The ion exchange property of MnO_2 was discussed by AKIYA KOZAWA [1959] proposing the Zn ion exchange determined experimentally as a measure for the ion exchange capacity of the different manganese oxides.

K. KRAUSKOPF [1961] dealing with the possibilities of the reduction of concentration of thirteen elements in sea water stated that among other adsorbents the

Delivered at the 2nd Symposium of the I. A. G. O. D. held in September 1967 in St. Andrews (Scotland)

$MnO_2 \cdot nH_2O$ plays an important role in the scavenging of some minor elements from sea water due to adsorption.

E. GOLDBERG [1954] stated that in the ferruginous sediments of the Pacific Ocean the adsorbed Ti, Co, Zr content is proportional to the iron oxide content, similarly the Cu, Ni content shows a linear correlation to the Mn content. It is very interesting that a considerable difference can be established between the amounts of Co and Ni adsorbed by manganese oxyhydrates of the deep-sea manganese nodules, though both double charged cations have similar ionic radii and both have the same geochemical character. According to E. GOLDBERG the concentration of Co shows parallelism with the iron content which fact may be interpreted so that the cobalt may be present in anionic state and thus adsorbed by the negative charged iron hydroxides.

It seems to be very reasonable that a fairly important and perhaps selective role may be attributed to the manganese oxyhydrates in the migration and distribution of certain minor elements and the results of such investigations may contribute to the detailed interpretation of genetic problems of manganese ore deposits as well as they may be useful how to solve some practical problems, too.

This fact encouraged us to start the systematic study of the adsorption properties of different natural and artificial manganese oxides and oxyhydrates, respectively, by model-experiments.

These investigations are readily carried out in two ways. 1. Introducing the minor element in known concentrations into the dilute aqueous solution of manganous salt, then precipitating the manganese oxyhydrate under well controlled conditions and determining the distribution of the minor element between the manganese oxyhydrate and the solution. In this way connections can be stated among the conditions of precipitation (pH, Eh, concentration, temperature, etc.), the composition of the solid phase and the adsorption of the ion introduced.

2. The other way in the set of experiments was as follows: starting from solid manganese oxide phases and treating them with solutions of different electrolytes of known concentration and measuring the decrease of the ion concentration of the solution owing to the adsorption.

These two ways complete each other as the first can be considered to be the model of processes taking place during the formation of manganese oxide and oxyhydrate mineral phases, the second set of experiments, however, can be taken for a model of processes occuring in manganese oxide deposits after their formation, in consequence of dilute aqueous solutions.

At present the aims and problems of the work will be merely outlined and the results obtained illustrated, however, it is not intended to give a theory on the basis of experimental data so far though it might be attractive and alluring. During these introductive experiments no effort has been taken to completeness rather a comprehension was aimed at concerning questions which may arise and be answered at least partly on the basis of experiences gained.

These questions may be outlined as follows:

a) Whether an essential adsorption may be established for the different ions on the manganese oxides investigated?

b) Whether an essential difference is revealed in the adsorption properties of different manganese oxides, that is, may a selective adsorption be established in relation to different manganese oxides as adsorbents and various ions, respectively?

c) How far is it possible to make use of the experimental data to interpret natural processes like the enrichment of certain ions and whether the data obtained

may be compared to those regarding the minor element concentration of different manganese oxide deposits.

The adsorption of Na^+, K^+, Ca^{2+} ions in chloride solutions and that of Cu^{2+}, Co^{2+} and Ni^{2+} ions in sulphate solutions on β-, γ-, η-MnO_2, α-Mn_2O_3, Mn_3O_4, manganite and cryptomelane were studied.

EXPERIMENTAL

Preparation of the samples

The preparation of MnO_2 modifications was carried out by the methods given in the papers of G. GATTOV and O. GLEMSER [1961 a, b].

1. β-MnO_2: $Mn(NO_3)_2 \cdot 4H_2O$ was tempered during 24 hours at 190—200 °C, the product pulverized in an agate mortar, boiled in 2—3 N nitric acid, filtered and washed free of acid then dried at 110 °C.

2. γ-MnO_2: A solution of 15 gramm $Mn(NO_3)_3 \cdot 4H_2O$ in 1000 ml of 3 N nitric acid was mixed with 200 ml solution of 2 per cent $KMnO_4$ at 20—40 °C. The precipitate was filtered by decantation and washed free of acid and dried at 60 °C.

3. η-MnO_2: α-Mn_2O_3 was boiled in 3 N nitric acid during 20 hours in a flask with reflux cooler then filtered, washed free of acid and dried at 60 °C.

The other manganese oxides were prepared as follows:

4. α-Mn_2O_3: A saturated ammonium oxalate solution was added to the boiling suspension of manganese carbonate in water till the supernatant liquid showed acidic reaction. The manganese oxalate precipitate was filtered, washed till neutral reaction and dried. The product was ignited in a Pt-dish in open air by constant stirring till the oxalate decomposed and then ignited at 650 °C up to the total transformation into α-Mn_2O_3.

5. Mn_3O_4: α-Mn_2O_3 was ignited to Mn_3O_4 in an electric oven at 1050 °C.

The natural samples were as follows:

6. Manganite.

7. Cryptomelane.

Both selected samples originated from the sedimentary manganese ore deposit of Urkut, Hungary. The fraction $<0{,}06$ mm was used to the adsorption experiments.

Identification of the samples

The identification of the samples was carried out partly by X-ray powder patterns partly by differential thermal analysis. The results were confirmed by infrared adsorption spectra.

The X-ray investigations were carried out by Fe/Mn radiation with 30 kV, 10 mA. Results are summarized in Tables 1 and 2.

Of the samples only the γ-MnO_2 proved to be roentgen-amorphous. The manganite from Urkut contains some pyrolusite as shown also by the D.T.A. curve.

The D.T.A. curves give valuable information on the modification of MnO_2 as the main endothermic peak appears at 620° C in the case of the most ordered, most stable β-modification while this endothermic peak appears at a somewhat lower temperature in the case of other modifications. According to G. GATTOW and O. GLEMSER [1961 a, b] in the case of different MnO_2 modifications the temperature of this endothermic peak is as follows: γ-MnO_2 500° C, $\gamma''MnO_2$

532° C, η-MnO_2 543° C, η''-MnO_2 548° C and β-MnO_2 620° C. According to the D.T.A. curves obtained the samples used for investigation correspond to the given modifications. The same is valid for the other manganese oxides too.

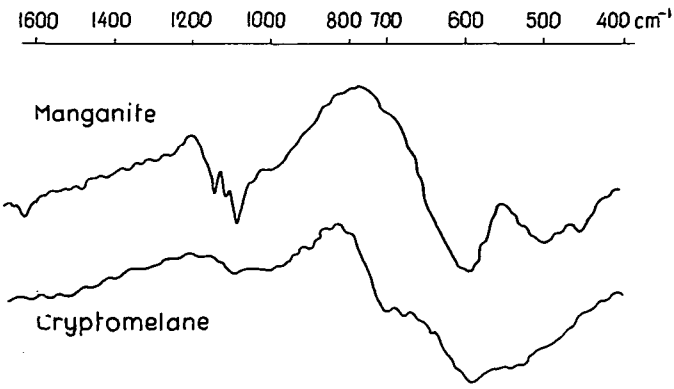

Fig. 1. Infrared absorption spectra of manganite and cryptomelane from Úrkút, Hungary

The infrared adsorption spectra can also be used to identify different manganese oxides. For the identification the absorption bands between 400—700 cm^{-1} wave number can be used as they are characteristic for the different manganese oxides [H. MOENKE, 1962]. Infrared adsorption spectra of different manganese oxides are also published in papers by G. GATTOW and O. GLEMSER [1961 a, b]. The infrared adsorption spectra of the samples investigated are shown in *Figs. 1—3.*

Table 1
X-ray powder data of the natural samples
d(Å) with Fe/Mn radiation

Manganite Úrkút				Cryptomelane Úrkút			
Measured		Michejev No 289		Measured		Michejev No 302	
d(Å)	I	d(Å)	I	(dÅ)	I	d(Å)	I
3,418	vs	3,40	100	6,869	w	6,81	4
3,107	m			4,813	vw	4,87	4
2,623	m	2,64	60	3,098	m	3,084	10
2,513	vw			2,447	vw	2,455	2
2,413	s	2,41	80	2,397	w	2,393	4
2,269	w	2,26	60	2,151	vw	2,148	2
2,192	w	2,18	60				
2,106	vw						
1,782	m	1,77	80				
1,703	w	1,70	70				
1,673	s	1,665	80				
1,628	w	1,630	70				
1,563	vw						
1,507	w	1,495	70				
1,453	w						

vs: very strong; s: strong; m: middle; w: weak; vw: very weak

Table 2

X-ray powder data of artificial samples, d(Å) with Fe/Mn radiation

β-MnO_2				η-MnO_2	
Measured		Michejev No 264		Measured	
d(Å)	I	d(Å)	I	d(Å)	I
3,116	vs	3,118	100	3,994	m
2,410	s	2,404	90	2,720	m
2,202	w	2,202	20	2,430	m
2,112	m	2,108	70	2,125	s
1,623	s	1,622	100	1,635	m
1,556	m	1,555	80		
1,435	m	1,434	60		

α-Mn_2O_3				Mn_3O_4			
Measured		A. S. T. M. 10—69		Measured		A. S. T. M. 8—17	
d(Å)	I	d(Å)	I	d(Å)	I	d(Å)	I
3,837	m	3,84	25	4,897	m	4,86	70
2,713	vs	2,72	100	3,079	m	3,05	50
2,508	vw	2,51	3	2,868	w	2,87	20
2,350	m	2,35	11	2,760	s	2,74	90
2,097	vw	2,10	1	2,479	vs	2,47	100
2,003	m	2,01	13	2,358	m	2,34	50
1,921	vw	1,92	1	2,032	m	2,02	60
1,840	m	1,845	13	1,824	vw	1,812	10
1,715	vw	1,719	3	1,796	w	1,779	50
1,658	s	1,664	30	1,698	w	1,689	20
1,610	vw	1,615	1	1,638	vw	1,629	15
1,562	vw	1,566	1	1,572	m	1,571	60
1,526	vw	1,524	5	1,541	s	1,537	80
1,452	w	1,452	9	1,436	m	1,434	50
1,417	m	1,419	15				

vs: very strong; s: strong; m: middle; w: weak; vw: very weak

Experimental conditions

During the expriments different quantities (0,1—0,5 gramm) of the samples were weighed into polyethylene bottles and 50—50 ml solutions containing the given ions in concentration of 0,01—0,1 mmol/100 ml (in some cases up to 0,2 mmol/100 ml) were added. As the equilibrium was reached within 30 minutes the samples were shaken for 60 minutes and filtered — after or without centrifugation as needed — and the ion concentration of the solution determined. From these values the decrease of the ion concentration and the adsorbed amount of the ions, respectively, were established.

The values referred to 1 gramm of adsorbent, the specific adsorbed quantity expressed in mmol/g, was obtained. Plotting these values against the measured equilibrium concentration of the solutions (the concentration of the solutions after the adsorption equilibrium having been reached), the adsorption isotherms could be drawn.

Specific adsorption can be calculated taking into consideration the volume of the solution (V), the difference between the starting (c_0) and equilibrium concentrations (c_e) of the solution and the mass of the adsorbent (m) weighed in:

$$\alpha = \frac{V(c_0 - c_e)}{100 \cdot m}.$$

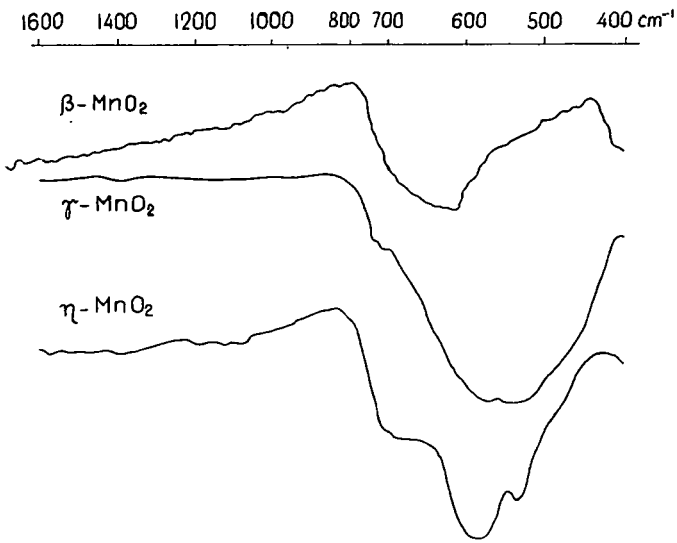

Fig. 2. Infrared absorption spectra of artificial MnO_2 modifications

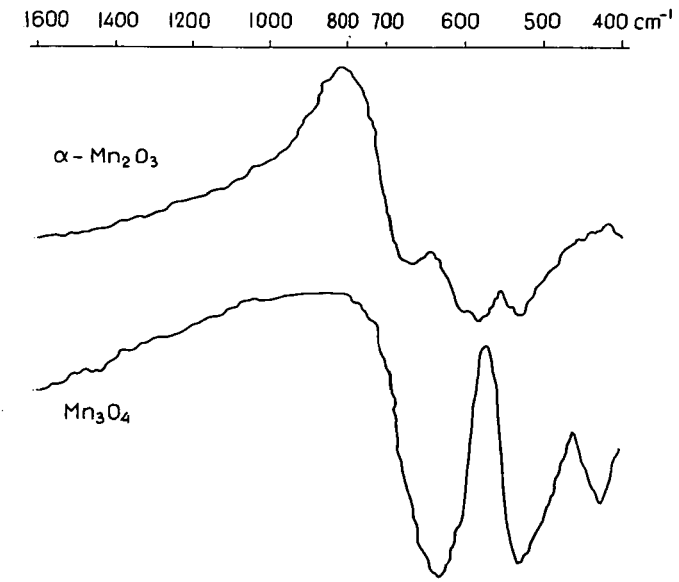

Fig. 3. Infrared absorption spectra of artificial α-Mn_2O_3 and Mn_3O_4

Determination methods applied

The concentration of Na^+, K^+ and Ca^{2+} was determined by flame-photometry.

To determine the concentration of Cu^{2+}, Co^{2+} and Ni^{2+} spectrophotometrical methods were used as found in different textbooks [e.g. B. LANGE, 1942; F. D. SNELL and CORNELIA T. SNELL, 1951; R. PŘIBIL, 1961]. The determination of the copper is based on the reaction with potassium ferrocyanide using gelatine as protecting colloid, that of the cobalt on the reaction with potassium bichromate in presence of EDTA and finally to determine the Ni content the well known dimethyl glyoxime reaction was used.

It is to mention that the determination of the equilibrium concentration of ions in the solution and that of their adsorbed amounts on the adsorbents would have been much more elegant and accurate by radiochemical methods using labelled ions for example Co-60, Cu-64 isotopes. The spectrophotometrical methods used — especially in the field of the lowest concentrations below 0,01 mmol/100 ml — may be accompanied by errors which make the initial part of the adsorption isotherms uncertain and inaccurate.

DISCUSSION OF THE RESULTS

Adsorption isotherms are shown in *Figs. 4—19*. The adsorption isotherms for the different ions are denoted by the same number in each Fig.: Na^+[1]; K^+[2]; Ca^{2+}[3]; Cu^{2+}[4]; Co^{2+}[5]; Ni^{2+}[6]. The abscissa is the equilibrium concentration measured and expressed in mmol/100 ml, the ordinata is the specific adsorption calculated and given in mmol/g. For the sake of comparison the scale of ordinata and abscissa is the same in each Fig.

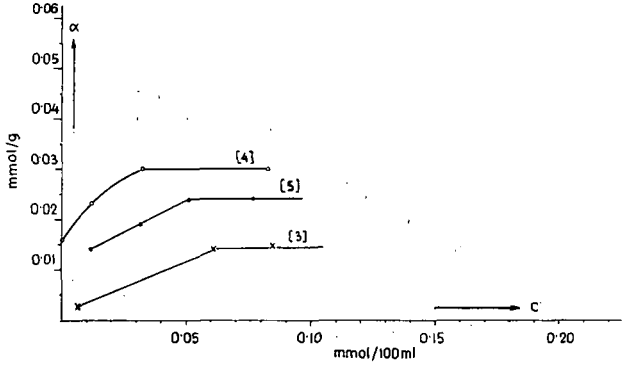

Fig. 4. Adsorption isotherms of Ca^{2+}, Cu^{2+} and Co^{2+} on natural manganite

The questions mentioned in the Introduction can be answered, at least partly, by the adsorption isotherms. According to their shape the isotherms obtained experimentally correspond either to those characteristic of electrolyte adsorption on polar adsorbent or to those of heterogeneous chemical reactions on the surface.

To use the terms unequivocally the expression „non-equivalent ion exchange adsorption" is used if the cations and anions of the electrolyte are not adsorbed at equal rate. In extreme cases only the cations of the solution are adsorbed on the surface of the adsorbent displacing the exchangeable cations from there while it is rather expedient to speak about chemo-sorption in the case of chemical reactions taking place on the surface.

Although it is hardly possible to decide surely the character of the process on the basis of the isotherms alone, some peculiar features, however, can be stated.

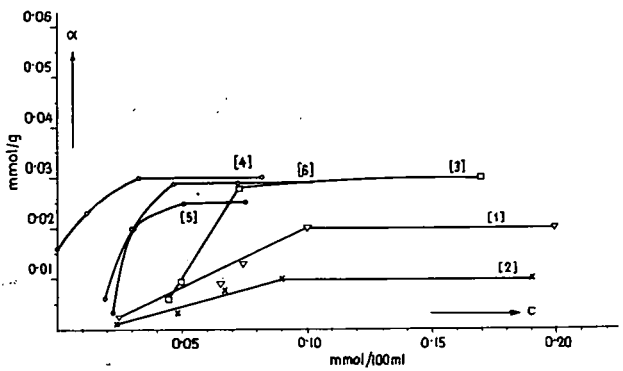

Fig. 5. Adsorption isotherms of Na^+, K^+, Ca^{2+}, Cu^{2+}, Co^{2+} and Ni^{2+} on natural cryptomelane

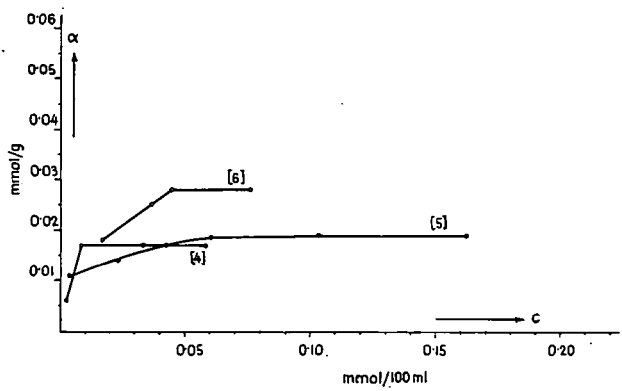

Fig. 6. Adsorption isotherms of Cu^{2+}, Co^{2+} and Ni^{2+} on artificial β-MnO_2

The steepness of isotherms gives rise to some conclusions concerning the exchange ability. The greater the exchange ability the steeper is the starting part of the isotherms. Of the samples investigated the isotherms of the ion adsorption on γ-MnO_2 are the steepest, especially in the case of Cu^{2+}, Ca^{2+} and Ni^{2+} ions. The flattest curves are those of β-MnO_2 and η-MnO_2. The adsorption was the most significant generally on γ-MnO_2 while the adsorption on Mn_3O_4 was always below 0,01 mmol/g.

The saturation was reached sometimes only at a relatively higher concentration as in the case of β-, γ-, and η-MnO_2 in respect of Co^{2+} or of α-Mn_2O_3 in respect

of K^+. It may be concluded that the strength of the bond of such ions is weaker than that of others reaching the saturation already at a lower concentration.

Sometimes the isotherms intersect the axis of equilibrium concentration (abscissa) as for example in the case of cryptomelane, γ-MnO_2 and η-MnO_2 in respect of Co^{2+} (*Figs. 5, 6, 8*, curve 5) or they intersect the axis of the specific adsorption (ordinata) e.g. the isotherms of manganite and cryptomelane in respect of Cu^{2+} (*Figs. 4, 5*, curve 4). It would be, however, a failure to draw conclusions from these

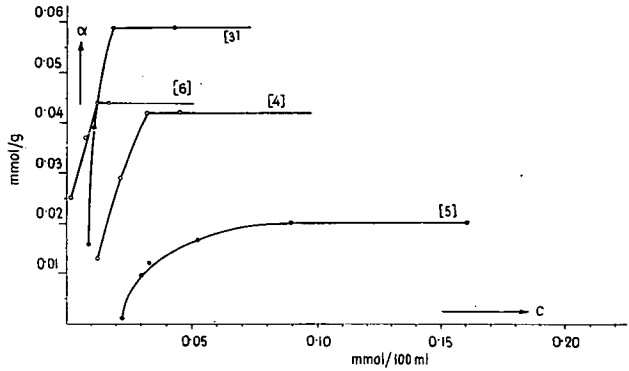

Fig. 7. Adsorption isotherms of Ca^{2+}, Cu^{2+}, Co^{2+} and Ni^{2+} on artificial γ-MnO_2

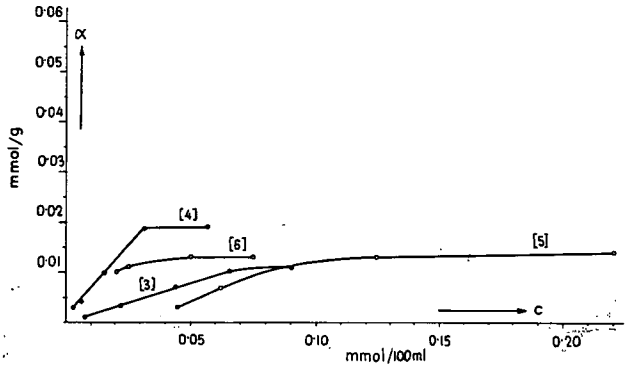

Fig. 8. Adsorption isotherms of Ca^{2+}, Cu^{2+}, Co^{2+} and Ni^{2+} on artificial η-MnO_2

facts as it was mentioned that the initial part of the isotherms is uncertain and inaccurate owing to the possible errors of the determination of fairly low concentrations. Some adsorption measurements with manganite and cryptomelane using radiochemical methods with Cu-64 and Co-60 isotopes showed that the adsorption isotherms start from the origo of the co-ordinata system. These control measurements were carried out by MR. ÁDÁM KOVÁCH and MRS. HUSZTI.

How could the processes of adsorption be outlined and what supports the assumption of a non-equivalent ion exchange adsorption?

The adsorption of cations demands a net negative charge on the surface. The manganese hydroxide sol is well known for its negative charge. The crystalline

solid phase carries a net negative charge owing to substitution of cations of higher valence by cations of lower valence in the lattice. This is also possible in the lattice of manganese oxides. There are many references to such substitution. For example the quadrivalent Mn ions can be substituted in γ-MnO_2 or in other manganese oxides by trivalent or bivalent Mn ions associated with substitution of O^{2-} by OH^-. In the case of ion exchange adsorption the cations of the solutions displace the exchangeable cations (H^+, Na^+ or K^+) on the surface.

In the case of manganese oxides the non-equivalent ion exchange adsorption is rendered probable also by the fact that on treating γ-MnO_2 with a chloride-solution of calcium ions of 0,1 mmol/100 ml concentration and determining the concentration of the chloride after the equilibrium having been reached, the concentration was equal to that of the starting solution, though, at the same time 0,059 mmol/g Ca ion was adsorbed.

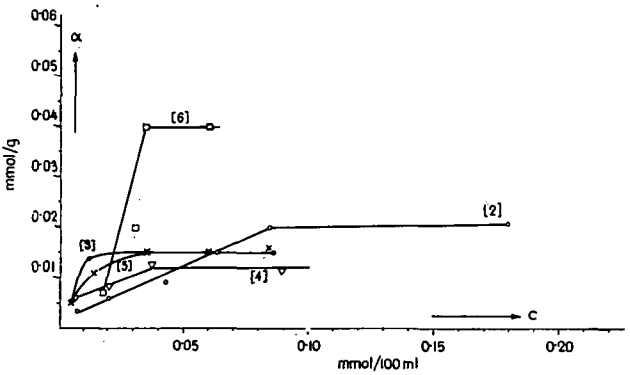

Fig. 9. Adsorption isotherms of K^+, Ca^{2+}, Cu^{2+}, Co^{2+} and Ni^{2+} on artificial α-Mn_2O_3

It was very instructive to confront the behaviour of suspensions of γ-MnO_2 and cryptomelane, respectively, in 0,1 mmol/100 ml Ca-chloride solution in respect of the change of the pH value. The pH of the solution has decreased after adding γ-MnO_2 to it. The decrease in the first ten minutes amounted to nearly three pH units (pH 5,71→pH 2,74), then a slight increase could be noted, and finally it became constant. On the contrary, the pH of the suspension of cryptomelane showed an increase only about one pH unit and reached a constant value. Treating γ-MnO_2 with distilled water a similar decrease of the pH value could be noted, however, Na^+-desorption could not be established, though, on the surface of γ-MnO_2 beside H^+ ions Na^+ ions were present as exchangeable cations. The decrease of the pH on treating the adsorbent with Ca-chloride solution suggests that calcium ions of the solution first exchanged the H^+ ions the surface resulting in a decrease of the pH and later also exchangeable Na^+ ions (or a part of them) were displaced by the Ca^{2+} ions effecting a slight increase of the pH. Treating cryptomelane with distilled water, desorption of K^+ ions could be established and a treatment with Ca-solution caused a K^+—Ca^{2+} exchange from the very beginning, leading to an increase of the pH value about of one pH unit.

Comparing the amounts of various ions adsorbed by different manganese oxides (Table 3) γ-MnO_2 possesses the greatest adsorption ability, especially in respect of Ca^{2+}, Cu^{2+} and Ni^{2+} ions, whereas that of β- and η-MnO_2 was much lower.

Table 3

Specific adsorption [α] in mmol/g

Adsorbent	Na^+	K^+	Ca^{2+}	Cu^{2+}	Co^{2+}	Ni^{2+}
Manganite	≪0,01	<0,01	0,015	0,011	0,024	<0,01
Cryptomelane	0,02	0,01	0,03	0,030	0,025	0,029
β-MnO_2	<0i01	<0,01	<0,01	0,017	0,019	0,028
γ-MnO_2	0,013	0,016	0,059	0,049	0,021	0,044
η-MnC_2	0,012	0,015	0,018	0,019	0,013	0,025
α-Mn_2O_2	≪0,01	0,02	0,015	0,01	0,01	0,04
Mn_3O_4	≪0,01	~0,006	~0,008	≪0,012	<0,015	<0,01

The adsorption of Na^+ and K^+ ions is generally low. The adsorbed quantity of Na^+, K^+, Ca^{2+} and even that of Cu^{2+} ion increases roughly according to the relative surface of MnO_2 modifications.

The Ni^{2+} adsorption on the oxides is higher than that of Co^{2+} ion except manganite. The manganite inclined to adsorb cobalt whereas cryptomelane adsorbed Co^{2+}, Ni^{2+} and Cu^{2+} roughly in equal rate. The worst adsorption ability was shown by Mn_3O_4.

The relatively considerable adsorption on γ-MnO_2 is to be ascribed to the fact that of the three MnO_2 modifications γ-MnO_2 has the relative largest surface, further, it proved to be amorphous and such adsorbents possess generally higher adsorption ability than the crystalline modifications. On the other hand, of the crystalline modifications the stable ones have lower adsorption ability than the less stable ones. This tendency seems to be prevalent in the case of β-, and η-MnO_2, too.

Comparing the adsorbed quantities of the different ions with their concentration determined in natural manganese oxides (Tables 4 and 5) found in the literature, it may be stated that the adsorbed quantities are considerably higher than the average concentration of these ions in the Earth's crust, in the different manganese ores from India in the Hungarian manganese carbonate and oxide ores.

The adsorbed amounts fit well into the lower and upper limits of analytical data as regards the different manganese ores of the United States published by D. F. HEWETT and M. FLEISCHER [1960]. However, the adsorbed quantities are

Table 4

Specific adsorption [α] recalculated in g/t

Adsorbent	Na^+	K^+	Ca^{2+}	Cu^{2+}	Co^{2+}	Ni^{2+}
Manganite	≪230	<930	601	699	1415	<587
Cryptomelane	460	390	1202	1906	1474	1703
β-MnO_2	<230	390	<400	1080	1120	1640
γ-MnO_2	299	626	2365	3113	1238	2583
η-MnO_2	280	586	720	1210	766	1467
α-Mn_2O_3	<230	785	601	763	884	2348
Mn_3O_4	<230	232	320	<635	590	<590

Table 5

Concentrations of Co^{2+}, Ni^{2+} and Cu^{2+} in different manganese minerals and other materials (g/t)

	Co^{2+}	Ni^{2+}	Cu^{2+}
Earth's crust, average (MASON, 1958]	23	80	45
Recent pelagic sediments:			
Indian Ocean (MÜLLER, 1967]			250 soluble in 2n HCl
Atlantic Ocean (WEDEPOHL, 1960]			130
Pacific Ocean (WEDEPOHL, 1960]			400
Indian manganese formations: [ROY, SUPRIYA, 1966]			
Metamorphic manganese ores	60—160	30—1400	50—140
Pyrolusites from colloidal dioxide ores	<100	<100	<100
Cryptomelanes from colloidal dioxide ores	<100	<100	100—1000
Manganese oxide minerals from deposits of U. S. A. (HEWETT, D. F. and M. FLEISCHER, 1960]			
Supergene manganese minerals	629—18 000	150—11 942	79—3100
Hypogene manganese minerals	78—4639	150	239—3515
Deep-sea manganese nodules from the Pacific Ocean (GOLDBERG, E., 1954]	120—7100	1600—11 500	1700—18 100
Manganese carbonate ores Úrkút, Hungary [NEMECZ, E., 1960]	100—500	~10	10—500

significantly lower than the upper limit of Co and Ni content determined in the supergene manganese minerals or the upper limit of Co in hypogene manganese minerals or than the considerable high Co, Ni, Cu content of deep-sea manganese nodules [E. GOLDBERG, 1954].

This comparison may give some information concerning the approximate quantity of ions that can be adsorbed by different minerals of manganese deposits from circulating solutions.

Naturally, it cannot be stated that the natural mineral phases corresponding to the samples studied at present will always adsorb the highest possible quantities experimentally found. It would be erroneous to assert that the amount of Co^{2+} hold by adsorption on manganite always reaches the value of 1,400 g/t or that of the copper on γ-MnO_2 reaches the significant 3,113 g/t value. These values were obtained under conditions when the adsorbent was in contact with solutions containing only one electrolyte. Such conditions can hardly be supposed in natural environments.

The statement of colloid chemistry is well known that in the case of simultaneous adsorption of two or more dissolved substances the adsorption of each substance will be lower than being dissolved alone.

The experiments show that this statement is valid also for manganese oxides. Repeating some of the experiments with mixtures of different electrolytes, an essential decrease in the adsorbed quantities could be noted, even more, in some cases adsorption was not to be determined at all or at least its rate was within the error of determinations.

So, in a mixture of Na^+-, K^+-, Ca^{2+}-chloride solutions of 0,1 mmol/100 ml concentration, the adsorption of Ca^{2+} ions could not be detected on β- and η-MnO_2 only on γ-MnO_2. However, the adsorption on the latter was only 1/3 of that measured in pure Ca-chloride solution. Na^+-adsorption in the same mixture could not be measured either in the case of β- and γ- or in that of η-MnO_2, on the contrary, Na^+-desorption could be measured in the case of β- and η-MnO_2. Still stronger decrease of adsorbed quantities could be determined in a mixture of Co^{2+}-, Ni^{2+}-, Cu^{2+}-sulphate solutions of the same concentrations using the three MnO_2 modifications. On the β- and η-MnO_2 adsorption of the mentioned ions could not be established, only on the γ-modification. The adsorption on the latter was, however, much lower than measured in pure solutions of the same concentration. So, the adsorbed quantity of Co^{2+} was only 1/40, that of Ni^{2+} 1/36 and that of Cu^{2+} 1/7 of the adsorbed quantities measured in solutions of single electrolytes.

Therefore, it seems not to be purposeful to attempt a conclusion that corresponding to the data obtained during the set of adsorption experiments an adequate part of the cobalt, nickel and copper content of natural manganese oxides can be considered as hold by adsorption. Even more, because it is proved that in simultaneous presence of several electrolytes the adsorption does not take place on some manganese oxides.

The experiences so far may be interpreted that the adsorbed quantities from solutions containing more electrolytes may be considered as a lower limit whereas the adsorbed quantity measured in solutions containing only one electrolyte would represent the upper limit that theoretically could be reached.

SUMMARY

Summarizing it can be said that the manganese oxides in contact with dilute aqueous solutions containing different electrolytes adsorb the cations mainly by non-equivalent ion exchange adsorption, however, the possibility of equivalent adsorption and chemical reactions on the surface are presumably not out of question. The quantity of ions adsorbed by the manganese oxides is not negligible, especially taking into consideration that the processes occuring first on the surface may be extended over the whole of the adsorbent and processes like topochemical reactions may be assumed. The quantity of ions adsorbed by the different manganese oxides may be compared to that determined in the different natural manganese oxide minerals. In respect of certain ions and manganese oxides, respectivelly, a specific adsorption ability could be established.

ACKNOWLEDGMENT

The writers are indebted to MR. Á. KOVÁCH and MRS. HUSZTI for the radiochemical control measurements and for their comments. Thanks are also due to MR. J. HIRES and MR. N. MAREK for carrying out the infrared spectra and to MRS. I. KISPÉTER and MR. Á. BERTALAN for their kind assistance in the laboratory work.

REFERENCES

GATTOW, G. and O. GLEMSER [1961a]: Darstellung und Eigenschaften von Braunsteinen. II. (Die γ- und η-Gruppe der Braunsteine.) — Z. f. anorg. u. allgem. Chem. *309*, p. 20—36.

GATTOW, G. and O. GLEMSER [1961b]: Darstellung und Eigenschaften von Braunsteinen. III. (Die ε-, β- und α-Gruppe der Braunsteine, über Ramsdellit und über die Umwandlungen der Braunsteine). — Z. f. anorg. u. allgem. Chem. *309*, p. 121—150.

GOLDBERG, EDWARD D. [1954]: Marine Geochemistry 1. Chemical Scavangers of the Sea. — Journ. Geol. *62*, 249—265.

HEWETT, D. F. and MICHAEL FLEISCHER [1960]: Deposits of the Manganese Ores. — Econ. Geol. *55*, 1—55.

KOZAWA, AKIYA [1959]: On an Ion-Exchange Property of Manganese Dioxide. — Journ. Electrochem. Soc. *106*, 552—556.

KRAUSKOPF, K. B. [1956]: Factors Controlling the Concentration of Thirteen Rare Metals in Sea Water. — Geochim. Cosmochim. Acta, *9*, 1—33.

LANGE, BRUNO [1942]: Kolorimetrische Analyse. — Verlag Chemie, Berlin.

Михеев, В. И. [1957]: Рентгенометрический определитель минералов. — Госгеолтехиздат, Москва.

MOENKE, H. [1962]: Mineralspektren. — Akademie-Verlag, Berlin.

MÜLLER, GERMAN [1967]: The HCl-soluble Iron, Manganese, and Copper Contents of Recent Indian Ocean Sediments off the Eastern Coast of Somalia. — Mineralium Deposita *2*, 54—61.

NEMECZ, E. [1960]: Report on the Investigations of the Manganese Carbonate Ores of Úrkút. — Manuscript, in Hungarian.

PŘIBIL, R. [1961]: Komplexone in der chemischen Analyse. — VEB Deutscher Verlag der Wissenschaften, Berlin.

ROY, SUPRIYA [1966]: Syngenetic Manganese Formations of India. — Jadavpur University, Calcutta.

SNELL, F. D. and CORNELIA T. SNELL [1951]: Colorimetric Methods of Analysis. — D. Van Nostrand Co., Inc. New York.

WADSLEY, A. D. [1950]: A Hydrous Manganese Oxide with Exchange Properties. — J. Am. Chem. Soc. *72*, 1781—1784.

WEDEPOHL, K. H. [1960]: Spurenanalytische Untersuchungen an Tiefseetonen aus dem Atlantic. — Geochim. et Cosmochim. Acta *18*, 200—231.

WEDEPOHL, K. H. [1961]: Natürliche Vorkommen und Geochemie von Höherwertigen Manganoxyden. — Batterien *15*, Nr. 3, 4. 4.

PROF. DR. GYULA GRASSELLY
MISS MAGDOLNA HETÉNYI
Institute of Mineralogy, Geochemistry
and Petrography
Attila József University at Szeged
Táncsics M. u. 2.
Szeged, Hungary

POTASSIUM METASOMATISM IN THE NEIGHBOURHOOD OF MÁTRASZENTISTVÁN (W-MÁTRA MOUNTAINS)

J. MEZŐSI

Institute of Mineralogy, Geochemistry and Petrography,
Attila József University, Szeged

ABSTRACT

In the W-Mátra Mountains, S from Mátraszentistván the Lower-Tortonian andesite series underwent potassium metasomatism to a considerable extent. The plagioclase feldspar of the sometimes compact, sometimes porous but owing to the marked silicification always resistant rock has been replaced by sanidine, easily identified by X-ray investigations. In the course of metasomatism the extent of silicification is so marked that in certain places instead of feldspar even quartz varieties are to be found. The cavities are covered by quartz and chalcedony, rarely by tridymite.

On the N parts of Mátra peaks the medial dacite tuff, appearing on the Helvetian-Tortonian boundary, is missing, here probably the andesite series is also settled immediately upon the Helvetian marly aleurite, thus likely the Burdigalian acidic detrital vulcanic substance may serve as a potassium source for the endometamagmatic potassium metasomatism.

OCCURRENCE

In the course of the detailed study of our mountainous regions newer and newer metasomatic areas are discovered. Such areas in Tokaj Mountains are mentioned by MRS. V. FUX—SZÉKY [1964], K. MÁTÉ—VARGA [1961], in Mátra Mountains by J. KISS [1960], I. KUBOVICS [1966], GY. VARGA [1959], and A. VIDACS [1962].

The mapping showed that the Lower-Tortonian andesite which had suffered metasomatism occurs in the surrounding of the 821,6 m altitude encircled by the streams Narád and Hutahely in W-Mátra, S from Mátraszentistván [J. MEZŐSI, 1968]. In the neighbourhood a younger, dark grey unaltered andesite, the so called capping-andesite is to be found, which closes the Helvetian-Tortonian volcanism. The sketching map *(Fig. 1)* yields some information on the geological built up of this territory.

In the W part of the occurrence on a lower terrain markedly siliceous rock can be found in large blocks. Its colour varies widely: whitish grey, pink, reddish grey, violet grey. Very often it contains smaller cavities with a few mm quarz crystal-

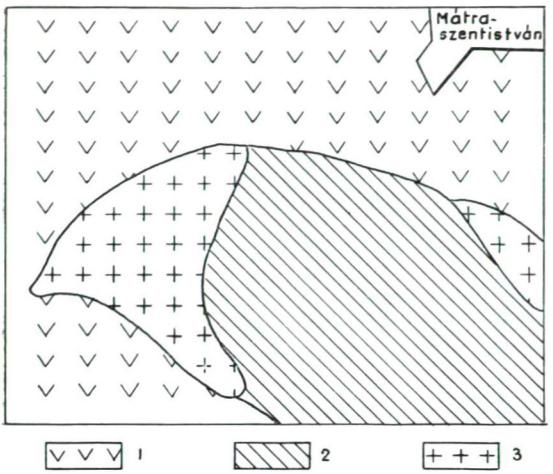

Fig. 1. Geological sketching map of the field investigated.
1. Lower-Tortonian andesite
2. Lower-Tortonian andesitogeneous potassium trachyte
3. Lower-Tortonian capping-andesite

groups or sometimes chalcedony in them. Among the surface rocks strongly leached, stripped rock debris occurs as well, appearing to be a part of some vein, however it does not contain ore minerals. It is especially easy to see in the violet grey rock that merely feldspar occurs in porphyritic form, traces indicating columnar pyroxene can be scarcely found. Owing to the too markde alterations the original texture in the case of the whitish grey rock cannot be detected at all.

Round the 821,6 m altitude a rock similar to the former type appears also in larger blocks, sometimes in stone rivers. In the cavities there are trigonal quartz crystals even as large as 1 cm. At places weak pyrite impregnation can be observed. Quartz crystals sometimes are covered by limonite crust of 1 mm thickness. In the debris similarly striped, chalcedony-opal vein fragments occur, however, without ore minerals. In some vein fragments rarely exsolutions indicating carbonate minerals are observed.

The hypocrystalline structure is well observable by microscopy. The columnar, mostly idiomorphic feldspar of 1—2 mm is always well separated from the matrix. Finer textural variations, however, could not be recognized, owing to the extensive silicification. Feldspar microlites are often replaced by SiO_2 variations *(Fig. 2)*, in some cases the matrix is completely impregnated by the SiO_2 variety *(Fig. 3)*.

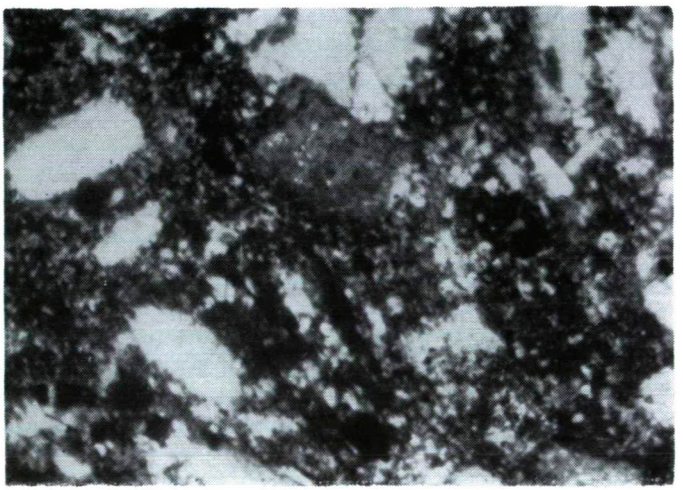

Fig. 2. Feldspar microlites replaced by chalcedony.
Crossed nicols, × 120.

The ore and femic microlites are completely dissolved in the matrix, and are replaced by limonite globules, or rarely by radial-fibrous aggregates of goethite. Unaltered magnetite, pyrite could not be found in the samples investigated, only some traces can be supposed. On the wall of smaller cavities, fissures first of all a thin crust of limonite globules appear then chalcedony follows — sometimes it completely fills the cavity.

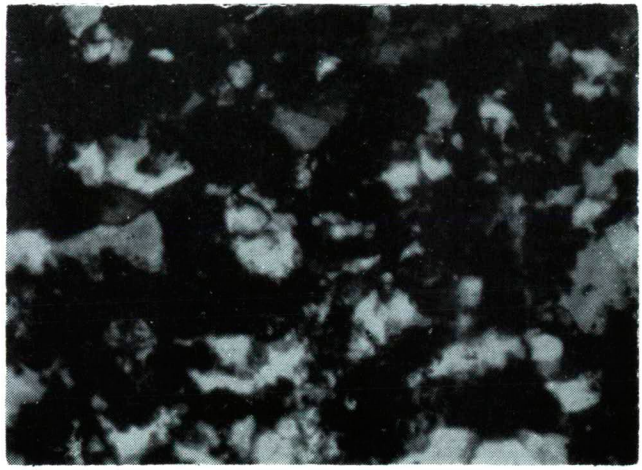

Fig. 3. Matrix of andesitogeneous potassium trachyte impregnated by chalcedony. Crossed nicols, × 120.

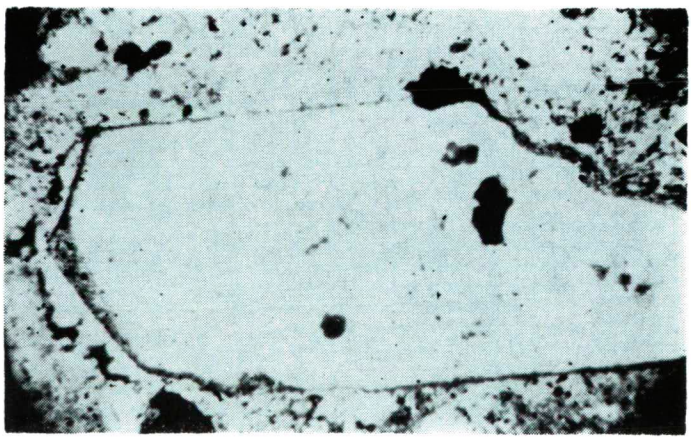

Fig. 4. Silicified feldspar with ramifying ore veinlet. Parallel nicols, × 90.

It is well known that the oxygen activity depends on the alkali content of the solutions. In the case of potassium metasomatism since iron has a higher oxidation degree, all the minerals, containing Fe^{2+}, are displaced. According to SCHELLMAN's investigations [1959], at pH 4—5 or in presence of Mg^{++} or Ca^{++} hematite is formed

already at usual temperature, and in presence of SO_4^{2-} goethite, in the neutral region. It is an explanation of the fact that in these rocks the above minerals can be found instead of magnetite. Hematite plays a role in the colouring of the rocks, too.

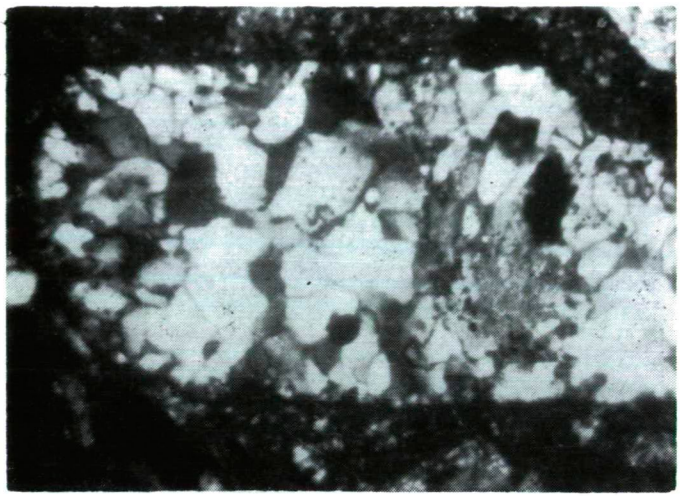

Fig. 5. Totally silicified feldspar.
Crossed nicols, × 90.

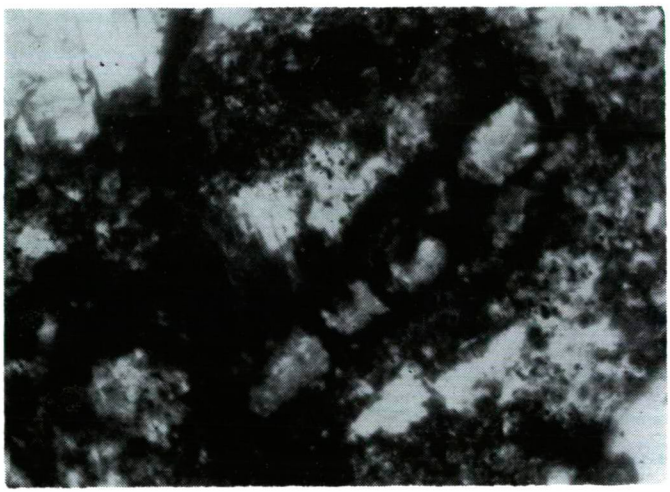

Fig. 6. Mineralized hypersthene.
Parallel nicols, × 60.

Original feldspar phenocrysts were mostly of columnar habit. Twinning and zonal development have either faded or completely disappeared, so their kind cannot be accurately determined in an optical way. In the initial stage of the alteration the crystal becomes mottled. A similar phenomenon has been experienced by

MRS. FUX—SZÉKY [1964] and KUBOVICS [1966] in feldspars of andesites suffered metasomatism. In other cases feldspar is completely replaced by quartz *(Figs. 4* and *5)*. In this case the amount of the ore mineral is minimal in the rock and a thin ore frame is to be found at the border of feldspar.

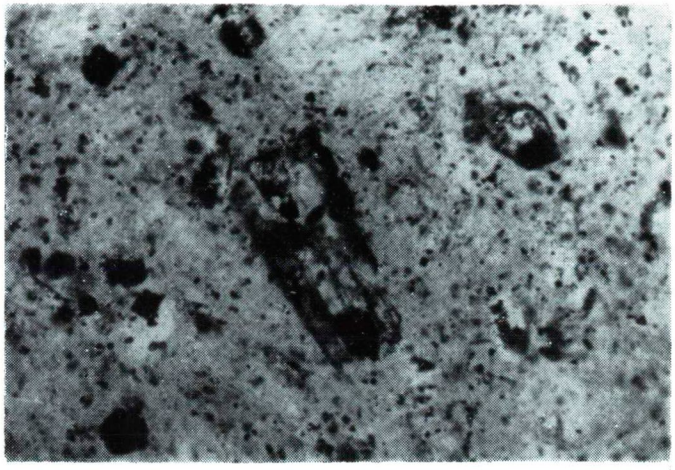

Fig. 7. Mineralized and seladonitized pyroxene.
Parallel nicols, × 90.

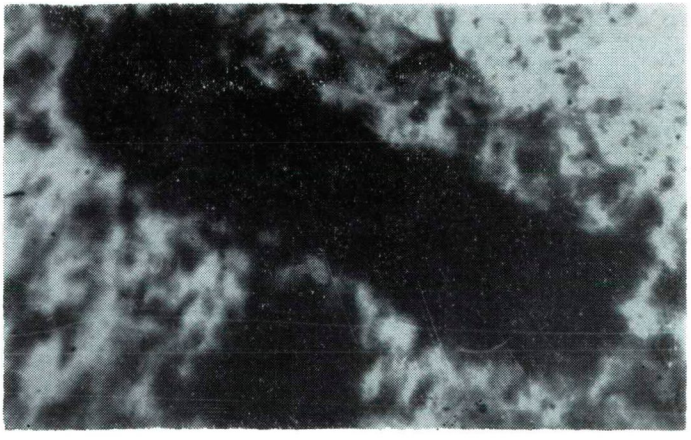

Fig. 8. Place of pyroxene crystal filled by limonite.
Parallel nicols, × 120.

In its present state the rock does not contain unaltered pyroxene, but its traces are detectable. When only mottled feldspars are observable in the rock, seladonite or perhaps a few quartz appear in the place of dark constituents. Sometimes the columnar pyroxene crystal is surrounded by an ore frame and even the cleavage directions parallel to the 001 plane are marked by limonite *(Figs. 6* and *7)*. Some-

times in the places of smaller crystals pseudomorphs consisting of limonite globules are found *(Fig. 8)*.

At larger cavities it is easy to observe that quartz crystal groups of trigonal habit are settled on chalcedony, on the walls of cavities *(Fig. 9)*.

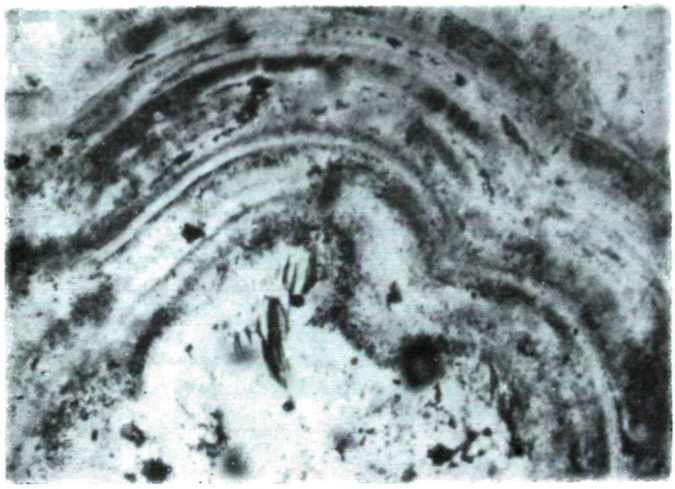

Fig. 9. Silica gel rhythmically separated.
Parallel nicols, × 30.

CHEMICAL INVESTIGATIONS

In view of the marked alterations the SiO_2 and alkali content of some of the samples has been investigated. Results are summarized in Table 1.

Table 1

Sample number	Description of sample	SiO_2	Na_2O	K_2O
1.	pink compact rock	64,34%	0,35%	7,11%
2.	faded pink compact rock	n.d.	0,10	7,29
3.	greyish white compact silicic rock	96,37	0,14	0,19
4.	compact flint rock	n.d.	none	none
5.	greyish yellow porous rock	n.d.	0,10	8,10
6.	light pink porous rock	n.d.	0,25	7,90
7.	rock of flesh-red colour	n.d.	0,20	7,91
8.	pink compact rock	n.d.	0,20	7,30
9.	pink, slightly porous rock	n.d.	0,20	7,90
10.	violet greyish rock,	n.d.	1,12	7,85
11.	unaltered Lower-Tortonian pyroxene andezite in the neighbouring territory	57,19	2,78	2,47

n. d. = not determined

The alkali percentage of rocks suffering potassium metasomatism in the Tokaj and Mátra Mountains are summarized in Table 2.

Table 2

	1.	2.	3.	4.	5.	6.	7.	8.
SiO_2	65,25%	65,20%	65,93%	68,75%	57,76%	57,39%	62,08%	67,92%
Na_2O	3,56	0,48	2,25	1,18	2,62	0,36	0,81	0,57
K_2O	6,07	9,67	6,00	4,36	7,82	11,28	11,69	11,27

1. Hidegkút Mt. According to I. KUBOVICS
2. Fekete-Lake. According to GY. VARGA
3. Világos Mt. According to A. VIDACS
4. SE from Világos Mt. According to A. VIDACS
5. Aranybánya-flow. According to J. KISS
6. Telkibánya, 2. drilling. According to MRS. FUX—SZÉKY
7. Telkibánya, peak Nagyhasdat. According to MRS. FUX—SZÉKY
8. Rudabányácska, Mt. Nagyszava. According to MRS. K. VARGA—MÁTÉ

The results show that both in the Mátra and Tokaj Mountains the alkali content as compared with the unaltered rock suffered considerable changes. The prevalent plagioclase feldspars were displaced in the course of metasomatic processes and were replaced by potassium feldspars. According to KORZSINSZKIJ [1965] in the intermediary rocks first alter the plagioclases and the femic components, the Ca^{++} and Mg^{++} content is displaced. Thereafter alkalies (Na^+ and K^+) are dissolved. The acting hydrothermal solutions were very rich in potassium and silicic acid, thus the Si/Al substitution and the degree of order, respectively, were changed too, together with the original triclinic feldspar structure. With the progress of Si/Al substitution a monoclinic structure developed.

X-RAY INVESTIGATIONS

Owing to the marked changes the kind of secondarily formed alkali feldspar could not be decided by microscopy. In view of earlier data in literature, partly formation of sanidine and partly of adularia has been pointed out in the course of metasomatism. Thus X-ray diffraction patterns of samples (except sample N° 6) enlisted in Table 1, were prepared with Cu Kα-radiation and Ni filter. Data are summarized in Table 3.

On the basis of microscopical investigations the strikingly large amount of SiO_2 varieties was surprising. A large part of this was chalcedony, a smaller low-quartz. Tridymite was possible to be pointed out merely in the greyish yellow porous rock No. 5. Cristobalite was absent in all the samples. According to FLÖRKE's studies [1954] carried out at higher temperatures the presence of K^+, starting from silica gel leads to formation of tridymite. It is likely that the lack of cristobalite was due to the presence of high K^+ content.

By microscopic investigations it could not be decided which mineral is the high K_2O content-bearing one. Therefore for sake of comparison X-ray patterns of pure sanidine and adularia have been taken. Since data of adularia could not be recognized in the material investigated, Table 4 does not contain them.

Table 4 shows that concerning the sanidine there is a fairly good agreement with data in literature, however, the number of values indicating plagioclase feldspar

is low. According to WRIGHT's investigations [1968] from 2Θ angles belonging to *d* values corresponding to the reflexions (201), (060) and (204) it is possible to estimate the amount of Or molecules. Data suggest 70 per cent Or content what is in harmony with results of chemical analysis.

Taking into consideration SZÁDECZKY-KARDOSS's principles of rock systematization, the Mátraszentistván andesitogeneous potassium trachyte can be regarded as an endometamagmatic formation where the original orthomagmatite was altered by solutions moving upwards through breaks and fissures. The strike of this trend is near to NW-SE thus is in agreement with trends around Nagybátony and with the direction of the tectonic valley of the upper part of Csörgő stream. Regarding that the Mátraszentistván mineralized area is near, (about 2—3 km,) by all probability the formation of this metasomatic area can be coupled with Gyöngyösoroszi mineralization both in respect of time and place. This is also indicated by spectrographic data showing that each sample contained Pb and Zn most of them Sb as well.

The considerably large amount of potassium moving towards the surface together with the solutions can be derived from Burdigalian „lower rhyolite tuff", since in Mátraszentistván the middle dacite-tuff is lacking, the Lower-Tortonian andesite series is deposited direct on the Helvetian marly aleurite. Further migration of potassium during metasomatism, the mechanism of displacement of Na^+ and Ca^{++} ions hat already been cleared by SZÁDECZKY-KARDOSS's investigations.

REFERENCES

BAMBAUER, H. U., M. CORLETT, E. EBERHARD and K. VISWANATHAN [1967]: Diagrams for the determination of plagioclases using X-ray powder methods. — Schweizerische min. und petr. Mit. *47*, p. 333.

BAMBAUER, H. U., E. EBERHARD and K. VISWANATHAN [1967]: The lattice constants and related parameters of plagioclases (low). — Schweizerische min. und petr. Mitt. *47*, p. 351.

BAMBAUER, H. U., F. LAVES [1960]: Zum Adularproblemen I. — Schweizerische min. und petr. Mitt. *40*, p. 177.

BÖHMER, M. [1961]: Relations between potassium trachytes, rhyolites and mineralization in the Kremnica ore field. — Geol. Práce Zosit *60*, p. 319.

FIALA, F., ZD. PÁCAL [1959]: Nekolik geochemických pozámek o kyselých diferenciáltech neovulkanitu v. Kremických horách. — Geol. Práce Zosit *54*, p. 5.

FLÖRKE, O. W. [1954]: Der Einfluss der Alkaliionen auf die Kristallisation des SiO_2. — Geologie *3*, p. 71.

GIUŞCĂ, D. [1961]: Die Adularisierung der Vulkanite in der Gegend von Baia Mare. — Acta Geologica *VII*, p. 173.

GOODYEAR, J. and W. J. DUFFION [1954]: Identification of plagioclase felspars by the X-ray powder methods. — Miner. Mag. *30*, p. 306.

KISS, J. [1960]: A new ore occurrence in the environment of Nagygalya, Nagylipót and Aranybányafolyás Mátra Mountains NE Hungary. — Annal. Univ. Sci. Budapestiensis de R. Eötvös nominatae. Sec. Geol. Tom. *III*, p. 55.

KORZSINSZKIJ, D. S. [1965]: Abriss der metasomatischen Prozesse. — Akad. Verlag, Berlin.

KUBOVICS, I. [1966]: A kálimetaszomatózis szerepe a nyugat-mátrai ércképződésben. — Földt. Közlöny *96*, p. 13.

MEZŐSI, J. [1968]: Földtani magyarázó a szorospataki térképlaphoz. Manuscript.

NEMECZ, E., GY. VARJÚ [1963]: Na-bentonit, klinoptilolit és káliföldpát képződése a Szerencsi öböl riolittufájából. Földt. Közlöny *93*, Anyagásvány füzet. p. 77.

ORVILLE, P. M. [1967]: Unit-cell parameters of the microcline-low albite and the sanidine-high albite solid solution series. — The Amer. Min. *52*, p. 55.

DE SÁENZ, I. M. [1967]: Alkali feldspar crystallisation under conditions from pneumatolytic, hydrothermal and diagenetic environments. — Schweizerische min. und petr. Mitt., *67*, p. 87

SCHELLMANN, V. [1959]: Experimentelle Untersuchungen über die sedimentäre Bildung von Goethit und Hämatit. — Chemie der Erde *20*, p. 104.

SZÁDECZKY-KARDOSS, E. [1958]: A vulkáni hegységek kutatásának néhány alapkérdéséről. — Földt. Közlöny *88*, p. 171.

Table 3

1.		2.		3.		4.		5.		7.		8.		9.		10.	
d	I	d	I	d	I	d	I	d	I	d	I	d	I	d	I	d	I
		6,654												6,628	1		
		6,531	1							6,580	1					6,531	1
								6,064	1	6,126	1						
		5,983	1							5,962	1	5,893	1	5,943	1		
								4,926	1								
						4,704	1	4,768	1								
		4,504	1					4,515	1								
		4,299	4					4,309	7			4,309	4				
4,268	5					4,247	8			4,279	5			4,268	3	4,247	3
				4,160	9												
3,966	1	3,993	1					3,985	2	3,958	1	3,985	1	3,958	1	3,941	1
3,791	3	3,832	5					3,832	5	3,800	4	3,816	3	3,800	3	3,784	5
						3,698	1			3,720	1					3,690	1
		3,653	1	3,616	1			3,661	1	3,631	1	3,662	1	3,631	1	3,660	1
		3,581	1							3,588	1						
		3,498	2					3,504	3			3,491	2				
3,465	2									3,477	3			3,477	2	3,456	3
3,344	10	3,344	10			3,344	10	3,374	10	3,356	10	3,356	10	3,350	10	3,325	10
3,229	8	3,241	8	3,277	10			3,277	6	3,247	7	3,252	6	3,252	5	3,224	10
								3,259	6		3						
2,997	2	3,011	4					3,026		3,006		3,026	2	3,006	2	2,986	3
2,907	1	2,920	2					2,939	3	2,907	2	2,935	1	2,920	1	2,892	2
2,778	1	2,778	1					2,795	2	2,822	1	2,795	1				
		2,650	1						1	2,770	1			2,775	1	2,762	1
2,608	1															2,697	1
2,591	2	2,584	2					2,598	2	2,591	2	2,598	1	2,584	1	2,584	2
2,552	1															2,527	1
2,527	1											2,473	1	2,460	1		
2,466	1	2,454	1	2,477	4	2,460	4	2,473	1								
		2,391	1					2,407	1	2,403	1			2,323	1		
		2,280	1	2,295	4	2,291	3	2,297	1	2,291	1	2,297	1	2,280	1		
		2,229	1	2,250	2	2,244	2			2,247	1	2,252	1	2,239	1		
2,174	2	2,159	2					2,182	1	2,179	1	1,182	1	2,169	2	2,167	2
2,133	1	2,116	1	2,140	3	2,136	3	2,140	1	2,140	1	2,150	2	2,128	1	2,126	1
2,017	1	2,005	1					2,022	1	2,022	1	2,024	1	2,011	1	2,013	1
1,984	1	1,976	1	1,992	2	1,984	2	1,988	1	1,988	1	1,980	1	1,976	1	1,980	1
		1,964	1														
		1,921	1									1,936	1	1,928	1	1,938	1
		1,880	1									1,858	1	1,850	1	1,851	1
1,823	1	1,837	1	1,829	9	1,823	8	1,825	2	1,829	1	1,823	1	1,817	1		
1,802	1	1,803	1					1,803	1	1,807	1	1,803	1	1,796	2	1,800	2
		1,782	2														
1,676	1	1,654	1	1,680	2	1,676	2	1,674	1	1,680	1	1,674	1	1,671	1		
		1,621	1														
1,545	1			1,550	5	1,543	4	1,543	2	1,548	1	1,544	1	1,543	1	1,578	1
1,503	1	1,522	1					1,500	1	1,510	1	1,501	1	1,501	1	1,505	1
		1,480	1	1,457	1	1,454	1					1,458	1			1,457	1
		1,430	1									1,440	1	1,440	1		
		1,421	1														
1,384	1			1,385	2	1,381	3	1,386	1	1,387	1	1,388	1	1,385	1		
1,376	1	1,369	1	1,378	4	1,373	4	1,378	1			1,379	1	1,376	1		
		1,357	1														
				1,291	1	1,287	1			1,299	1			1,291	1		
		1,273	1														
		1,261	1	1,259	1	1,256	1	1,260	1	1,267	1						
				1,229	1	1,228	1										
				1,201	1			1,201	1								
				1,183	1												
		1,153	1	1,154	1												
				1,083	1												
				1,048	1												
				1,047	1												
				1,037	1												
				1,018	1												
				0,979	1												
				0,963	1												
				0,917	1												

Table 4

1.		2.		3.		4.		5.		6.		7.		8.		9.		10.		11.	
d	I	d	I	d	I	d	I	d	I	d	I	d	I	d	I	d	I	d	I	d	I
6,555	1			6,65	0,6					6,580	1									6,531	1
6,483	1	6,37		6,51	0,9	6,48	2														
		5,85		5,869	0,9	5,806	0,3			5,983	1			5,962	1	5,893	1				
		4,59								4,504	1	4,515	1								
4,188	2			4,241	5	4,118	2,5					4,075	1	4,169	1			4,121	1		
				3,947	2			3,966	1	3,993	1	3,935	1	3,958	1	3,985	1	3,958	1		
3,923	1	3,86		3,870	0,3	3,880	1,2													3,941	1
3,776	3	3,74		3,789	8	3,746	3,5	3,791	3											3,784	5
3,595	1	3,59		3,623	1,5	3,600	0,4											3,631	1		
				3,557	1,2																
3,465	2	3,49		3,459	5	3,453	1,2	3,465	2					3,477	3			3,477	2	3,456	3
				3,328	10																
				3,287	6																
3,241	10	3,24		3,258	3,5	3,245	10,0	2,229	10	3,241	8	3,259	6	3,247	7	3,252	6	3,252	5		
				3,223	8	3,212	4,0													3,224	10
2,997	2	3,00		2,995	5			2,997	2	3,011	4			3,006	3	3,026	2	3,006	2	2,986	3
		2,96		2,932		2,962	1,2					2,939	2			2,935	1				
2,910	2	2,92		2,905	2	2,900	1	2,907	1	2,920	2			2,907	2			2,920	1		
		2,88		2,889																	
2,770	1	2,77		2,766	1,5	2,757	0,5	2,778	1	2,778	1	2,795	1	2,770	1	2,795	1	2,775	1	2,762	1
		2,61		2,608				2,608	1												
2,582	2			2,582	3			2,591	2	2,584	2	2,598	2	2,591	1	2,598	1	2,584	1	2,584	2
		2,52				2,547	1,5														
						2,50	0,4														
2,422	1	2,44				2,41	0,4							2,403	1						
2,373	1	2,34				2,334	0,3											2,323	1		
		2,30												2,291	1	2,297	1	2,280	1		
		2,21								2,229	1										
2,174	3	2,18		2,171	2	2,161	3	2,174	1	2,159	2	2,179	1	2,179	1	2,182	1	2,169	2	2,167	1
		2,12						2,133	1	2,116	1							2,128	1	2,126	1
		2,09																			
2,064	1	2,06																			
2,000	1							2,017	1	2,005	1	2,022	1	2,022	1	2,024	1	2,011	1	2,013	1
1,967								1,984	1	1,976	1	1,988	1	1,988	1	1,980	1	1,976	1	1,980	1
1,911	1	1,93								1,921	1					1,930	1	1,928	1	1,938	1
1,853	1	1,82						1,823	1			1,825	1	1,829	1	1,823	1	1,850	1	1,851	1
		2,81												1,807	1			1,817	1		
1,800	2	1,80		1,793				1,802	1	1,803	1	1,803	1			1,803	1	1,796	2	1,800	1
1,767	1																				
		1,70																			
1,626	1	1,64								1,621	1										
		1,63																			
		1,59																			
1,565	1	1,57						1,545	1			1,54	2	1,548	1	1,544	1	1,543	1	1,578	1

Samples of Table 4 are as follows:

1. Sanidine, Vesuvio [WRIGHT, 1968]
2. Sanidine, Vesuvio [WRIGHT, 1968]
3. ASTM 10—353.
4. ASTM 10—357.
5. Mátraszentistván 1.
6. Mátraszentistván 2.
7. Mátraszentistván 5.
8. Mátraszentistván 7.
9. Mátraszentistván 8.
10. Mátraszentistván 9.
11. Mátraszentistván 10.

SZÁDECZKY-KARDOSS, E. [1959]: Über die Migrationserscheinungen magmatischer und metamorpher Gesteinsbildungsprozesse. — Freiberger Forschungsh. *58*, p. 66.
SZÁDECZKY-KARDOSS, E., A. VIDACS, K. VARRÓ [1959]: A Mátra hegység neogén vulkanizmusa. - MTA. Geokémiai Konf. Munk.
SZÉKY-FUX, V. [1964]: Propilitesedés és kálimetaszomatózis Tokaji hegységi vizsgálatok tükrében. — Földt. Kötlöny *94*, p. 409.
VARGA, GY. [1959]: Részjelentés a Nagygalya környéki földtani térképezésről. Manuscript.
VARGA-MÁTÉ, K. [1961]: Kálimetaszomatózis és kálium feldúsulás a Sátoraljaújhely és Kovácsvágás közti területen. Földt. Közlöny *91*, p. 391.
VIDACS, A. [1962]: A Mátra hegység radiológiai vizsgálata. MÁFI Évi jelentés az 1959. évről. p. 63.
WRIGHT. TH. L. [1968]: X-ray and optical study of alkali felspar: II. An X-ray method for determining the composition and structural state from measurement of 20 values for three reflections. — Amer. Miner. *53*, p. 88.

DOC. DR. JÓZSEF MEZŐSI
Institute of Mineralogy, Geochemistry
and Petrography
Attila József University at Szeged
Táncsics M. u.2.
Szeged, Hungary

TECTONIC CONTROL OF SEDIMENTATION IN THE UPPER PANNONIAN SECTION OF A BOREHOLE AT MACS, GREAT HUNGARIAN PLAIN, HUNGARY

B. MOLNÁR

Institute of Geology, Attila József University, Szeged

INTRODUCTION

The Upper Pliocene (Levantine) sequence is absent at many places below the Pleistocene fluviatile and eolian formation of the Great Hungarian Plain, so that the Pleistocene is immediately underlain by the Pannonian stage representing the earlier Pliocene.

In the Great Plain basin the upper boundary of the Upper Pannonian sequence is at very different depths (0 to 800 m). On the edges of the basin, however, the Upper Pannonian is represented even at 400 m height a.s.l. or more. Considering the average 100-m elevation a.s.l. of the Great Hungarian Plain, this would mean

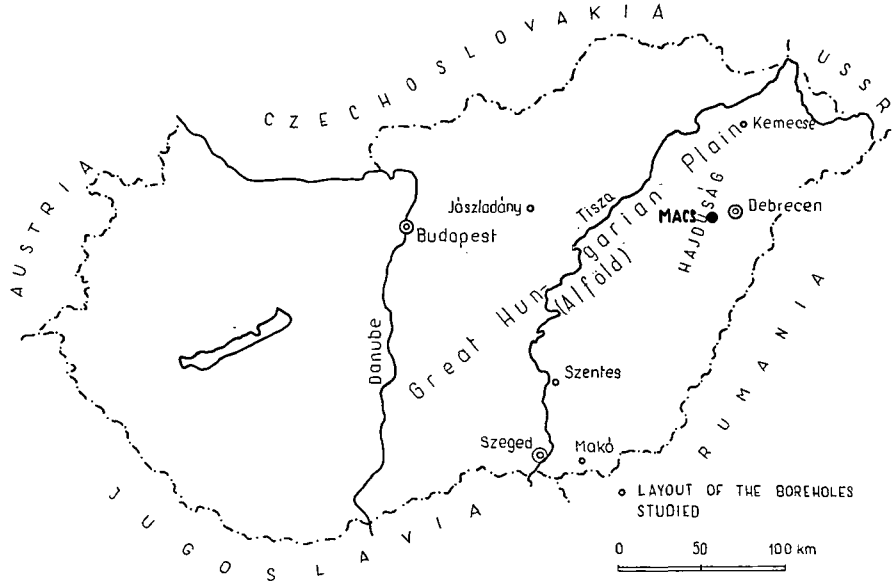

Fig. 1. Layout

some 1100 m of difference in elevation as a maximum caused by heavy post-Pannonian tectonic movement.

In the north part of the Great Plain, the Hajdúság, there is a structurally higher-perched Pannonian table-land; hence, the Hajdúság is an area, where the upper surface of the Pannonian sequence lies close to the present-day surface [M. ERDÉLYI, 1962; B. MOLNÁR, 1966] *(Fig. 1)*. Several investigators of the Hajduság's geology have realized that it differs in character from the surrounding area [GY. ÉBÉNYI—E. R. SCHMIDT, 1931, 1938, 1939; K. FERENCZ, 1956; I. FERENCZI, 1939—1940; L. KŐRÖSSY, 1956; I. DOBOS, 1953; A. RÓNAI, 1955; J. SÜMEGHY, 1944; P. SZÓFOGADÓ, 1958; J. URBANCSEK, 1953]. As regards the Pleistocene sedimentary sequence, this difference is known as a result of the exhaustive study of the Pleistocene member of the Macs borehole [M. ERDÉLYI, 1962; B. MOLNÁR, 1966] *(Fig. 1—2)*. The nearly 50-m-thick Pleistocene sequence here has proven eolian, in contrast with the fluviatile filling of the surrounding area. Within the sequence, ten (*Fig. 2.* I—X.) phases of loess deposition, a minimum of six phases of soil genesis, and five interlayers of wind-blown sand can be distinguished (see simplified profile in *Fig. 2*). The eolian sequence could be deposited thank to the high-perched position of the Hajdúság against its background in Pleistocene time, a reason why fluvial accumulation was impossible here and only eolian sediment was deposited.

Core-drilled by the staff of the Hungarian Geological Institute between 1958 and 1959, the borehole at Macs traversed, beside the above-mentioned Pleistocene eolian sequence, an additional 453 m of Upper Pannonian sediment [M. ERDÉLYI, 1962]. The interesting geological setting of the Hajdúság within the Great Plain basin required — and the reliability of the drill-core material enabled — the Pannonian sequence to be also examined in detail.

The megascopic description of the material could already reveal that the Upper Pannonian here had been deposited in a shallow lake — mainly marshy environment [M. ERDÉLYI, 1962]. Accordingly, the Upper Pannonian lake was, in what is now the Hajdúság, generally shallower than in the rest of the basin. Thus, it can be supposed that the contemporaneous tectonic deformation of the area is readily reflected by the sedimentary sequence deposited that time.

Therefore, the purpose of the present investigation is to gain — by studying the Upper Pannonian sediments of the Macs borehole sunk in the Hajdúság — an understanding of the relationship between tectonic movement and sedimentation in the north part of the Great Plain.

The lithologic log of the Macs borehole of 501 m bottom hole depth (where the Upper Pannonian is represented by the interval of 48 to 501 m) and a considerable part of the analyses (grouped as A, B, C, and D in four parts) are shown in *Figs. 2—5*. In each figure, on the left side of the log, the elevation a.s.l. and the depths of drilling have been indicated. Additional explanation has been given in the legend *(Fig. 6)*.

SEDIMENTOLOGICAL REVIEW OF THE MACS BOREHOLE

Granulometric composition and its statistic evaluation

The lithologic log, recorded macroscopically, and then analysed for grain size composition, of the borehole is illustrated by *Figs. 2—5*. In the graphic representation, the finer-grained and darker sediments have been more densely, the coarser and lighter ones less densely hachured.

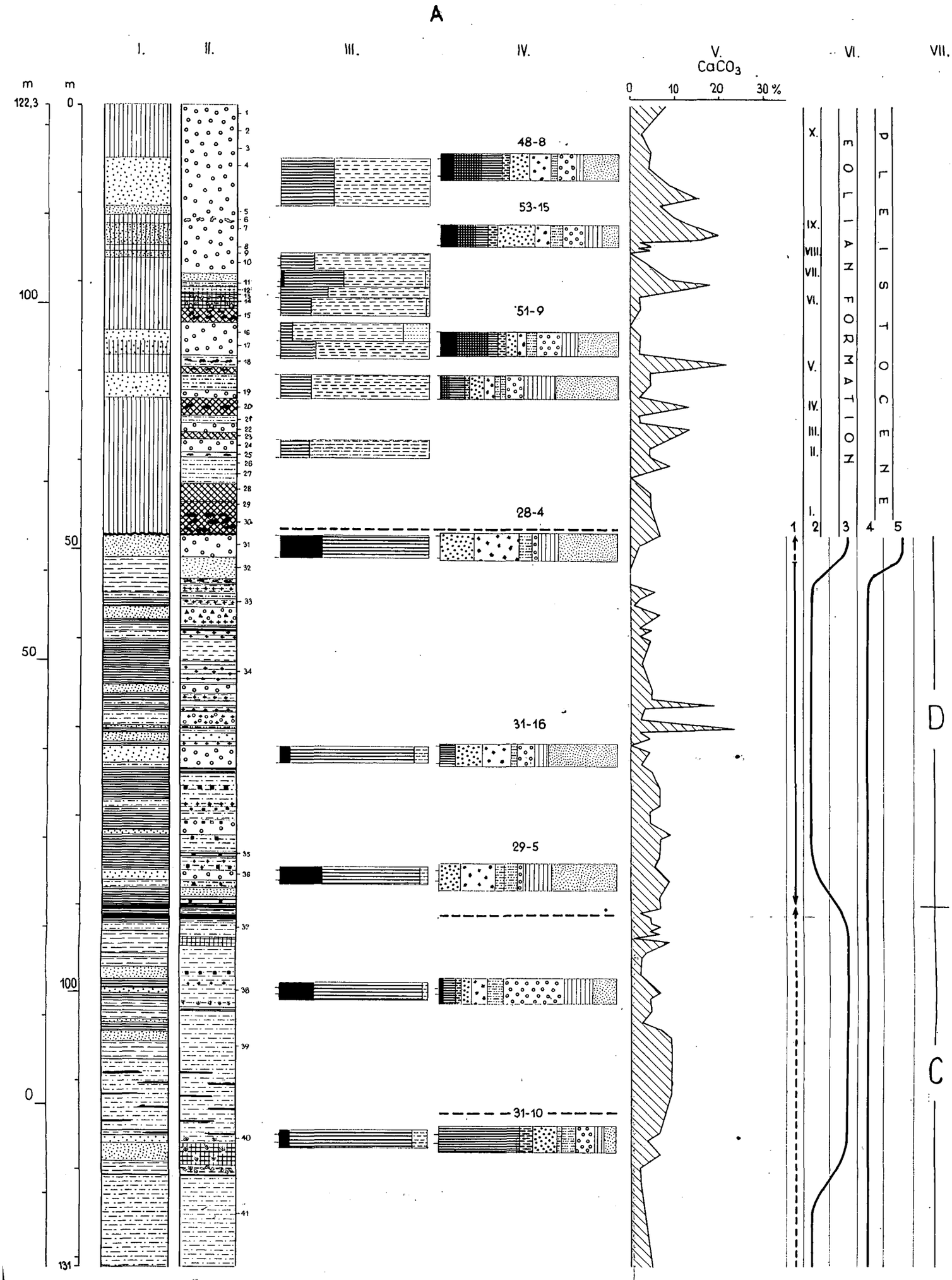

Fig. 2. Lithologic log of the Macs borehole, interval of 0 to 131 m

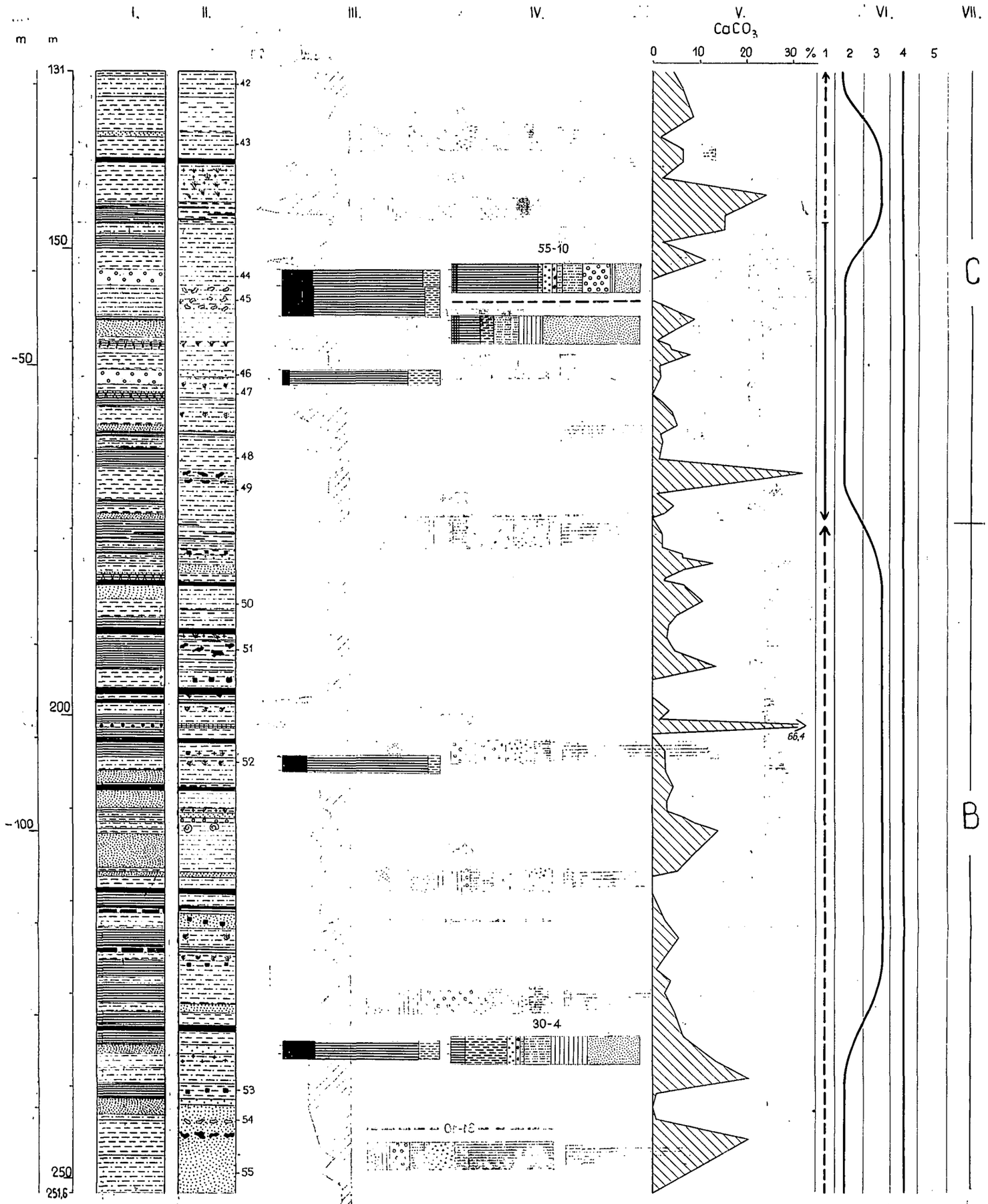

Fig. 3. Lithologic log of the Macs borehole, interval of 131 to 251,6 m

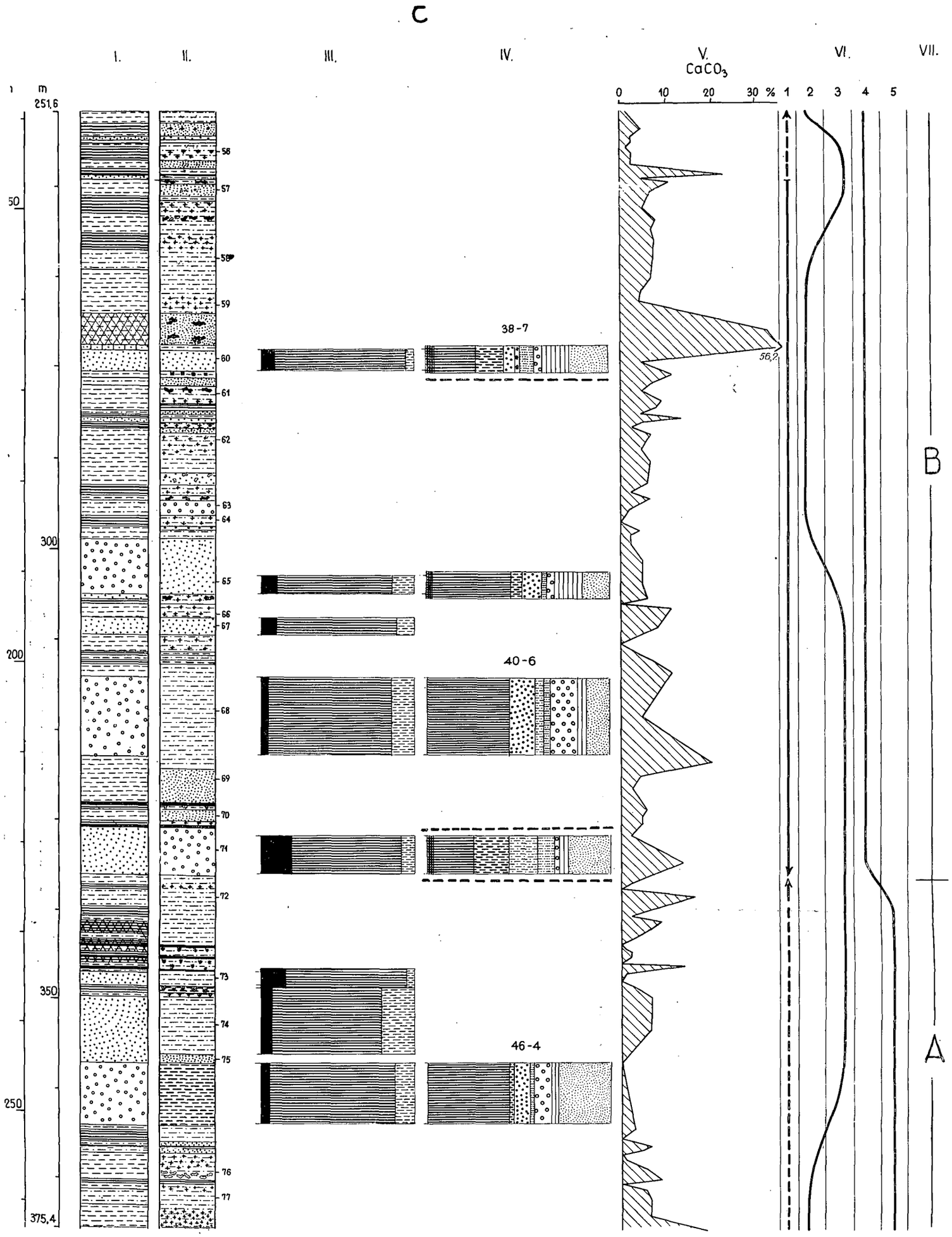

Fig. 4. Lithologic log of the Macs borehole, interval of 251,6 to 375,4 m

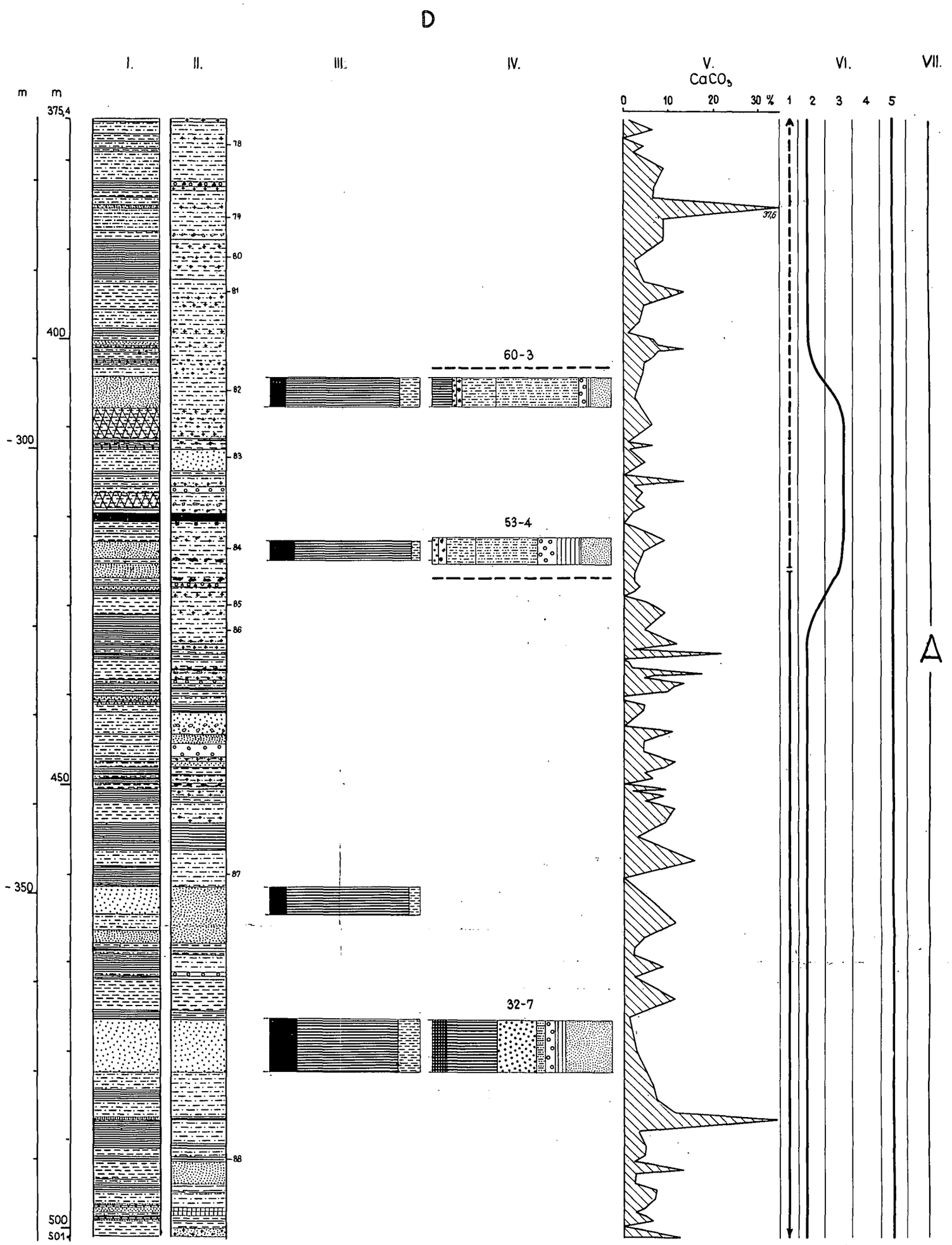

Fig. 5. Lithologic log of the Macs borehole, interval of 375,4 to 501 m

LEGEND

I. Lithologic composition

1 Clay <0,005 mm Ø
2 Fine silt 0,005-0,02 mm Ø
3 Coarse silt 0,02-0,06 mm Ø
4 Claystone (argillite) 0,005 > mm Ø
5 Mudstone (siltstone) 0,005-0,02 mm Ø
6 Loess 0,02-0,05 mm Ø
7 Loessic sediment
8 Fine sand 0,06-0,1 mm Ø
9 Small sand 0,1-0,2 mm Ø
10 Medium sand 0,2-0,5 mm Ø
11 Lignite
12 Lignite stringers
13 Shaly coal or carbonaceous shale
14 Limestone
15 Limonite
16 Flint (silica)
17 Sandstone

II. Colour, and changes in colour of the sediment

1 Yellow
2 Greyish-yellow
3 Brownish-yellow
4 Reddish-yellow
5 Yellowish-grey
6 Light grey
7 Brownish-grey
8 Greenish-grey
9 Medium grey
10 Dark grey
11 Black
12 Greyish-green
13 Green
14 Yellowish-brown
15 Brown
16 Reddish-brown
17 Brownish-red
18 Dark red
19 Chalk precipitate
20 Chalk concretions
21 Limonite mottles
22 Limonite concretions
23 Grey mottling
24 Yellow mottling
25 Plant remains
26 Gastropod shells

III. Grain shape

1 Sharp, splintery
2 Slightly rounded
3 Rounded
4 Intensively rounded

IV. Mineralogical composition

1 Hypersthene
2 Augite
3 Basaltic hornblende
4 Hornblende
5 Magnetite
6 Limonite
7 Biotite
8 Chlorite
9 Garnet
10 Other minerals
11 Weathered minerals
12 — — — Changes in source are

48-8 First group of numerals : feldspar factor
Second group of numerals : ratio of weathered minerals as referred to total minerals

V. $CaCO_3$ content

VI. Miscellaneous

I/a Phase of emergence
I/b Phase of subsidence
2 Lacustrine sedimentation
3. Near-shore sedimentation
4. Transgressive trend
5 Regressive trend

VII. Symbol of the cycle

Fig. 6. Legend to *Figs. 2 to 5*

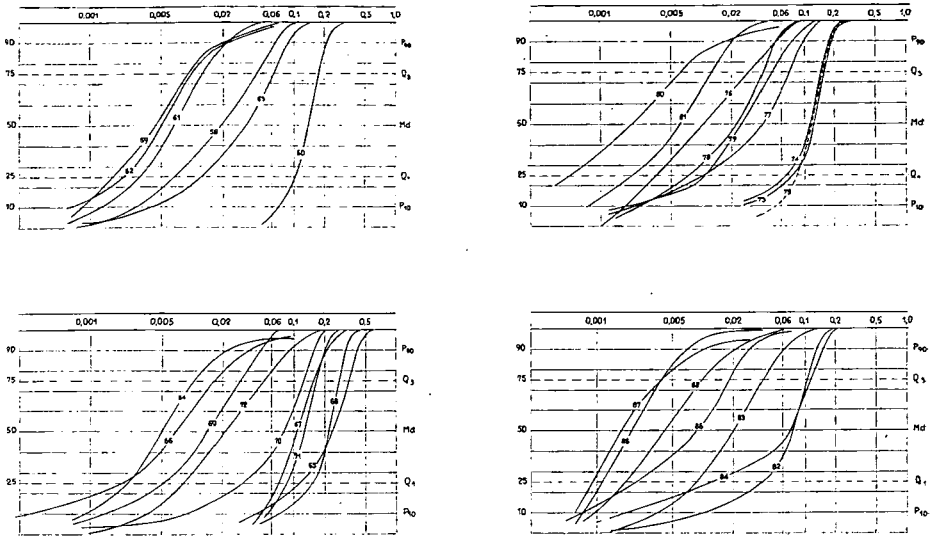

Fig. 7. Granulometric curves of the analysed samples from the interval of 267 to 492 m

The numbers written on the side of Column II of *Figs. 2—5* correspond to the serial numbers of Table 1 and of the samples analysed.

According to the results of the granulometric analysis, the sediments of the borehole are dominantly fine-grained, mainly corresponding to clay and fine- and coarse-silt fractions. Sand is scant and what is available is chiefly fine- or coarse-grained, so that even the greatest grain size does not exceed the size of medium sand (*Figs. 7—8*, samples 31—88). The fineness of the granulometric composition is also indicated by the *median* (*Md* = diameter of grains accounting for 50 per cent of the sediment) and the representative grain size (diameter of grains represented by the highest percentage in the sample) values (see *Md* and *M* values in Table 1). The interval characterized by the coarsest grain size composition within the lithologic log of the borehole is between 298 and 363 m. This sandy interval is interrupted, however, by a

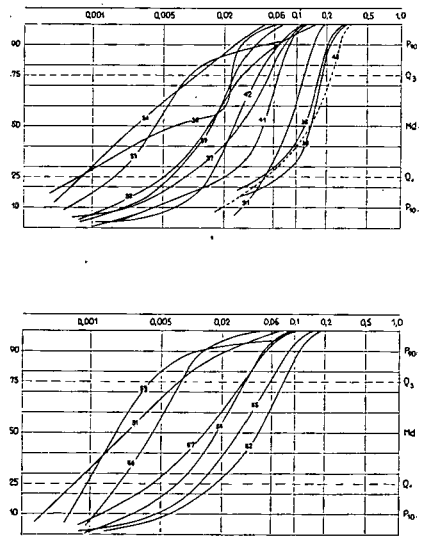

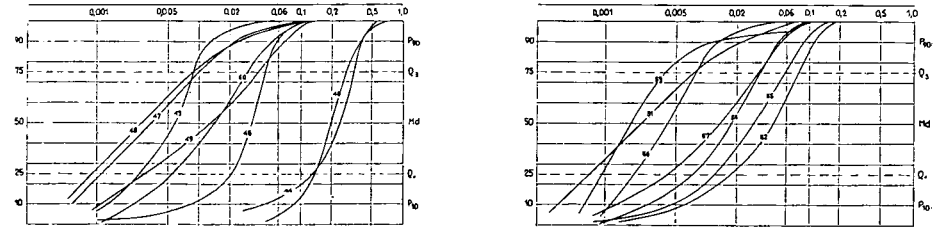

Fig. 8. Granulometric curves of the samples from the interval of 48 to 261 m

Table 1
Lithologic statistics of the studied Upper Pannonian material of the Macs borehole

Number	Depth m	P_{10}	Q_1	Md	M	Q_3	P_{90}	$So=\sqrt{\frac{Q_3}{Q_1}}$	$K=\frac{Q_3-Q_1}{2(P_{90}-P_{10})}$	$Sk=\frac{Q_1\cdot Q_3}{Md^2}$	$CaCO_3$	Type of Sediment
31.	48,3—50,8	0,03	0,05	0,085	0,098	0,12	0,16	1,55	0,27	0,83	2,2	F.S.
32.	50,8—53,3	0,0015	0,0052	0,014	0,015	0,03	0,067	2,40	0,19	0,80	—	F.Si.
33.	55,5—56,4	0,00057	0,0016	0,0042	0,005	0,0095	0,055	2,44	0,52	0,86	0,9	CL.
34.	59,9—65,2	0,00039	0,0080	0,0027	0,0045	0,011	0,026	3,70	0,59	1,20	2,2	CL.
35.	84,0—84,7	—	0,00078	0,007	0,0026	0,024	0,030	5,55	—	—	6,6	CL.
36.	86,0—88,0	—	0,045	0,12	0,15	0,17	0,21	1,94	—	0,53	8,8	S.S.
37.	92,9—93,3	0,0024	0,0082	0,028	0,03	0,055	0,077	2,58	0,18	0,52	6,6	C.Si.
38.	98,8—100,4	—	0,067	0,14	0,16	0,18	0,22	1,64	—	0,61	6,6	S.S.
39.	105 —107,5	0,0022	0,006	0,015	0,016	0,026	0,043	2,08	0,49	0,69	8,8	F.Si.
40.	115,8—117	0,019	0,047	0,13	0,15	0,21	0,25	2,11	0,42	0,58	3,5	S.S.
41.	120,5—131	0,0038	0,019	0,045	0,05	0,062	0,080	1,80	0,28	0,74	5,3	C.Si.
42.	131,4—132,7	0,0062	0,014	0,024	0,025	0,040	0,065	1,69	0,22	0,97	6,6	C.Si.
43.	138,1—140,3	0,0013	0,0026	0,0058	0,0065	0,0085	0,013	1,81	0,25	0,66	6,6	F.Si.
44.	153,0—154,0	0,042	0,13	0,24	0,027	0,32	0,35	1,57	0,32	0,72	—	M.S.
45.	154,0—157,6	0,009	0,021	0,033	0,036	0,044	0,058	1,44	0,23	0,85	—	C.Si.
46.	163,8—165,3	0,087	0,14	0,2	0,24	0,28	0,36	1,43	0,26	0,98	1,3	M.S.
47.	165,3—166,0	0,00057	0,0012	0,0036	0,0042	0,01	0,024	2,89	0,19	0,92	—	CL.
48.	171,4—173,6	0,00045	0,0009	0,0028	0,0038	0,009	0,026	3,16	0,16	1,02	1,3	CL.
49.	175,0—177,0	0,0011	0,003	0,013	0,016	0,039	0,072	3,60	0,25	0,69	0,9	F.Si.
50.	186,0—188,8	0,0022	0,0057	0,014	0,016	0,030	0,062	2,29	0,20	0,87	9,7	F.Si.
51.	191,8—194,0	0,0003	0,00065	0,002	0,0038	0,0068	0,02	3,17	0,16	1,10	4,4	CL.
52.	204,5—207,6	0,0054	0,013	0,04	0,042	0,072	0,098	2,35	0,32	0,59	2,2	C.Si.
53.	239,7—241,5	0,00056	0,00087	0,0016	0,0019	0,0036	0,01	2,03	0,29	1,22	0,9	CL.
54.	243,2—244	0,0022	0,0065	0,016	0,017	0,029	0,045	2,11	0,26	0,73	0,9	C.Si.
55.	247,6—251,6	0,004	0,01	0,026	0,03	0,052	0,08	2,28	0,28	0,89	—	C.Si.
56.	255,5—257,0	0,0098	0,0019	0,0038	0,0044	0,007	0,011	1,91	0,21	0,91	2,2	CL.
57.	259,7—261,0	0,0011	0,0036	0,012	0,012	0,029	0,048	2,84	0,27	0,73	6,6	F.Si.
58.	267,0—270,6/*a*	0,0028	0,0067	0,019	0,022	0,044	0,066	2,56	0,30	0,82	6,6	C.Si.
59.	273,2—274,0	0,0008	0,0017	0,0045	0,0055	0,0095	0,02	2,36	0,13	0,80	4,4	F.Si.
60.	277,7—280,4	0,071	0,11	0,14	0,14	0,18	0,21	1,30	0,25	1,00	4,4	S.S.
61.	282,5—283,8	0,0012	0,0031	0,0066	0,0075	0,013	0,022	2,04	0,24	0,93	8,8	F.Si.
62.	287,1—290,0	0,00055	0,0022	0,0048	0,0058	0,01	0,021	2,13	0,19	0,96	4,4	F.Si.
63.	294,5—296,4	0,0039	0,012	0,034	0,028	0,066	0,090	2,34	0,31	0,70	2,2	C.Si.
64.	296,4—297,5	0,00085	0,0024	0,005	0,0055	0,011	0,022	2,14	0,20	1,07	—	CL.
65.	303,0—305,0	0,042	0,12	0,24	0,26	0,34	0,43	1,68	0,28	0,71	2,2	M.S.
66.	307,0—307,2	0,00024	0,002	0,0069	0,007	0,017	0,036	2,92	0,21	0,71	11,1	F.Si.
67.	307,5—309,5	0,047	0,07	0,11	0,12	0,18	0,22	1,60	0,32	1,04	6,0	S.S.
68.	314,2—322,9	0,067	0,15	0,22	0,24	0,27	0,32	1,34	0,24	0,84	4,4	M.S.
69.	324,1—328,0	0,0014	0,0052	0,014	0,016	0,029	0,046	2,36	0,27	0,77	4,4	F.Si.
70.	328,6—330,0	0,0084	0,032	0,077	0,090	0,12	0,16	1,93	0,29	0,65	4,4	F.S.
71.	331,7—336,0	0,055	0,080	0,12	0,13	0,16	0,21	1,41	0,26	0,89	13,7	S.S.
72.	337,5—339,6	0,0034	0,0082	0,02	0,023	0,05	0,058	2,47	0,38	1,03	16,4	C.Si.
73.	347,0—348,4	0,024	0,080	0,12	0,13	0,16	0,19	1,41	0,24	0,89	2,2	S.S.
74.	349,1—356,0	0,02	0,069	0,11	0,13	0,15	0,18	1,47	0,25	0,86	2,2	S.S.
75.	356,0—357,0	0,056	0,085	0,12	0,13	0,15	0,18	1,33	0,26	0,89	—	S.S.
76.	369,0—369,5	0,0018	0,0035	0,010	0,011	0,03	0,055	2,92	0,25	1,05	0,9	F.Si.
77.	371,2—372,8	0,0023	0,011	0,04	0,05	0,075	0,1	2,61	0,33	0,52	6,6	C.Si.
78.	378,0—378,8	0,0025	0,0075	0,022	0,026	0,040	0,055	2,31	0,31	0,62	4,4	C.Si.
79.	385,4—388,1	0,0019	0,011	0,025	0,03	0,050	0,080	2,13	0,25	0,88	8,8	C.Si.
80.	388,9—393,5	—	0,0005	0,0022	0,003	0,0065	0,018	3,60	—	0,67	2,2	CL.
81.	393,9—395,0	0,0008	0,0021	0,0062	0,007	0,015	0,021	2,67	0,32	0,82	13,3	F.Si.
82.	404,3—408,0	0,0092	0,039	0,075	0,08	0,11	0,13	1,67	0,29	0,75	4,4	F.Si.
83.	412,4—415	0,0034	0,0085	0,020	0,023	0,04	0,062	2,16	0,27	0,98	4,4	C.Si.
84.	422,8—424,9	0,0018	0,012	0,07	0,08	0,12	0,16	3,16	0,21	0,29	4,4	F.S.
85.	428,9—430,0	0,00062	0,0022	0,009	0,01	0,019	0,029	2,94	0,30	0,59	4,4	F.Si.
86.	431,0—433,8	0,00065	0,0010	0,002	0,0022	0,004	0,0072	2,00	0,23	1,00	4,4	CL.
87.	459,3—461,5	0,00055	0,00082	0,0016	0,002	0,0039	0,011	2,18	0,15	1,25	—	CL.
88.	492,0—492,6	0,0008	0,0018	0,0043	0,005	0,01	0,021	2,35	0,20	0,97	2,2	CL.

CL. = CLAY = 0,005 > mm ⌀, F.Si. = FINE SILT = 0,005—0,02 mm ⌀, C.Si. = COARSE SILT = = 0,02—0,06 mm ⌀ F.S. = FINE SAND = 0,06—0,1 mm ⌀, S.S. = SMALL SAND = 0,1 —0,2 mm ⌀, M.S. = MEDIUM SAND = 0,2—0,5 mm ⌀

Table 2

Heavy mineral composition of the Upper Pannonian and Pleistocene sands of the Macs borehole

Number	Depth m	DOMINANTLY MAGMATIC MINERALS											DOMINANTLY METAMORPHIC MINERALS											OTHER MINERALS				Total quantity minerals in the examined fraction	Dominant grain diameter mm	Age
		Hypersthene	Other rhombic piroxenes	Augite	Diopside	Basaltic-Hornblende	Magnetite	Ilmenite	Biotite	Olivine	Apatite	Zircon	Chlorite	Tourmaline	Epidote	Zoizite	Rutile	Hornblende	Actinolite-tremolite	Garnet	Staurolite	Cyanite	Glaukophane	Calcite-dolomite	Limonite	Other micas	Weathered minerale			
1.	6—8	7,0	1,0	16,2	1,0	11,1	11,1	—	0,5	0,5	2,5	—	3,0	1,0	1,0	—	—	4,5	0,5	11,6	—	0,5	—	0,5	12,1	0,5	19,3	0,69	0,1—0,2	
2.	15,5—16,0	9,2	1,1	10,3	0,6	7,0	21,2	—	0,6	—	1,7	0,6	6,3	3,4	0,6	—	—	5,2	0,6	12,6	0,6	0,6	—	—	9,2	—	8,6	0,72	0,06—0,1	
3.	24,5—26,5	9,5	0,6	16,9	1,3	6,3	6,3	—	—	—	0,6	—	5,6	3,1	0,6	—	—	4,4	—	14,4	2,5	0,6	—	—	5,0	—	22,5	0,87	0,1—0,2	
4.	32,2—34,9	1,1	3,3	4,9	2,2	7,8	8,4	—	2,7	—	0,6	0,6	3,8	4,4	2,7	—	1,1	3,8	—	9,9	2,2	—	—	—	6,0	—	34,5	0,46	0,1—0,2	Pleistocene
5.	48,3—50,8	—	2,4	—	0,8	0,8	19,5	—	—	—	2,4	0,8	7,1	1,6	—	—	0,8	—	0,8	3,2	0,8	—	—	—	25,4	—	33,6	0,46	0,1—0,2	
6.	72,0—74,0	—	—	—	0,8	9,0	14,7	—	—	—	1,6	—	4,1	4,9	—	—	0,8	—	—	9,8	—	—	—	—	16,6	—	37,7	0,62	0,1—0,2	
7.	86,0—88,0	—	2,0	—	1,4	—	11,8	0,7	4,8	—	3,4	—	7,5	2,7	0,7	—	2,0	—	—	3,4	—	0,7	—	—	19,9	2,0	37,0	0,52	0,1—0,2	
8.	98,8—100,4	1,6	2,3	—	0,8	6,8	6,0	1,6	0,8	—	4,5	—	8,3	0,8	1,6	—	1,6	3,0	0,8	34,8	0,8	0,8	—	—	9,0	—	14,1	1,04	0,1—0,2	
9.	115,8—117	—	—	—	—	45,5	13,9	—	2,2	—	1,4	0,7	8,8	1,4	0,7	—	1,4	7,3	—	10,2	0,7	—	0,7	—	0,7	—	6,6	1,48	0,1—0,2	
10.	153 —154	—	—	2,2	—	43,3	5,6	—	2,8	—	0,6	—	12,0	0,6	—	—	0,6	2,2	—	14,7	—	—	—	—	2,2	—	14,0	3,39	0,2—0,5	
11.	157,8—157,9	—	2,8	1,4	1,4	11,7	—	—	—	—	2,1	—	13,2	2,1	0,7	0,7	—	7,5	1,4	2,9	—	0,7	—	—	—	—	51,4	4,10	0,06—0,1	
12.	235,6—236,6	—	2,1	0,7	2,9	6,6	4,4	—	1,4	—	2,9	—	15,1	2,2	2,2	2,2	—	22,9	3,7	0,7	—	—	—	—	2,2	—	27,8	0,68	0,06—0,1	
13.	277,7—280,4	—	—	3,8	4,8	23,2	5,7	—	—	—	0,9	—	8,6	1,9	1,9	—	0,9	16,3	5,7	3,8	—	—	—	—	1,9	—	20,6	2,40	0,1—0,2	
14.	303 —305	—	1,8	1,8	1,2	44,4	11,2	—	—	—	5,4	0,6	2,4	1,8	—	—	—	5,4	3,6	5,4	0,6	—	—	—	—	—	14,4	4,60	0,2—0,5	
15.	314,2—322,9	—	—	0,6	—	44,0	15,0	—	4,2	—	—	—	3,5	1,8	—	—	0,6	0,6	—	15,5	0,6	0,6	—	—	—	—	13,0	4,45	0,2—0,5	
16.	331,7—336	0,6	0,6	2,5	—	23,0	1,2	—	16,0	—	—	—	9,9	0,6	—	—	0,6	19,2	0,6	1,8	—	—	—	—	1,2	0,6	21,6	1,84	0,1—0,2	
17.	357 —364	—	—	0,8	—	44,4	9,8	—	—	—	1,6	—	1,6	0,8	—	—	—	1,6	0,8	9,8	—	—	—	—	—	—	28,8	3,80	0,2—0,5	
18.	404,3—408,0	—	0,7	—	—	10,7	2,0	—	19,7	—	2,7	—	47,0	1,4	—	—	—	1,4	0,7	4,0	—	—	—	—	2,7	3,4	13,6	0,43	0,06—0,1	
19.	422,8—424,9	0,6	0,6	—	—	—	2,8	—	16,8	—	8,5	—	43,5	1,7	0,6	—	0,6	—	—	11,3	1,1	—	—	—	4,5	0,6	15,8	0,38	0,06—0,1	
20.	476 —482,9	—	—	6,8	—	28,7	21,9	—	0,8	1,7	0,8	—	5,1	0,8	—	0,8	—	0,8	—	5,1	—	—	—	—	0,8	—	25,9	1,00	0,1—0,2	Upper pannonian

Grain shape

The shape of the sand grains was studied by the method of I. MIHÁLTZ—T. UNGÁR—P. DÁVID [1954, 1955] distinguishing four types of grains: from water-transported sediments (types 1 and 2) to dominantly wind-blown ones (types 3 and 4). The method being a statistical one, the origin of the sand sediment is determined by the grain types prevailing in the strata. In the Upper Pannonian samples examined this way, the types 1 and 2 have been found to predominate in every case, type 3 has been represented by a low percentage only, a fact testifying to transportation by — or deposition in — water. In the Pleistocene sequence — whose data have been presented for comparison in *Fig. 2* — has been dominated throughout by types 2 and 3, and also type 4 appeared in several cases, a phenomenon reflecting the different conditions of sedimentation referred to above.

Mineral composition

1. Heavy minerals. Within the 453 m of the Upper Pannonian sequence, changes in mineralogic composition, i.e. in source area, can be observed nine times. Proceeding from the bottom to the top, the following types could be distinguished: *a)* The sample of the interval 476 to 483 m is dominated by augite, basaltic hornblende, and magnetite (*Fig. 5*, Table, 2, Sample 20). *b)* The samples from 404 m and 422 m depths (*Fig. 5*, Table 2, Samples 18 and 19) show the abundance of micas (chlorite, biotite). *c)* The composition of the sample from 357 m depth is nearly the same as that of the lowermost sample (*Fig. 4*, Table 2, Sample 17). *d)* Between 331 and 336 m, the common hornblende is fairly abundant (19%). a phenomenon distinguishing this interval from the sequences lying below and above it (*Fig. 4*, Table 2, Sample 16). *e)* Between 303 and 314 m, the basaltic hornblende is, again, of considerable amount (*Fig. 4*, Table 2, Samples 14 and 15). *f)* Between 157 and 280 m, the weathered minerals increasing upwards and basaltic and common hornblende, are of importance (*Figs. 3* and *4*, Table 2, Samples 11 and 13). *g)* Between 115 and 154 m, the mineralogic composition is characterized, again, by the abundance of basaltic hornblende (43—45%) (*Figs. 2* and *3*, Table 2, Samples 9, 10). *h)* The sample deriving from 98 m depth is conspicuous for its high garnet content (35%). A connection with the earlier source area is still indicated, however, by augite and basaltic hornblende present in low percentages (*Fig. 2*, Table 2, Sample 8). *i)* The rest of the Upper Pannonian sequence (depth interval of 48 to 88 m) shows a completely different composition: high percentage of magnetite and limonite. In these samples too, the weathered minerals are represented by a very marked percentage (*Fig. 2*, Table 2, Samples 5 to 7).

For a comparison, in *Fig. 2* and Table 2 the heavy minerals composition of the Pleistocene sequence is also shown. The sample from 32 m still exhibits transitions between the underlying, Upper Pannonian, samples and the overlying, later Pleistocene, ones. The transitional character is due to an admixture from the Upper Pannonian sandy surface (*Fig. 2*, Table 2, Sample 4). The rest of the Pleistocene shows an identity with the sediment being transported by the Tisza river and its tributaries in the northern Trans-Tisza Region. In these samples, the hypersthene, barely attaining 1 to 2 per cent in the above-discussed sediments, is enriched to 7 to 9 per cent, being associated with abundant augite (10—16 per cent) and basaltic hornblende (7—11 per cent). (*Fig. 2*, Table 2, Samples 1 to 3).

Beside the minerals listed above, other minerals have though been also present in the samples, but the examplified ones are representative and readily charac-

number of clay, silt and lignite layers testifying to a marked unsteadiness of sedimentation even in this phase of high-rate accumulation.

The statistical values of the lithology of the strata studied are shown, in depth oderr, in *Fig. 9* and Table 1. Although not every layer has been analysed in detail, the investigation included all types of sediment, and the analysed samples have been selected evenly, as possible, throughout the profile. Thus, the vertical succession and variation of the results obtained are suitable for depicting the character of the processes.

The value of *sorting (So)* varies within very ample limits (1.3—5.5). This variation is fairly irregular, yet it is possible to select such intervals within the profile, where the sediment is well sorted or rather badly sorted. For instance, well-sorted sediments occur in samples 67 to 75 and 38 to 46. Less sorted are the samples 76 to 86 and 47 to 53, and, particularly so, the samples 31 to 37 representing the topmost Upper Pannonian.

Kurtosis (K) does not show any regular change. What is noteworthy is, however, that the greatest deviation from the average occurs in the samples 32 to 41 of the topmost Upper Pannonian. Just the same phenomenon can be observed in the variation of *skewness (Sk)*. The last-mentioned two characteristics, however, could not be computed for all samples, of the uppermost part of the profile, as the finer size fraction is very abundand there (curves 35, 36, 38).

Consequently, the statistical characteristics of grain size and the grain size itself show, in the Upper Pannonian interval, a substantially greater range of variation than do in the 48 -m-thick Pleistocene sequence. This very fact readily shows the essential difference between lacustrine sedimentation and eolian deposition on a dry surface, as was the case with the two formations of dissimilar age, respectively.

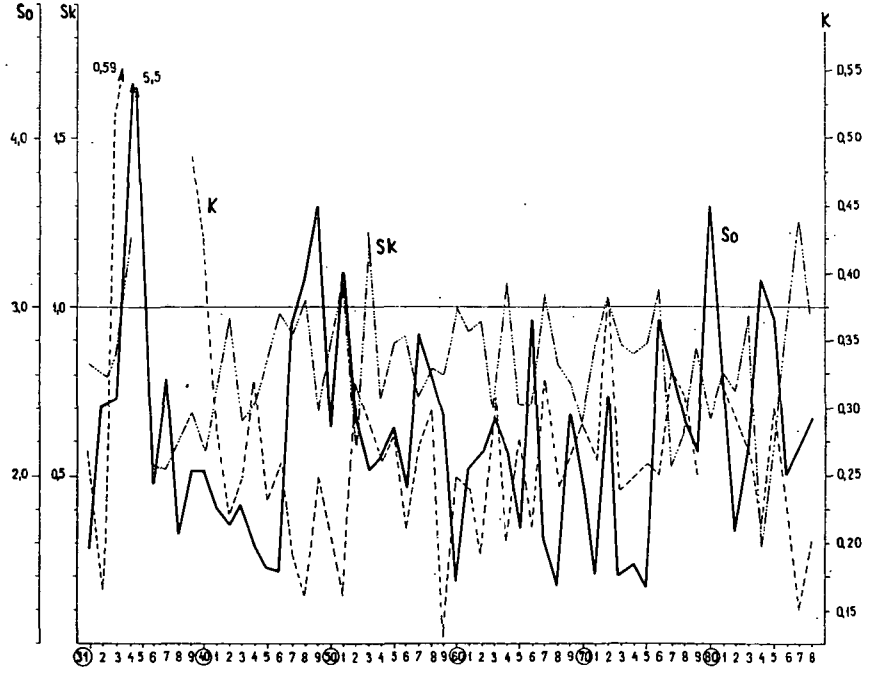

Fig. 9. Lithological statistics of the analysed samples (The numerals equal the serial numbers on the side of Column II, *Figs. 2—5* as well as those of Table 1.)

teristic of the particular heavy mineral levels, both with their aggregate appearance and relative proportions.

Such frequent changes in the heavy minerals composition are indicative of the rapid variation of the source area, a phenomenon which can be ascribed to crust movements. Associated with the predominant magmatic minerals, the repeated concentration peaks of chlorite also indicate that erosion was not confined to the volcanics of the marginal zone; on the contrary, the basin-deposited sediment has partly come from a crystalline-schist-built area, or possibly from the deposition of older sedimentary rocks.

2. Light minerals. First of all, the quantitative changes of feldspar grains in the sequence was studied. A. CAILLEUX (1965) developed a method for the evaluation of the amount of feldspar in clastic sediments. On the basis of the results obtained for a number of samples from different places, he could prove the dependence of the petrographic composition not only on the rejuvenation of the morphology (tectonics) but also on the climate and the vegetation.

Under cold and arid climate — and because of the rapidity of erosion in many mountains — there is no time for chemical weathering, the rock is only mechanically disaggregated, so that feldspar is enriched in the sandy sediment. On a hot and humid, forest-clad plain, however, it is the chemical weathering that gains prominence, so that the feldspars are altered into clay or bauxite minerals. The amount of heavy minerals removed from granite or gneiss surfaces into the sedimentation basin, is rather low. For this reason, the sand grains primarily consist of quartz.

Feldspar-rich sediments can be formed under various conditions. Beside climatic effects, the erosion of volcanic rocks, for instance, may also provoke an enrichment of feldspar. On the contrary, a decrease in the concentration of feldspar is always due to chemical weathering (rather than to physical disintegration). This fact was proved by F. J. PETTIJOHN [1949] on Mississippi-transported sediments in which the originally 25% concentration of feldspar decreased by mere 5 per cent after being transported for 1800 km in the river.

The *Cailleux feldspar factor* can be calculated by using the following formula:

$$\text{Feldspar factor} = \frac{100 \times \text{feldspar}}{\text{feldspar} + \text{quartz} + \text{mica} + \text{other minerals}}$$

„other minerals", the carbonates (calcite, dolomite) and the minerals indeterminable because of their advanced weathering or coating, have been omitted. Sediments showing 10- to 80% concentration are held for feldspar-rich, those of 4- to 5% concentration, for feldspar-poor.

The material of the Macs profile can be considered feldspar-rich. Within the Upper Pannonian sequence, the *Cailleux factor* varies between 28 and 60, the highest value occurring in the interval of 150 to 501 m (*Figs. 2—5*, column IV, first group of numerals). So high a ratio of feldspar in the Pannonian has not been found heretofore anywhere in the more central, southern, part of the basin, the average value has varied within the range of 20 to 35 [B. MOLNÁR, 1967 *c*, 1967 *d*].

The high feldspar ratio here is a proof for the rapid removal of considerable amounts of volcanic material, a fact confirmed by the heavy minerals already presented above.

Between 48 and 150 m, the feldspar ratio decreases from 28 to 31. This fact can only partly be due to a change of source area. Nota bene, the heavy minerals composition of the sample from 115 m depth is identical with that of the deeper-

sited, but more feldspar-rich, deposits. The lower concentration of feldspar may be due to the lower rate of accumulation, conditions under which the chemical weathering could have time enough for influencing the feldspars of the sediment. No information suggesting a latest Pannonian climate, considerably warmer than formerly, is available. And given the subequal climate, the chemical weathering could attain a comparatively higher intensity only in case of a lower rate of deposition.

In accordance with the colder climate, the Pleistocene samples yield a higher feldspar factor — from 48 to 53.

The percentage ratio of the weathered, coated grains to the total of mineral grains has been established. In the Upper Pannonian section, the samples which were generally more abundant in feldspar, showed lower concentrations in the lower part of the section (3—10%) and higher concentrations in the less feldspar-rich interval (4—16%) (Legend, *Figs. 2—5*). In the upper part of the Upper Pannonian section, this fact is an evidence of the more intensive effect of chemical weathering.

Carbonate content

After the samples had been attacked by hydrochloric acid, the weight loss of CO_2 was calculated for $CaCO_3$. It can be considered rather low throughout the profile, as compared to the rest of the Great Hungarian Plain [B. MOLNÁR, 1967 *b*]. Layers with a carbonate content attaining 30 per cent have not been numerous, and only five samples showed a higher figure. A strikingly high value, 37 to 66 per cent, was obtained for three intervals only.

Relationship between tectonic movement and sedimentation

The Lower Pannonian of the Hajdúság is 200 to 250 m thick, the Upper Pannonian attains 1,000 m thickness [L. KÖRÖSSY, 1962]. Hence, the 453 m thickness of the Macs profile exposes nearly the half of the Upper Pannonian sequence. Exhibiting a swift variation in lithology throughout the vertical range of the borehole, the profile is represented by about 18 layers of lignite, 7 stringers of lignite, shaly lignite and carbonaceous shale as well as by 17 diagenized interlayers. The matrix of the latter is not always a carbonate one. So, e.g. the samples taken from 487.5 or 277.5 m depths have a siliceous matrix. The diagenized matter, immediately overlying these points, however, shows again a calcareous matrix, the sample from 201 m being, in addition, limonitized.

The colours of the sediments being considered are very diversified (*Figs. 2—5*, Column II). Concretions or precipitates of chalk and limonite are frequent. The mottled nature of the sediments is indicative of reduction and oxidation processes.

In the lithofacies-dated Upper Pannonian interval, M. FARAGÓ [1960] has identified a rich pollen assemblage which is considered to comprise shallow-water and swamp communities of Upper Pannonian flora.

The representatives of fauna are very scant throughout the profile; F. BARTHA [in M. ERDÉLYI, 1962] identified *Viviparus sadleri* PARTSCH, *Melanopsis fuchsi* HANDM., *Limnocardium* sp. and *Anodonta* sp. from the 217,3 to 220,6 m interval. From the interval of 211,4 to 212,3 m, he described *Viviparus sadleri* PARTSCH, *Congeria* sp., *Limnocardium* sp., *Anodonta* sp. According to him, these forms are indices of the Upper Pannonian brackwater facies. On the basis of the lithologic composition of the 453 m thick profile, four periods of subsidence (a) and four

periods of emergence (or standstill) (b), forming — couple by couple — individual sedimentation cycles (A to D), can be distinguished.

Aa) Most difficult to qualify is the lower, 425 to 501 m, interval, as its downward continuation is unexplored. At a depth of some 420 m, however, the heavy minerals composition will change, as shown above, giving rise to the first lignite seam. The worse sorting of the sediment also applies to this interval. Taken all together, these data are data evidencing the tectonic movement of the area.

The role of sandy sediments declines from bottom to top (the samples from 463, 466, 480, and 490 m depths are represented by sand, whereas the interval of 425 to 463 m — i.e. a thickness of nearly 40 m — includes but a few decimeters of sand). Consequently, between 425 and 501 m, a subsidence of the area and a deepening of the contemporaneous lake can be revealed (*Fig. 5*, Column VI, 1 and Legend).

Ab) At 420 m depth, the appearance of the first lignite layer, the variegated stain of the sediments, their limonite and chalk concretions, and the changes of the source area are indicaters of a movement of geometrically opposite sence— emergence or, possibly, a static condition leading to accumulation of sediment. The appearance of the lignite layer also is an evidence of shallowing, i.e. of the rate of emergence. In fact, the sediment now occurring at 420 m depth may have been deposited nowhere else but at the water front (*Figs. 4—5*, Column VI, 1, 2, 3).

The rise-causing effect of tectonic movement resulted — as opposed to the formerly magmatic nature of the heavy minerals — in the predominance of the metamorphic minerals — such as chlorite which must have come from a metamorphic source area. Farther upwards within the same interval, however, it is again the magmatic character that begins to dominate. In the lower portion of the interval the sediments is more badly sorted, the parts farther up show a better sorting. The greatest number of diagenized layers is found here within the entire profile. This type of sedimentation can be traced from 420 m to 334 m depth. Consequently, the interval of 334 to 501 m as a whole represents a minor cycle of sedimentation (A).

Ba) At 334 m a new change in source area, manifested by the comparatively higher percentage of common hornblende, sets in. From this depth upwards, the amount of sandy sediment will suddenly increase, a penomenon indicating the final sedimentation of the preceding cycle and the initial, coarser-grained, one of the new cycle, respectively. Between 258 and 334 m, no lignite layer or stringer can be found and the sediment becomes gradually finer farther upwards. All these phenomena combined, are indicative of a subsidence of the area *(Fig. 3)*.

Above 334 m — a level where the growth of the ratio of hornblende has shown an inversion of crust movement — the magmatic mineral paragenesis becomes, again, characteristic.

Bb) In the interval of 180 to 258 m there are many lignite layers attaining the highest frequency here in the entire profile. The Upper Pannonian mollusks determined by F. BARTHA have come from this interval. Within this interval the heavy minerals composition has shown the first change before the appearance of the first lignite layer, at 283 m, a change indicative of an inversion of crust movement. At the base of the interval, the sediments are well sorted, in the upper part less sorted *(Fig. 8)*. The calcareous-limonitic hardground occurring at 202 m is an evidence for swamp sedimentation. The higher amount of weathered minerals can also be accounted for by an oxidation in swamps.

As suggested by the above features, the sediments deposited within the interval

of 180 to 258 m may have been formed in the ascendent, or possibly static, phase of tectonic movement.

Consequently, the 180- to 334 m interval indicates a new sedimentation cycle (B).

Ca) Between 148 and 180 m, the characters of lithofacies, including the smaller thickness of the sediment, suggest a sedimentation of short duration due to subsidence.

Cb) In the interval of 90 to 148 m, however, a phase of emergence or static condition can be shown to have taken place, again.

Between 90 and 180 m, appears, in turn, a third sedimentation cycle as counted from the bottom of the hole upwards. This cycle is, however, represented by a thickness considerably lower than the preceding ones are (C).

Da) The last phase of subsidence within the profile under consideration occurs between 51 and 90 m.

Db) Finally, between 48 and 51 m there are small-grained sands—regressive sediments corresponding to the complete withdrawal of the Pannonian lake. They may be partly absent, as in the Levantine the sedimentation was replaced by erosion. As shown above, the Pannonian sediments were redeposited even in the Pleistocene.

Consequently, it is the last cycle of the profile that appears between 48 and 90 m (D).

SUMMARY

In conclusion, it can be stated that the 453-m-thick Upper Pannonian of Macs is composed of four minor cycles of sedimentation. The sedimentation cycles differ in grain size from one another, as the grains first become finer, then, again, coarser from bottom to top. Here in the regression phase, the kinetics of the crust — subsidence, emergence or static condition, respectively — are indicated, in several cases, by the lignite seams and by the general changes of sedimentation (sorting and heavy minerals composition of the sediments) rather than by grain-size variation.

In Table 3 the thicknesses of the subsidence and emergence phases (or possibly of static phase) of the individual cycles as well as the thickness of the sediments of the particular cycles have been shown. The upward-decreasing thickness of the individual sedimentation cycles is conspicuous.

Table 3

Thickness of the sedimentation cycles of the Upper Pannonian sequence of Macs

Symbol of cycle	Thickness of subsidence-recording sediments m	Thickness of sediments recording emergence or static conditon m	Total thicknes of sedimentation cycle m
D	39	3	42
C	32	58	90
B	76	78	154
A	79	88	167
Total thickness m	226	227	453

Accordingly, the latest Pannonian tectonic movement was a rhythmical one. Preceding the overall latest Pannonian regression, these rhythms were of shorter and shorter duration. The thickness of the second — emergent or static — phase of the particular cycles is always higher than that of the sedimentary sequence formed in the subsidence phase. (Table 3). Hence, the Pannonian lake vanished in such a way that subsidence was gradually outscored by emergence or static condition which became longer and longer.

Within the 453-m-thick Upper Pannonian section, at a depth of about 354 m, the over-all trend of tectonic movements and their cumulative effect have changed with the appearance of the coarsest sediment. Heretofore rather subsiding and slowly deepening (with simultaneous accumulation), the lake-covered area now began to become shallower, despite the minor subsidences which intervened from time to time (*Figs. 2—5*, Column VI, 5).

In other parts of the Great Hungarian Plain, e.g. at Jászladány and Kemecse, the above cycles could also be shown to occur within the Pannonian sedimentary sequence (*Fig. 1*). The lignite layers, however, played a less significant role there, the lithofacies of the individual cycles being different. The cyclicity is, however, an evidence for rhythmical tectonic movements, here too [A. RÓNAI, 1968].

In the southern Great Plain, where the Pleistocene epoch witnessed fluviatile accumulation, the rhythmicity of crust movement is proven [MOLNÁR, 1967 *a*, 1968] for the Pleistocene, too (Szentes, Makó). Consequently, this peculiarity of tectonic movement was preserved in the Pleistocene.

REFERENCES

CAILLEUX, A. [1965]: Petrographische Eingenschaften der Gerölle und Sandkörner als Klimazeugen. — Geologische Rundschau B *54/1*, pp. 5—15.

DÁVID, P. [1955]: A Duna—Tisza közi futóhomok koptatottsága. — (Manuscript, only in Hungarian).

ERDÉLYI, M. [1960]: A Hajdúság vízföldtana. — Hidrológiai Közlöny (Hydrological Journal), Budapest, pp. 90—105.

EBÉNYI, GY., SCHMIDT, E. R. [1931, 1938, 1939]: Magyarázatok Magyarország geológiai és talajismereti térképéhez 2/a, Nagybátony, 2/b, Hajdúböszörmény, 2/c, Balmazújváros.

FARAGÓ, M. [1960]: A macsi fúrás pollenvizsgálata. — (Manuscript, only in Hungarian).

FERENCZ, I. [1939—40]: Hajdúböszörmény környékének földtani felépítése. — M. Kir. Földtani Int. Évi Jel. *III*, pp. 99—104.

FERENCZI, K. [1965]: Szakvélemény Debrecen város és környéke hidrológiai viszonyairól. Magyar Állami Földtani Intézet (Manuscript, only in Hungarian).

KŐRÖSSY, L. [1956]: A Tiszántúl északi részén végzett kőolajkutatás földtani eredményei. — Földtani Közlöny (Bulletin of the Hungarian Geological Society) *86*, pp. 391—403.

KŐRÖSSY, L. [1962]: A Nagy Magyar Alföld mélyföldtani és kőolajföldtani viszonyai. — (Manuscript, only in Hungarian.)

MIHÁLTZ, I., UNGÁR, T. [1954]: Folyóvízi és szélfújta homok megkülönböztetése. — Földtani Közlöny (Bulletin of the Hungarian Geological Society) *84*, pp. 17—28.

MOLNÁRNÉ-DOBOS, I. [1953]: A Nyírség Ny-i pereme. — Földtani Int. Évi Jel. I. pp. 297—303.

MOLNÁR, B. [1966]: A Hajdúság pleisztocén eolikus üledéksora. — Földtani Közlöny (Bulletin of the Hungarian Geological Society) *96*, pp. 306—316.

MOLNÁR, B. [1967/a]: A Dél-Alföld pleisztocén feltöltődésének ritmusai és vízföldtani jelentőségük. — Hidrológiai Közlöny (Hydrological Journal) *47*, pp. 537—552.

MOLNÁR, B. [1967b]: Lithological and Geological Study of the Pliocene Formations. Part II. — Acta Miner. Petr., Acta Univ. Szegediensis *18/1*, pp. 35—46.

MOLNÁR, B. [1967c]: A dunaújvárosi felső-pannóniai és pleisztocén képződmények üledékföldtani vizsgálata. — (Manuscript, only in Hungarian).

MOLNÁR, B. [1967d]: Algyői fúrások ásványvizsgálata, — (Manuscript, only in Hungarian).

MOLNÁR, B. [1968]: Sedimentationszyklen in den pleistozänen Ablagerungen des südlichen Ungarischen Beckens. — Geologische Rundschau B. *57/2*, Stuttgart, pp. 532—557.

PETTIJOHN, F. I. [1949]: Sedimentary rocks. — Harper E. Brothers Publishers, New York.
RÓNAI, A. [1955]: A Nyírség, Hajdúság és Hortobágy talajvízviszonyai. — Hidrológiai Közlöny (Hydrological Journal) *7—8*, pp. 1—16.
RÓNAI, A. [1967]: Pliocén és negyedkori üledékképződés és éghajlattörténet a Déljászsági-medencében. — Magy. Áll. Földtani Int. (Manuscript, only in Hungarian).
SÜMEGHY, J. [1944]: A Tiszántúl. — Magyar tájak földtani leírása. Budapest.
SZÓFOGADÓ, P. [1958]: Felszín alaktan és mélyszerkezet kapcsolatának felhasználása Hajdúböszörmény vízellátására. — Hidrológiai Közlöny (Hydrological Journal). *38*. 4. 309—312.
URBANCSEK, J. [1953]: A Hortobágy földtani képződményei. — Földt. In. Évi Jel. *II*, p. 465.

DR. BÉLA MOLNÁR
Institute of Geology
Attila József University at Szeged
Táncsics M. u. 2.
Szeged, Hungary

ON THE RELATIONSHIP BETWEEN THE DEGREE OF OXIDATION OF MANGANESE OXIDE-HYDRATE PRECIPITATES AND THE CONDITIONS OF THEIR PRECIPITATION

MRS. E. MOLNÁR

Institute of Mineralogy, Geochemistry and Petrography,
Attila József University, Szeged

INTRODUCTION

One of the essential problems in the research of sedimentary manganese ore deposits is the effect of the various factors (pH, Eh, temperature, saturation of solutions, presence of foreign ions, etc.) on the composition of manganese oxide-hydrate precipitates. Since manganese can be present in the state of 2-, 3-, and 4-valency in both artificial and natural compounds, from this point of view the role of pH and Eh and the relationship between the pH and Eh conditions of the system and the oxidation degree of the resultant oxide-hydrate, respectively, are of great importance.

It seems to be obvious that the dependence of the measured oxidation degree of a manganese oxide-hydrate on the conditions of precipitation — pH and Eh, first of all — will be justified only if the possibility of any change in the oxidation degree of oxide-hydrate during post-precipitation treatment (filtering, washing, drying) is excluded. Nota bene, post-precipitation changes are independent of the factors of precipitation, so that such changes cannot be correlated with them.

Apart from a few exceptions, the composition of manganese oxides, manganese oxide-hydrates (their degree of oxidation) is variable and the circumstances of precipitation and the production techniques are largely responsible for these changes. As regards the technology of production of various MnO_2 modifications and various types of manganese oxides and/or manganese oxide-hydrates of higher valency, a considerable number of references are available. Various production techniques of MnO_2 modifications α, β, γ, δ, ε, and η as well as the results of the examination of modifications produced by different techniques were discussed in detail by O. GLEMSER, G. GATTOW, and H. MEISIEK [1961].

Numerous production techniques of MnO_2 modifications have been described in the papers of W. F. COLE, A. D. WADSLEY and A. WALKLEY [1947]; information on the means of producing various manganese oxides and/or oxide-hydrates were presented and the relevant literature reviewed by A.D. WADSLEY and A. WALKLEY [1951]; the relationships between the production techniques and characteristics of the oxidation products of manganese (II)-hydroxide — in the first place, manga-

nese(II)-manganites and δ-MnO_2 — were dealt with by W. FEITKNECHT and W. MARTI [1945a, 1945b] and by W. BUSER, P. GRAF and W. FEITKNECHT [1954], respectively.

As shown in the afore-mentioned papers, the determination of the composition and of the oxidation degree — and, consequently, the characterization of the sample — was done on filtered, washed and dried products. The experiences suggest that manganese(II)-hydroxide and the products of comparatively lower degree of oxidation, if wet, are readily oxidizable.

Avoiding of oxidation requires very thorough preparatory measures to be undertaken, as referred to by W. FEITKNECHT and W. MARTI [1945a]. These authors noted, however, that filtering in an oxygen-free nitrogen atmosphere and washing in water, alcohol and acetone, and then the expelling of the traces of acetone in a high vacuum have proved efficient measures for the samples of comparatively lower oxidation degree rather than for the more highly oxidized ones where the organic solvents induced various kinds of secondary reactions no matter how great care was taken during the treatment. In most cases the final product is filtered, washed with water acid-free and dried either above P_2O_5, or in a vacuum at a temperature of 50° to 60° C. In manganese dioxide modifications the composition of the final product, the Mn/O ratio, is difficult to reproduce, if at all possible, or it cannot be reproduced unequivocally. This fact is readily illustrated by the 21 different powder patterns given for γ-MnO_2 by the various authors [O. BRICKER, 1965 and G. GATTOW, 1961].

In many cases, it would be important first of all to find out the relationship between the factors of precipitation (pH, Eh) and the oxidation degree, Mn/O ratio, of the resultant solid product. Since this relationship may be influenced by possible changes due to filtering, washing, and drying, it seems to be advisable to determine the Mn/O ratio in the aqueous suspension. Nota bene, such a method would permit to bring the Mn/O ratio of the fresh suspension into a direct and clear-cut correlation with the factors of precipitation. To put it frankly, what can be determined this way is the Mn/O ratio alone, even though there is a reference [O. BRICKER, 1965] suggesting that the resultant product is identifiable by means of X-ray powder pattern, if an aliquot part taken from the suspension is passed through a 0,22-μ millipore filter and then carried out the X-ray investigation. In the reference quoted here the method of the treatment of the extremely low amount of solid product before the X-ray investigation has not been shown. As believed by the author of the present paper, the determination of the oxidation degree in suspension is particularly advantageous if the stability ranges of manganese oxides and/or oxide-hydrates of different oxidation degree are to be determined.

EXPERIMENTAL

For the determination of the oxidation degree of extremely small quantities of manganese oxide products, G. GATTOW [1961] has developed a method permitting to analyse each particular weighed sample (10 to 30 mg) for both manganese and active oxygen. The method is suitable for the examination of products devoid of foreign ions or at least cations which would disturb the complexometric determination of manganese or the iodometric one of oxygen.

Since the determination of the Mn/O ratio in aqueous suspension has been aimed at, the following two problems has to be settled first of all: Is the aqueous suspension properly homogenizable in order that the sampling might be made

volumetrically rather than gravimetrically, by using weighed samples and how much is the reliability of sampling influenced by the aging of the manganese hydroxide — manganese oxide-hydrate precipitate?

Various manganese(II)-hydroxide suspensions were obtained (Table 1) in such a way that 0,1 M solution of KOH or 0,1 M solution of NaOH was added to 0,05 M solution of $MnCl_2$ until precipitation took place. During this procedure the alteration of pH was measured. The suspension was homogenized for a quarter of an hour by a vibrating mixer and then six 25-ml aliquots were pipetted with a one-sign pipette. Three of these aliquots were used for the determination of Mn, three for that of active oxygen.

The suspension devoted to the determination of manganese was added to by 1—2 drops of concentrated hydrochloric acid and 1 drop of 30% hydrogen peroxide. This led to immediate dissolution of the precipitate. Peroxide was decomposed by slight boiling and the solution was diluted to 100 ml and then 0,1 g of ascorbic acid and 5 ml of NH_4Cl-NH_4OH buffer (pH = 10) were added to it. Afterwards the solution was titrated for manganese by EDTA of 0,05 M in presence of indicator Eriochromblack T (1:200 NaCl).

The determination of active oxygen in suspension can be done at an extremely swift rate and with a high accuracy, if the method developed at the Institut für Magnetische Werkstoffe, Jena, German Democratic Republic [P. KLEINERT, 1962], is applied in the following simplified form. The 25 ml aliquot is put into an Erlenmeyer flask of 200 ml capacity equipped with a Contat-Göckel attachment and containing 10 ml 15% hydrochloric acid and 15 ml of 0,05 N solution of Mohr-salt ($Fe(NH_4)_2(SO_4)_2$). To expel the air from the flask, a few tiny sodium hydrogen carbonate crystals are dropped into it. And after the weighed suspension sample is added, the flask is immediately closed by the sodium-hydrogen-carbonate-filled Contat-Göckel attachment. The solution devoted to blank test is submitted to the same procedure. The precipitate will immediately dissolve as it is put into the flask. The excess of Mohr-salt is titrated back with 0,05 N solution of Ce(IV)-sulphate. In doing so, 1 drop of 0,025 M ferroin is used as indicator. Its colour is to change from orange-red to green. It should be noted that the suspension added to the hydrochloric-acidic Mohr-salt solution will dissolve in a few moments, so there is no need in using sodium-hydrogen-carbonate stopper. If not a suspension but a solid manganese oxide sample of high solubility is to be analysed for active oxygen, the air can be expelled in the way described above, i.e. by using a Contact-Göckel attachment filled with sodium-hydrogen-carbonate solution. On the other hand, samples of low solubility require the use of a nitrogen flow for expelling the air from the device as shown in P. KLEINERT's quoted paper. In Column 1 ot Table 1 the time data of aging of the precipitate have been presented in an attempf to show the time limits of reliable homogenization in dependence on aging due to coagulation, consequently — the time range of reliable sampling and determinations.

In Column 2 the mg values of the Mn found for sets of parallel samples taken from different suspensions (3 of each), in Column 3 the mg values of active oxygen of the same samples, in Column 4 the composition of the precipitate — precisely its x value (MnO_{1+x}) — have been listed.

Grain size and rate of deposition will increase and, beyond certain limits, this may influence the reliability of sampling. Parallel determination in suspension of fresh precipitates show a good agreement, but after two- or three-week aging the suspension can no longer be homogenized, as the parallel measurements will

Table 1

Time of aging of the precipitate	Mn mg	Active O mg	Composition of the precipitate (MnO_{1+x}) $x=$
	in 25-ml aliquots		
1	2	3	4
Mn/O ratio determined immediately after preparation of the suspensions	31,78	0,57	0,0616
	31,73	0,57	0,0603
	31,73	0,57	0,0603
	29,46	3,63	0,4230
	29,41	3,63	0,4237
	29,41	3,63	0,4237
	28,90	0,84	0,0998
	28,93	0,84	0,0997
	28,93	0,84	0,0997
	29,41	0,34	0,0388
	29,41	0,35	0,0399
	29,34	0,37	0,0434
Determination after 1-day aging	28,05	0,93	0,1138
	27,69	0,94	0,1165
	27,75	0,94	0,1163
Determination after 2-day aging		etc.	
	26,27	0,88	1,1150
	26,13	0,90	1,1183
	26,54	0,89	1,1151
Determination after 7-day aging	26,90	2.11	1,2705
	27,09	2,06	1,2611
	26,81	2.11	1,2715

show inacceptably great divergences. It is possible, however, that acceptable results may be obtained even for long-aged precipitates, if homogenization techniques, outscoring the intensity of the vibratory mixer, are introduced. At any rate, as proven by the tabulation, volumetric sampling from homogenized suspensions permits to determine, with proper accuracy, both the Mn and active oxygen contents of the suspension and to calculate the Mn/O ratio.

Table 2

Composition (MnO_{1+x}) found	
in suspension $x=$	in filtered, washed and dried product $x=$
0,0296	0,3700
0,0466	0,3688
0,0338	0,3667
0,0389	0,3514
0,0356	0,3768
0,0409	0,3594
0,0436	0,3580
0,0416	0,3500

Another aim of the work reported here has been to find out the differences in oxidation degree and Mn/O ratio determined in the suspension itself (as shown above), on the one hand, and in the filtered, washed and dried solid product, on the other. Therefore, on the one hand, the MnO_{1+x} composition was determined directly in manganese(II)-hydroxide suspensions precipitated

from 0,05 M $MnCl_2$ solution by 0,1 M KOH or 0,1 N NaOH; on the other hand, other suspension aliquots were filtered, washed with ion-free water, dried at 60° C for 24 hours and then the composition of the resultant product was determined. The results are shown in Table 2.

As shown by the results, the precipitation-dependent oxidation degree, determined in the suspension itself, is much lower than the figure obtained for the filtered, washed and dried solid product which was precipitated under the same conditions and had a composition close to, and an oxidation degree somewhat higher than that of Mn_3O_4 ($MnO_{1.33}$).

So as regards the relationship between precipitation conditions and resultant product, it appears from the above that what is more logical to consider dependent on precipitation conditions is the oxidation degree of the fresh suspension rather than the figure found for the solid product after filtering and drying.

SUMMARY

An investigation into the oxidation of manganese(II)-hydroxide in aqueous solution and into relationships between the oxidation degree of precipitates and conditions of precipitation has revealed substantial differences between the Mn/O ratio in the suspension, on the one hand, and the oxidation degree of the product that resulted from the filtering, washing and drying of the precipitate, on the other. The techniques described here make it possible to determine the oxidation degree of manganese(II)-hydroxide and/or manganese oxide-hydrate directly in the fresh suspension. This fact seems to justify the view that it is the oxidation degree found in fresh suspension that depends on the conditions of precipitation rather than the composition and the Mn/O ratio determined in the filtered and dried solid product. In this latter case any change in oxidation degree is no longer dependent on the conditions of precipitation, but is provoked by post-precipitation processes such as filtering, washing, and drying.

REFERENCES

BRICKER, O. [1965]: Some Stability Relations in the System $Mn-O_2-H_2O$ at 25° and one Atmosphere Total Pressure. — Amer. Miner. *50*, pp. 1296—1351.

BUSER, W., P. GRAF, W. FEITKNECHT [1954]: Beitrag zur Kenntnis der Mangan (II)-manganite und des δ-MnO_2 — Helv. Chim. Acta *37*, pp. 2322—2333.

COLE, W. F., A. D. WADSLEY, A. WALKLEY [1947]: An X-ray Diffraction Study of Manganese Dioxide. — Trans. Electrochem. Soc. *92*, pp. 133—353.

COPELAND, L. C., F, S. GRIFFITH, C. B. SCHERTZINGER [1947]: Preparation of a Dry Cell Depolarizer by Air Oxidation of Manganous Hydroxide. — Trans. Electrochem. Soc. *92*, pp. 127—132.

FEITKNECHT, W., W. MARTI [1945a]: Über die Oxydation von Mangan (II)-hydroxyd mit molekularem Sauerstoff. — Helv. Chim. Acta *28*, pp. 129—148.

FEITKNECHT, W., W. MARTI [1945b]: Über Manganite und künstlichen Braunstein. — Helv. Chim. Acta *28*, pp. 149—155.

GATTOW, G. [1961]: Die Chemische Analyse von natürlichen und künstlichen Braunsteinen. — Batterien *15*, pp. 164—172.

GLEMSER, O., G. GATTOW, H. MEISIEK [1961]: Darstellung und Eigenschaften von Braunsteinen (I). — Z. Anorg. Allg. Chem. *309*, H. 1—2.

GATTOW, G., O. GLEMSER [1961a]: Darstellung und Eigenschaften von Braunsteinen (II). — Z. Anorg. Allg. Chem. *309*, H. 1—2.

GATTOW, G., O. GLEMSER [1961b]: Darstellung und Eigenschaften von Braunsteinen (III). — Z. Anorg. Allg. Chem. *309*, H. 3—4.

JOHNSON, R. S., W. C. VOSBURGH [1952]: The Reproducibility of the Manganese Dioxide Electrode and the Change of Electrode Potential with pH. — J. Electrochem. Soc. *99*, pp. 317—321.
KLEINERT, P. [1962]: Die analytische Untersuchung sogenannter anomaler Wertigkeiten in hochgeglühten Ferriten. — Acta Chim. Hung. *31*, pp. 339—345.
WADSLEY A. D., A. WALKLEY [1951]: The Structure and Reactivity of the Oxides of Manganese. — Rev. Pure and Applied Chem. *1*, pp. 203—212.

MRS ERIKA MOLNÁR
Institute of Mineralogy, Geochemistry
and Petrography
Attila József University at Szeged
Táncsics M. u. 2.
Szeged, Hungary

SOME CONTRIBUTIONS TO THE KNOWLEDGE OF ZEOLITES

MRS. É. PÉCSI-DONÁTH

Institute of Petrography and Geochemistry, Eötvös University, Budapest

INTRODUCTION

Of the 20 or so species of zeolite minerals lately investigated by the present author, rigorous structure determinations on unheated samples have been carried out recently for the following: laumontite [COOMBS, 1952], harmotome [SADANAGA et al., 1955], gmelinite, levyne [H. STRUNZ, 1956], faujasite [BERGERHOFF et al., 1958], natrolite [MEIER, 1960], stilbite [GALLIET al., 1960], ptylolite [J. BAUER et al., 1962], phillipsite [STEINFINK, 1962], gismondite [K. FISCHER, 1963], brewsterite [PERROTA et al., 1964]. Furthermore, the structure of dehydrated natrolite was determined by FANG [1963] and that of dehydrated and chlorinated chabasite by J. V. SMITH [1962]. These workers have determined by electron density measurements and Fourier analysis the atomic distances and the accurate atomic coordinates as well as the dimensions of the unit cells. Moreover, besides establishing the lattice structure, they provided information also about the positions of the cations and in some cases of the water molecules. However, several questions remained unanswered:

A) I. The temperatures at which zeolites heated to 1000 °C become amorphous roentgenographically.

II. The nature of the crystalline phases and structure variants, formed as a result of heating to lower temperatures.

III. Whether in the course of thermal decomposition up to 1000° C a new crystal lattice comes to exist, and if so, how, and what is the new mineral thus formed.

To answer these questions, the author has performed X-ray diffractometry on unheated zeolite samples and on samples heated to characteristic temperatures (the temperature of exo- and endothermic peaks on the DTA graphs).

B) Up till the last decade, the water content of zeolites was considered a function of ambient water vapour pressure, whose removal from the mineral caused no structural change and whose distribution within the structure was random. Water of this kind was called zeolite water. In most recent literature, however [AVERBUCH et al., 1950, J. V. SMITH, 1962, 1964, ROSHKOVA et al., 1962] it is stated as a result of research by the most up-to-date techniques that not all zeolites contain zeolite water and not all the water held in zeolites is zeolite water. It was KOIZUMI [1953] and PENG [1955] who, first applying the DTA method to the water content of zeolites, obtained some important results concerning the nature of zeolite water. Rigorous structure analysis [MEIER, 1960, J. V. SMITH, 1962] has shed light in some cases also

on the nature of the water bond, but these investigations did not establish the water loss *vs.* temperature relationship, and its correlation with structural changes, nor the precise nature of the initial and final phases and of the intermediate phases formed during the experiments. The complex approach resorted to in the present author's investigations (chemical analysis complemented with spectroscopy, X-ray diffractometry, infrared spectroscopy, DTA, dehydration, devolatilization analysis, derivatography and regeneration methods applied to the initial zeolite phase as well as to phases heated to the characteristic temperatures) made it possible to clean information as to the nature and the manifold aspects of water in zeolites.

C) Zeolites were first classified on the basis of morphological features; consequently,

1. fibrous, platy and cubic zeolites were distinguished, at first.

2. DEER's classification [1963] essentially rested on this basis, but also took into account whether the bond strengths of the $(SiAl)O_4$ tetrahedra in the tectosilicate lattice are stronger in one or two directions or equally strong in all three directions. DEER could thus distinguish the natrolite, heulandite and harmotome groups.

3. In his structural system, J. V. SMITH [1962] chose the number of interlinked tetrahedra and the mode of linkage as a basis. He distinguished the following main groups: 1. analcite, 2. sodalite, 3. chabasite, 4. natrolite, 5. phillipsite, 6. mordenite, 7. bikiatite, 8. zeolites of unknown structure.

4. Studying the escape of water from the zeolites, KOIZUMI [1953] classified them on the basis of their dehydration in to 1. natrolitic, 2. analcitic, 3. combinations of the two, and 4. zeolites belonging to neither of these types.

EXPERIMENTAL

A) I. Heating some natural zeolites, KOIZUMI [1960] observed the transitions

phillipsite →	wairakite + H_2O	at 260° C
scolecite →	wairakite + H_2O + anorthite	300° C
laumontite →	wairakite + H_2O	410° C
heulandite →	wairakite + H_2O + SiO_2	320° C
epistilbite →	wairakite + H_2O + SiO_2	350° C
wairakite →	anorthite + H_2O + SiO_2	465° C

at the temperatures listed on the right side. He found that the five natural zeolites listed above decomposed to wairakite at relatively low temperatures. On heating to higher temperatures (1000° C), it is known by common results of several researches that zeolites transform into feldspars.

Heating our zeolites we have determined their temperatures of decomposition or transformation. Listed according to J. V. SMITH's system, these are as follows.

1. Zeolites of the analcite type:	wairakite	465° C
2. Zeolites of the sodalite type:	faujasite	400° C
3. Zeolites of the chabasite type:	chabasite	700° C
4. Zeolites of the natrolite type:	natrolite mesolite scolecite	500—600° C
	thomsonite gonnardite	350° C

5. Zeolites of the phillipsite type:

phillipsite	400° C

6. Zeolites of the mordenite type in general

7. Zeolites of unestablished structure

heulandite	400° C
clinoptylolite, mordenite	above 1000° C
laumontite	800° C
the stilbite family	350° C

The figures mean those temperatures at which the mineral can still be identified by a few d(Å) values but above which it turns roentgenographically amorphous.

A) II. We could prove the presence of wairakite, first produced by KOIZUMI [1960] after the heating of some of our zeolites: phillipsite, laumontite, heulandite, epistilbite, chabasite and desmine [É. PÉCSI-DONÁTH, 1965, 1966]. The transformation of stilbite produced, besides wairakite, also heulandite in some cases and clinoptylolite in others [É. PÉCSI-DONÁTH, 1965] could also be shown.

A) III. We have established that

1. On heating, the d(Å) values of the new substance appear in some cases beside those of the old one as the new crystal lattice starts to develop. (Chabasite, gmelinite, levyne, mordenite, harmotome, brewsterite).

2. Some other zeolites pass through a roentgenographically amorphous state into a new crystalline phase. This is the case with species of zeolite not mentioned above.

3. Heating to 1000° C invariably produces a feldspar or feldspathoid, with the single exception of clinoptylolite which has proved to be roentgenographically amorphous at that temperature. The new lattices are mostly well-formed, with well-defined d(Å) values, but some are poorly crystallized. The products of transformation obtained at 1000° C are as follows:

Zeolite	Feldspar		Feldspathoid		Other
wairakite	anorthite				
chabasite	anorthite				
gmelinite	oligoclase				
levyne	oligoclase				
natrolite	albite	+	nepheline		
scolecite	anorthite				
mesolite	bytownite				
thomsonite	anorthite	+	nepheline		
phillipsite			nepheline		
harmotome	bytownite	+	$BaAl_2Si_2O_8 + KAlSi_3O_8$		
gismondite	anorthite				
mordenite	—				
heulandite	bytownite				
clinoptylolite	—				
laumontite	oligoclase				
brewsterite	anorthite	+	celsian	+	Sr-metasilicate
stilbite	anorthite				
epistilbite	anorthite				
parastilbite	anorthite				

4. In some zeolites the fact that the mineral turns amorphous roentgenographically merely means that the new structure is cryptocrystalline. Scolecite becomes almost completely amorphous roentgenographically beyond 350° whereas the DTA graph exhibits a sharp endothermic peak between 500 and 550° C. This suggests that on heating above 350° C scolecite develops a cryptocrystalline structure not resolved by the diffractometer. For this reason we experimented with imbibition with glycerine, as usual in clay mineral research, and with silicon oil, applied by us for the first time to zeolites. Scolecite heated to 350° C after such treatment gave an X-ray structure differing by slight intensity decreases from the unheated one. The substance treated in this same way and heated at 400° C still gave identifiable d(Å) values in spite of intensity decreases. Samples heated to 500 and 700° C, respectively, gave no structure in spite of the treatment, and at 1000° C, we obtained the anorthite structure.

B) As regards the nature of water in zeolites, we have studied:

1. The temperatures of formation of some partly or entirely dehydrated zeolite species and the nature of water contained in them.

a) On heating natrolite passes into metanatrolite, which is monoclinic as opposed to the original orthorombic structure. The unit cell dimensions, a_0 and b_0, change and so does the space group (from Fdd2 to F112). The temperature of formation of the „meta" variety was given by several authors [F. RINNE, 1890, G. TAMMAN, 1897, F. ZAMBONINI 1906—08, more recently M. H. HEY 1952, ROSHKOVA et al., 1962] as 300° C. It was, however, pointed out already by PENG [1955] and KOIZUMI [1957] that there is a temperature gap of about 100° C between the escape of water and the transformation of the structure. This was proved by more recent observations also by ROSHKOVA et al. [1962] and É. PÉCSI-DONÁTH [1962]. Metanatrolite is not, however — as contrary to prior opinion — fully dehydrated, as has been proved particularly by infrared spectroscopy, After losing the crystal water between 300 and 400° C and transforming between 500 and 600° C into the monoclinic variety called metanatrolite, the mineral still contains some water which escapes gradually up to 1000° C. From 500 to 600° C, the infrared absorption bands characteristic of the bond Si-O-Al[4] disappear and are replaced by the absorption band of Si-O-Al[6] which proves that the small amount of water still present in metanatrolite is adsorbed water adhering to the lattice (cf. Table 1.).

b) The following up of the scolecite-metascolecite transformation has also provided some new evidence. According to F. RINNE [1896], there are two varieties of metascolecite: from 180 to 220° C, partial dehydration produces metascolecite I, which, on further heating, assumes an orthorombic structure whilst retaining its pyroelectric property. According to M. H. HEY [1936], the metascolecite variety with $2H_2O$ occurs also as a natural mineral. According to KOIZUMI and ROY [1960], heating scolecite at 300° C produces anorthite and wairakite under the escape of water. Tracing the changes brought about by heating by means of the DTA method, the present author obtained the following results.

It could thus be established that the peak beginning at 170° C with its crest at 300° C, corresponding to a weight loss of 4,57 or 4,70 per cent, respectively (i.e. to the loss of one molecule of water), is the zone of formation of metascolecite I.

The further endothermic reaction with peaks given by KOIZUMI at 460, by PENG at 500° C indicates the formation of metascolecite II. We have found this peak to be double, with a total water loss of exactly, 4,57 and 4,70 per cent, respectively, indicating the escape of another molecule of water in two steps. As our sample was already amorphous roentgenographically at 500° C, the peaks at 540°

Table 1

Infrared absorption bands of natrolite (Fassa Valley, Tirol)

Unheated sample	Sample heated at		
	300° C	500° C	500° C
	in KBr		in nujol
	wave number (cm^{-1})		
400—460	400—465	400—460	400—460
415	415	425	415
425	420		430
445	445	445	
	485	490	500
510	510	510	570
545	545	545	
580	580	580	
600	600	600	
625	625	630	630
675	675	680	
730	720	720	730
		750	
		770	
		790	
800—1500	800—1500	820—1500	
840	850	840	
	880		
940	940	900	
970	970	930	
980	980	—	—
		1000	
1040	1040		
1060	1060	1050	
		1080	
1090	1090	1090	
	1630		
1640	1650	1630	
1670			
3700—3000	3700—3000	3520—3000	3720—3500
	3330	3330	3330
3400			
3540	3540	3540	3550
4540			
5100			

Table 2

Koizumi [1953]	Peng [1955]	É. Pécsi-Donáth [1962]	É. Pécsi-Donáth [1966]
100° C end.			
170 end.	170° C end.		
	weak	200° C end.	
240 double	310	310	310° C big broad end.
275			
300 small			
460 big sharp	500	460	480 small sharp
		490	520 big sharp
550	560	540	570 small sharp
			770 flat end.
			950 weak ex.

and 570° C indicate the transition into the amorphous state, that is, the water escapes inevediately thereafter. This water is presumably bound somewhat stronger as its escape gives rise to a small sharp endothermic peak. The water still left over in the lattice gradually escapes up to 1000° C, in two steps, but without giving rise to sharp endothermic peaks [É. PÉCSI-DONÁTH, 1966].

The transition scolecite → metascolecite can be traced also by means of infrared spectroscopy.

Table 3

Infrared absorption bands of scolecite (Attlitz Valley, Switzerland)

Unheated sample	Sample heated at			
	350° C	400° C	500° C	1000° C
	wave number (cm^{-1})			
470—400	520—400	525—400	535—400	450—400
410	410	410	410	410
425	425	430	430	430
	450	445	445	440
	460			
	475			
540				535
585	585			570
625	635	625		
		645		650
690				
720	740	720	720	780
	780			
800—1400	1350—810	1350—820	1140—820	1600—800
	840	830		840
		860		
		880		880
910	920	910	920	920
			980	940
1020	1150	1000		
		1100	1080	1100
		1170	1180	
		1220		
1110				
1470		1650		
1600				
1670	1680			
2850				
2920				
2960				
3800—3000	3740—3000	3700—3100	3300—3700	3300—3700
3230	3220			
	3240			
3330	3450	3450		
3410			3580	
3510	3550	3570		
	3580			
3610				
3640	3630	3640	3640	3640
			3680	
3690		3680		3690
3760	3760	3710		
5060				

The transformation into metascolecite I, up to 350° C, changes the infrared spectrum of the unheated material: besides the 3000 to 3800 cm^{-1} range with 5 or 6 sharp absorption bands, there turn up now 3 absorption bands also in the 1600 cm^{-1} range. These decrease in both number and intensity on heating to 350° C. (To 4 in the 3000 to 3800 cm^{-1} range, and to 1 in the 1600 cm^{-1} range.) Also in the absorption ranges typical of the silicate structure, the formation of the crypto-crystalline structure indicated by the DTA graph is reflected by substantial changes. The one molecula of water escaping on the scolecite — metascolecite I transformation is, in our opinion, bound like crystal water, because:

a) Its escape is accompanied by the disappearance of several sharp bands of absorption.

b) The unheated sample exhibits in the 4000 to 6000 cm^{-1} absorption range a sharp absorption band at 5060 cm^{-1}, which suggests the presence of crystal-water (Table 3).

The infrared spectrum of scolecite heated at 400° C already exhibits a more substantial change. The absorption bands suggesting the presence of some water have disappeared and there have remained in the silicate structure some almost indefinable areas of absorption. However, the transition metascolecite I—II lies about 100° C higher, at 500° C, because the second water molecule is expelled in two stages and the size of the second endothermic peak is incremented by a contribution from the process of formation of metascolecite II. This transition could not take place at a temperature higher than 500° C, either, because X-ray diffractometry has revealed the substance heated at 500° C to be amorphous roentgenographically. The endothermic peak at 540° C is due to the escape of the OH radicals bound to the tetrahedra. The regeneration graph proves that the crystal-water-like water of metascolecite I can be regenerated by rehydration, whereas the water of metascolecite II cannot, since the structure has become crypto-crystalline. The water imprisoned on lattice collapse — less than one molecula — escapes at a higher temperature, in two steps without any sharp endothermic reaction. (For figures see É. PÉCSI-DONÁTH [1965, 1966].)

c) As regards thomsonite, it was M. H. HEY [1952] who stated that this mineral reversibly passes into metathomsonite at 270 to 300° C or slightly above: the temperature of transition is a function of water content (thomsonite higher in water transforms at a lower temperature). In the course of her investigations, the present author has found the following DTA peaks, as compared with those of KOIZUMI [1953] *(Fig. 1)*.

X-ray diffractometry gave for thomsonite from three localities temperatures of structural transitions as seen in Table 5.

The dehydration graph *(Fig. 2)* shows the release of 5 molecules of water up

Table 4

KOIZUMI [1953]	É. PÉCSI-DONÁTH [1962]	É. PÉCSI-DONÁTH [1966]
75° C endo.	100° C endo.	250° C endo.
358 endo	350—360 endo.	—
428 endo.	420—430 endo.	420 endo.
523 endo.	460—520 endo.	460 endo.
	930—960 exo.	510 endo.
		560 endo.
		1010 exo.

Table 5

Origin	Base	300—325° C	425° C	460° C	500° C	525° C	560—580° C	600—800° C	1000° C
Theiss, Tirol	all thomsonite lines as in literature	thomsonite whith 1—2 lines of changed intensity (stronger or weaker)	1—2 very weak peaks resembling faroelite plus an amorphous phase	—	amorphous phase only	—	amorphous phase only	amorphous phase only	very strong lines of anorthite and nepheline
Dunbarton, Scotland			intensity weakened but still sharp peaks, amorphous phase subordinate	amorphous phase only	—	amorphous phase only	amorphous phase only		
Faröer Is. Iceland			a few lines all very weak, amorphous phase abundant	—	—	—	a few very weak lines plus an amorphous phase		

to 400° C. The escape of water in connection with the endothermic peak at 360° C indicates at the same time also the transformation into metathomsonite. The infrared spectrum of the unheated sample *(Fig. 3)* presents within the wide absorption range of water from 3800 to 2900 cm^{-1} a few narrow bands, at 3280 and 3400 cm^{-1} and also at 1680 and 1610 cm^{-1}. Heating to 350° C makes these disappear, so that only the wide band remains and even that with a much reduced intensity. Simultaneously, the absorption bands of the silicate structure also disappear (Table 6). The regeneration experiments have also shown that the mineral is capable of regeneration up to 250° C, whereas at higher temperatures rehydration takes place only immediately before the formation of the new phase *(Fig. 4)*.

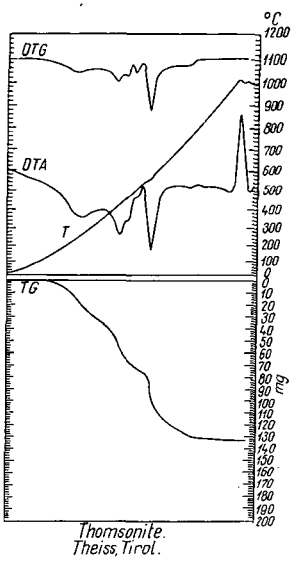

Fig. 1. Derivatogram of thomsonite (Fassa Valley, Tirol)

TAYLOR's [1933] rigorous examination of the structure revealed that thomsonite contains three types of water. These were called Aq1, Aq2 and Aq3 by TAYLOR. In his opinion, Aq1 and Aq2 are bound more strongly than Aq3 which is of the type found in natrolites.

Comparing this statement with our own findings we can state concerning the transition thomsonite → metathomsonite and the nature of the water involved that thomsonite loses half its water content (3 molecules, Aq3) up to 300° C, whereas on heating to 400° C it loses another two molecules in crystal-water-type bond (Aq1 and Aq2) while it passes into metathomsonite. The removal of these latter gives rise to a sharp peak in the DTA graph and to the

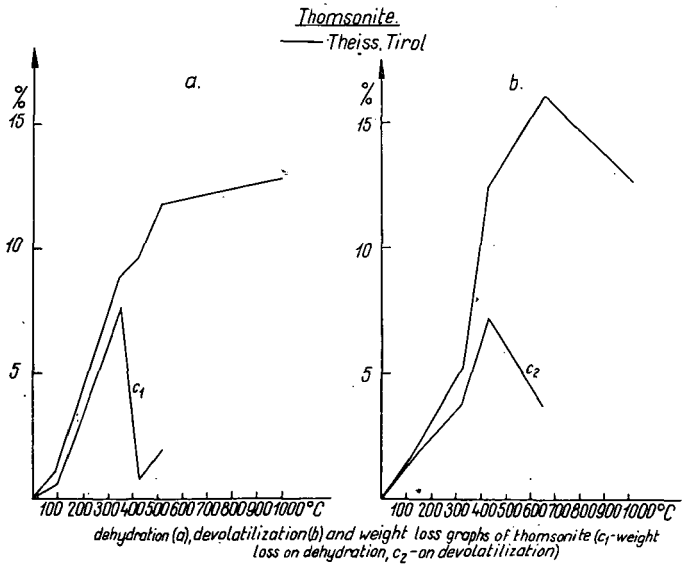

Fig. 2. Dehydration and devolatilization graphs of thomsonite

disappearance of the narrow bands of absorption in the wide range from 3850 cm^{-1} to 2800 cm^{-1} in the infrared spectrum. Dehydration is accompanied by loss of structure up to 430° C. The one molecule of water left in the structure then escapes up to 700° C.

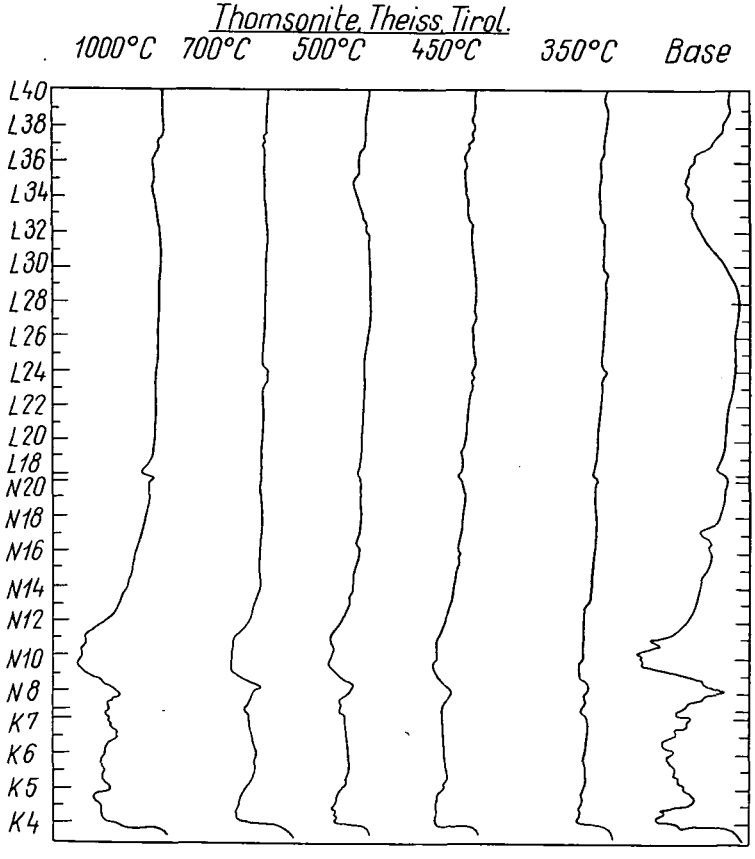

Fig. 3. Infrared spectra of thomsonite; unheated, and after heating to 350 and 1000 °C, respectively; with KBr pills

2. As regards water in the various sorts of zeolite, it has been pointed out in the papers already cited of KOIZUMI, PENG, ROSHKOVA, AVERBUCH, SMITH etc. that „zeolite water" is a complicated notion. An evaluation of the complex experiments performed by the present author on some of the zeolite species has made it possible to establish the nature of the water bond, and moreover to find out wether the water is typical zeolite water or not. Water in natrolite is largely crystal-water and so is water in scolecite, mesolite, thomsonite and laumontite. The presence of crystal-water in crystal-water-type bond is proved *a)* by repeated weight loss at given temperatures on the TG graph, *b)* by sharp endothermic peaks on the DTA graph, *c)* by narrow bands of absorption in the infrared spectrum, *d)* by characteristic bands in the long-wave infrared (4000 to 6000 cm^{-1}), *e)* fine structure investigations published in literature (natrolite: MEIER et al. [1960], laumontite: COOMBS [1952]

Table 6

Infrared absorption bands of thomsonite (Theiss, Tirol)

Unheated sample	Sample heated at				
	350° C	450° C	500° C	700° C	1000° C
wave number (cm^{-1})					
410	405	410	410		
435	425	440	440	440	450
455		475			
505			500		
540		520	520		535
585	585				570
630		610			
660	680	670	690		
710		710	710	710	675
910		920			720
940	940		950	960	930
1000			1030		1030
1070	1070	1050			1090
1230	1270	1170			1370
1430					
1480	1480		1480		1460
1530	1530				
1610		1610	1640		1630
1680	1690				
	2080				
		2400			
3850					
2800	3500	3700	3750		3720
	2940	3100	3180		3100
3400	3400				
3580		3550	3460		3460
3630		3670	3630	3680	3620
		3690		3690	
		3740	3740	3740	3700

etc.) have proved that the water molecules occur in definite positions, annexed to definite cations by hydrogen bridge bonds.

In some other zeolites (chabasite, levyne, gonnardite, harmotome, stilbite) the above-mentioned measurements have also proved the presence of crystal-water, even if in a less striking form. In the course of the dehydration of chabasite, the weight loss measurable up to and above 500° C, the narrow absorption band at 3400 cm^{-1} and the drawn-out one between 3000 and 3700 cm^{-1} even at 560° C indicate that water is still present in chabasite at this temperature although not in the form of crystal-water. Thus water stays in the structure up to fairly high temperatures (to 800° C) and forms on the DTG graph a well-defined peak corresponding to the OH radicals bound to the $(Si,Al)O_4$ tetrahedra. Hence, this water is present in hydroxyl form. According to several authors it is largely bound to the Al substituting the Si in the $(Si, Al)O_4$ tetrahedra of the silicate lattice.

A small group of zeolites (gmelinite, edingtonite, gismondite, brewsterite, clinoptylolite, heulandite, mordenite) largely contains „zeolite water" in the classical sense: this water moves freely about in the structure, without being bound to any well-defined position or cation. Its distribution is random. One of its types is water around the cations, in coordination with it, which represents a special type among

zeolites. It is not bound by a strong OH bond to the cation: on the contrary, it forms a hydrate shell about it without the development of any strong cation-OH bond.

The weak binding of these H_2O molecules is proved:

a) by the endothermic trough without a well-defined peak, indicative of gradual water escape, on the DTA graph,

b) by the gradual weight loss indicated by the TG graph,

c) by the broad, elongate absorption band about the 3000 cm^{-1} wave number, characteristic of water, and the complete absence of any absorption in the higher wave number range (4000 to 6000 cm^{-1}),

d) by a largely constant ability of almost total rehydration, in spite of heating up to 1000° C, or, more precisely speaking, up to the temperature of transformation of the structure.

Most of the zeolites contain besides the much-examined and easily distinguished types of water enumerated above one or two molecules of water which gradually escape on heating at higher temperatures. This water escapes in most cases in a temperature range where diffractometry already reveals a roentgenographically amorphous substance. Considering that e.g. in the case of scolecite a cryptocrystalline structure could be surmised in spite of this, the water in question is in our opinion a water bound to the disintegrating tectosilicate lattice, imprisoned by the collapsing structure up to quite high temperatures.

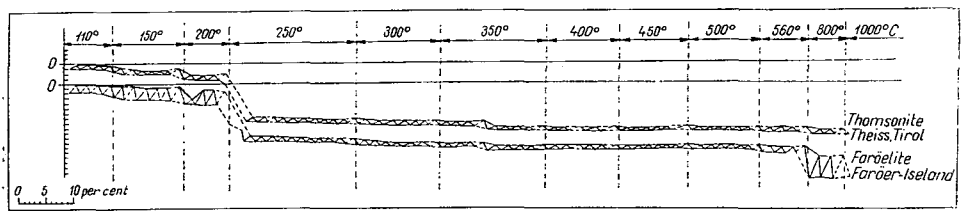

Fig. 4. Regeneration graphs of thomsonite and faroelite

It is recorded in literature that silica gels are capable of storing water and gradually letting it escape up to quite high temperatures. The escape of this type of water is not accompained by a sharp endothermic reaction. Water loss is indicated partly by weight loss (dehydration measurements), and partly by the prolonged descent of the TG graph also at high temperatures. We are of the opinion that this type of water is lattice-bound and we have found it invariably in zeolites which carry water bound to the lattice in the form of OH radicals (e.g. in natrolite).

3. The rehydration properties of zeolites are partly structure dependent and partly determined by the nature of the water content.

a) It is a general experience that zeolites heated to constant weight at a given temperature can always be rehydrated, provided the structure was not destroyed to a roentgenographically amorphous state.

b) Natrolite, scolecite, etc., that is, the zeolite species largely containing crystal-water lose very little water if any, up to a temperature characteristic of the mineral species, and hence they do not rehydrate, either *(Fig. 5)*. Heated at a given temperature, these minerals lose most of their water content, but on rehydration they take in one or two per cent more than they have lost (they are strongly „activated"). This feature is preserved over a temperature interval of 100 to 150° C. On heating to higher temperatures these minerals lose their capacity of rehydration,

and take in but small quantities of water, presumably by adsorption on the surface. The amount of the water thus attached remains below 0,5 per cent. The zeolites containing crystal water and water in hydroxyl bond, as well as the minerals largely containing zeolite water (chabasite, harmotome, clinoptylolite, mordenite etc. which become reontgenographically amorphous only at high temperatures) rehydrate almost completely *(Fig. 6)*. A drop in rehydration takes place after the loss of crystal-water, but rehydration is still significant up to the complete collapse of the structure.

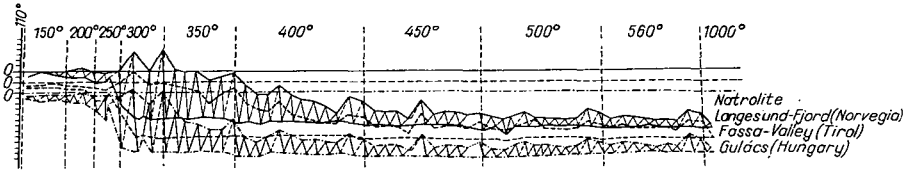

Fig. 5. Regeneration graph of natrolite

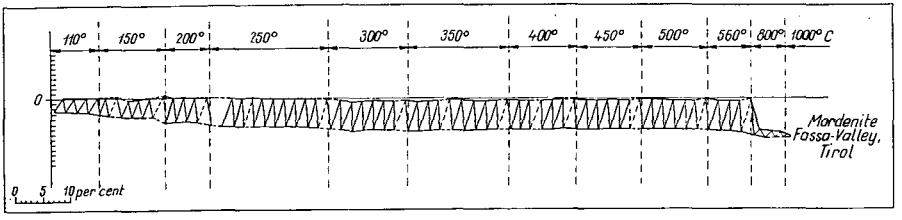

Fig. 6. Regeneration graph of mordenite

A peculiar group as regards the capacity of rehydration is that of thomsonite, which, when heated to higher temperatures, exhibits a second rehydration at the beginning of the formation of the new crystalline phase. It was proved by X-ray analysis that at the given temperature the new lattice was not as yet fully developed whereas the old one was considerably disintegrated. The capacity of rehydration dissappeared with the full development of the new crystalline phase.

C) On the basis of their manifold and typical water contents, zeolites can be classified, according to a new system, as follows:

1. Zeolites with water mainly in crystal-water form:
natrolite, scolecite, mesolite, etc.

2. Zeolites containing water in the crystal-water form but also in the form of OH radicals bound to the lattice:
chabasite, desmine, etc.

3. Zeolites with typical zeolite water, in which some of the water forms hydrate shells about the cations:
mordenite, clinoptylolite, etc.

All three groups contain, however, besides the above-mentioned types of water also the so called lattice-bound water.

SUMMARY

For the 20 or so species of zeolite studied, transformation temperatures have been established. The transformation into wairakite, of some zeolites and to heulandite or clinoptylolite of others, have been observed. As a new technique, imbibiton with siliconoil has been introduced in the X-ray diffractometry of certain zeolite structures.

Concerning the nature of the water content of the several „meta" varieties coming to exist on heating and of the water in unheated zeolites it is possible to state that

1. natrolite, scolecite and thomsonite contain water in a crystal-water-type bond, and the meta variety is formed about 100° C above the escape of this water,

2. the lattice that became roentgenographically amorphous by heating still imprisons about one molecula of water until much higher temperatures;

3. Zeolites contain

a) water in crystal-water-like bond,
b) the above type of water plus water bound to the lattice by OH bonds,
c) typical zeolite water.

It is characteristic of all three types that some small amounts of water are preserved strongly bonded to the tetrahedra of the disintegrating lattice.

4. On the basis of rehydration properties, the above groups containing various types of water are easily distinguished, and this may serve as a basis for a new classification.

REFERENCES

AVERBUCH, P., P. DUCROS, X. PARÉ [1950]: Resonance magnétique nuclaire des protons dans la chabasie. — Cr. Acad. sci. vol. *250*, N. 2.

BAUER, J., R. HRICHOVÁ [1964]: Ptilolit (Mordenit) von Teigerhorn, Island. Slomik Vys. Skoly Chem. Techn. Miner. Praha. 27—36.

BERGERHOFF, G., W. H. BAUR, W. NOWACKI [1958]: Über die Kristallstruktur des Faujasites. — Neues Jahrb. Mineral. *9*, 193—200.

COOMBS, D. S. [1952]: Cell size, optical properties and chemical composition of laumontite and leonhardite. — A. Mineral. *37*, 812—830.

DEER, W. A., R. A. HOWIE, J. ZUSSMANN [1963]: Rock-forming Minerals IV. London, Longmans.

FANG, J. H. [1960]: Ph. D. Dissertation, Pennsylvania State University, Part 2. Dehydrated Natrolite.

FISCHER, K. [1962]: The crystal structure determination of the zeolite gismondite, $CaAl_2Si_2O_8 \cdot 4H_2O$. Submitted to Am. Mineral.

GALLI, J., G. GOTTARDI [1966]: The crystal structure of stilbite. — Min. Petr. Acta. 1—10.

HEY, M. H., F. A. BANNISTER [1932]: Studies on the zeolites, Part III. Natrolite and metanatrolite. — Mineral. Mag. *23*, 243—289.

HEY, M. H., F. A. BANNISTER [1936]: Studies on the zeolites, Part IX. Scolecite and metascolecite. — Mineral. Mag. *24*, 227—253.

HEY, M. H., F. A. BANNISTER [1932]: Studies on the zeolites. Part II. Thomsonite, faroelite and gonnardite. — Mineral. Mag. *23*, 51—125.

KOIZUMI, M. [1953]: The differential thermal analysis curves and dehydration curves of zeolites. — Mont. Journ. (Japan) I. 36.

KOIZUMI, M. and R. ROY [1960]: Zeolite studies I. Synthesis and stability of the calcium zeolites. — Journ. Geol. *68*, 41.

MEIER, W. M. [1960]: The crystal structure of natrolite. — Zeitschr. f. Krist. *113*, 430—444.

MEIER, W. M. [1961]: The crystal structure of mordenite (ptilolite). — Zeitsch. f. Krist. *115*, 439—450.

PENG, C. J. [1955]: Thermal analysis of the natrolite group. — The Amer. Miner. *40*, 834.

PERROTA, A. J., J. V. SMITH [1964]: The crystal Structure of Brewsterit (Sr, Ca, Ba) $(Al_2Si_{10}O_{16})5 \cdot H_2O$. —Acta Cryst. *17*, 857—862.

PÉCSI-DONÁTH, É. [1965]: On the individual properties of some Hungarian zeolites. — Acta Geol. *IX*, 235.
PÉCSI-DONÁTH, É. [1966]: On the relationships between lattice structure and „zeolite water" in gmelinite, heulandite and scolecite. — Acta Miner. Petr. Szeged *XVII*, Fasc. 2. 143—158.
PÉCSI-DONÁTH, É. [1962]: Investigation of the thermal decomposition of zeolites by the DTA method. Acta Geol. *VI*, Fasc. 3—4. 429—442.
RINNE, F. [1890]: Über die Veränderung welche die Zeolithe durch Erwärmung bei und nach dem Frübewerden erfahren. — Sitzungsb. d. k. pr. Ak. der Wiss. 1163.
RINNE, F. [1894]: Beitrag zur Kenntnis des Skolezite. Ebenda, 11, 51—68.
Рожкова, Е. В. — К. С. Ершова, — Н. И. Андруценко [1962]: О воде в цеолитах. Москва Минеральное сырье, вып. 6.3.
SADANAGA, R. F., Y. RAKÉUCHI [1961]: The crystal structure of harmotome, $Ba_2Al_4Si_{12}O_{32} \cdot 12H_2O$. Acta Cryst. *14*, 1153—1162.
SMITH, J. V. [1963]: Structural classification of zeolites. — Min. Soc. of Am. Spec. Paper 1. 281.
SMITH, J. V. [1962]: Crystal structures with a chabazite framework: I. Dehydrated Ca-chabazite. — — Acta Cryst. *15*, 835—845.
SMITH, J. V., F. RINALDI and L. S. DENT GLASSER [1963]: Crystal structures with a chabazite framework: II. Hydrated Ca-chabasite at room temperature. — Acta Cryst. *16*, 45—53.
SMITH, J. V., C. R. KNOWLES, F. RINALDI [1964]: Hydrated Ca-chabasite at ± 20 and — 150 °C. — Acta Cryst. *17*, 374—384.
SMITH, J. V., J. H. FANG [1964]: IV. Reconaissance of the complex. — Journ. Chem. Soc. 3749—3758.
STEINFINK, H. [1962]: The crystal structure of zeolite, phillipsite. — Acta. Cryst. *15*, 644—651.
STRUNZ, H. [1956]: The zeolites gmelinite, chabazite, levyne. — Neues. Jahrb. Mineral. Mh. *11*, 250—259.
TAYLOR, W. H., C. A. MEEK, W. W. JACKSON [1933]: The structures of the fibrous zeolites. — Zeitschr. Krist. *84*, 373—398.
TAMMAN, G. [1898]: Über die Dampfspannung von Kristallisierten Hydraten deren Dampfspannung sich kontinuierlich ändert. — Zeitschr. f. phys. Chem. *27*, 323.

Mrs ÉVA PÉCSI—DONÁTH
Institute of Petrography and Geochemistry, Lóránd Eötvös University
Budapest VIII, Muzeum krt. 4/a, Hungary

ÜBER GRANITISCHE VERDRÄNGUNGSGÄNGE IM DIORIT DER BROCKENMASSIV-OSTRANDZONE (Harz)

ROLF SEIM und JÜRGEN EIDAM

Sektion Geologische Wissenschaften der Ernst-Moritz-Arndt-Universität Greifswald

1. EINFÜHRUNG

In einer vorausgegangenen Arbeit wurden metasomatische Prozesse an einem Diorit-Granitkontakt im Brockenmassiv beschrieben. Aus einem Gabbrodiorit entstanden durch K(Na)-Feldspat- und Quarzeinsprossung granodioritische Gesteine. Dünnschliffintegrationen ergaben, daß die Metasomatose mit einem Abbau von Bronzit/Diopsid und Plagioklas verbunden ist.

Inzwischen haben wir bei Geländearbeiten in der Ostrandzone des Brockenmassivs festgestellt, daß metablastische Diorite ziemlich verbreitet sind. Solche Gesteine häufen sich im Grenzbereich Diorit-Granit. Außerdem fanden wir an einigen Stellen innerhalb des Diorits recht instruktive Beispiele für die Entwicklung von *Verdrängungsgängen* (replacement dikes), wie sie von GOODSPEED [1940] definiert und von BURKE [1959], JANARDAN [1959], EFIMOV & IVANOVA [1963] und anderen Autoren in ähnlicher Ausbildung beschrieben wurden. In diesen Fällen handelt es sich jedoch meist um Verdrängungsgänge in Metamorphiten bzw. Migmatiten. In solchen Gesteinen vor sich gehende Prozesse sind nicht immer leicht überschaubar, so daß bisweilen mehrere Deutungsmöglichkeiten bestehen. Das gilt insbesondere für die Zone zwischen dem Altbestand und dem neugebildeten Ganggestein, die sich durch eine Anreicherung femischer Bestandteile auszeichnet. Die beiden Möglichkeiten — basische Front oder Melanosom — hat MEHNERT [1959] in seiner ausführlichen Besprechung des Granitproblems gegenübergestellt (Abb. 5, S. 142). Im ersten Fall entstand die an Mafiten angereicherte Zone durch Exsudation leukokrater Minerale (Quarz und Feldspäte) im Verlauf einer hochgradigen Metamorphose: wir sprechen von partieller Anatexis. Die Stoffmobilisation ist dabei an bestimmte pT-Bedingungen gebunden, die das *gesamte* Gestein betreffen und die durch experimentelle Untersuchungen recht gut bekannt sind [WINKLER & v. PLATEN, 1957 bis 1960]. Im anderen Fall haben sich die femischen Komponenten vor einer Verdrängungszone angereichert, wobei die Umbildung ein unterschiedliches Ausmaß erreicht haben kann. Sichere Beispiele einer solchen Verdrängung und Mobilisation sind in erster Linie in magmatischen Ausgangsgesteinen zu erwarten, in denen es durch Zufuhr alkalisilikathaltiger Lösungen, verbunden mit einer lokalen Temperaturerhöhung, zu engräumigen Stoffaustauschprozessen kam.

In diesem Zusammenhang darf darauf hingewiesen werden, daß REITAN [1960] sich mit der genetischen Bedeutung von zwei Typen basischer Zonen, die schmale Pegmatitadern begleiten, ausführlich befaßt hat. Bei dem ersten, oft zu beobachtenden Typ sind die immobilen Elemente — gewöhnlich Mg, Fe und zum Teil Ca — in unmittelbarer Nachbarschaft der Pegmatitadern angereichert, während die mobilen Elemente Si, Al und die Alkalien eine gegenläufige Tendenz zu erkennen geben. Bei dem zweiten, bisher selten beobachteten Typ, bildet sich eine Konzentration der immobilen bzw. eine Verarmung der mobilen Stoffe in einer gewissen Entfernung vom Pegmatit-Nebengesteinskontakt ab. Schließlich erwähnt dieser Autor, daß durch K-Zufuhr bewirkte Umbildung von Amphibol zu Biotit eine „basische Zone" vortäuschen kann, so daß Modalanalysen und/oder chemische Analysen erforderlich sind, um sicher zu gehen.

Die petrographische Untersuchung von Verdrängungserscheinungen liefert ganz allgemein wichtige Hinweise zur Stoffmigration und -akkumulation. Natürlich sollten im Handstück- und Aufschlußbereich gewonnene Resultate nicht auf größere Räume übertragen werden, sondern vielmehr Prozesse im Kleinbereich eindeutig von großräumigen Metasomatosen abgegrenzt werden. Nach unserer Auffassung ist es abwegig, Saumbildungen von basischen Einschlüssen in einem Granit als Beispiel einer „Granitisierung" oder „an example of the initial phase of granitization" [HÄRME & LAITALA, 1955] zu bezeichnen, wenn die entstandene Mineralassoziation weder im Mineralbestand noch im Chemismus granitähnlich wurde. Biotitreiche Reaktionszonen um (Meta-) Basiteinschlüsse im Granit oder Gneis sind verbreitet, ohne daß dabei an Granitisationsvorgänge gedacht werden muß.

Metasomatische Vorgänge sind oft schwer zu beweisen, weil die Umbildung nur selten vom Ausgangsgestein bis zum Endstadium über alle Zwischenstufen hinweg verfolgt und durch Mineral- bzw. Gefügerelikte belegt werden kann. Meist läßt sich die stoffliche Gleichartigkeit benachbarter Gesteinstypen vor der Umwandlung nur annehmen, nicht aber beweisen. Es ist kein Zufall, daß in Verbindung mit Granitisationshypothesen, trotz eingehender Gelände arbeiten und petrographischer Studien, gelegentlich Fehlurteile zustande kamen. So hat zum Beispiel BOWES [1953] die Granitisation eines australischen Tillites beschrieben und durch chemische Analysen ergänzt, obgleich die „granitisierten" Bereiche, wie später CHINNER, SANDO & WHITE [1956] zeigten, ehemalige Granitgeschiebe darstellen.

Verhältnismäßig klar sind Metasomatosen, wenn sie sich auf einem engen Raum abspielen und wenn die Umbildung auf Grund eines steilen Temperaturgefälles oder kurzzeitiger Stoffzufuhr nicht durchgreift. Als derartige „Initialstadien" der Metasomatose, die nicht selten den Schlußakt einer magmatischen Entwicklung des betroffenen oder eines benachbarten Gesteins darstellen, haben wir einen Teil der Verdrängungsgänge zu betrachten. ABDULAEV [s. PALIVCOVA, 1960] schlägt vor, solche Gangbildungen als „Meta-Gesteinsgänge" zu benennen. Diese Bezeichnung wird von uns abgelehnt, weil sie im deutschsprachigem Schrifttum zu Mißverständnissen führen würde. Man verstünde darunter metamorphe Ganggesteine, wie z.B. epizonal beanspruchte (mylonitisierte) Granitgänge. Indessen erscheint ABDULAEV's Einteilung der metasomatischen Gangbildungen in

a) Gesteinsgänge der magmatischen Metasomatose als Resultat der Granitisation in den Gesteinen des Rahmens und

b) Gesteinsgänge der postmagmatischen Metasomatose als Ergebnis der Verdrängung durch postmagmatische Lösungen innerhalb des Intrusivkörpers

als brauchbar, wenngleich die Trennung zumeist schwierig sein dürfte.

2. VERDRÄNGUNGSGÄNGE IM DIORIT

Geländebefund: Unser Material entstammt dem Dioritsteinbruch im Braune-Wassertal 700 m nördlich vom Großen Thumkuhlenkopf und dem Steinbruch an den Hippeln westlich vom Kantorkopf (Meßtischblatt Wernigerode, Nr. 2305). Im Braune-Wassertal grenzt der Quarzbiotitaugitdiorit des Brockenplutons an mittel- und oberdevonische Schichten des sudetisch oder asturisch gefalteten Rahmens. In diesem Steinbruch sind die Verdrängungsgänge besonders gut ausgebildet. Sie erreichen eine Mächtigkeit bis zu 20 cm und unterscheiden sich von ausgesprochenen Dilatationsgängen, die im gleichen Gebiet beobachtet werden können, durch starke Mächtigkeitsschwankung und eine ausgesprochen buchtige Grenze zwischen der granitoiden Gangfüllung und dem benachbarten Diorit *(Abb. 1)*.

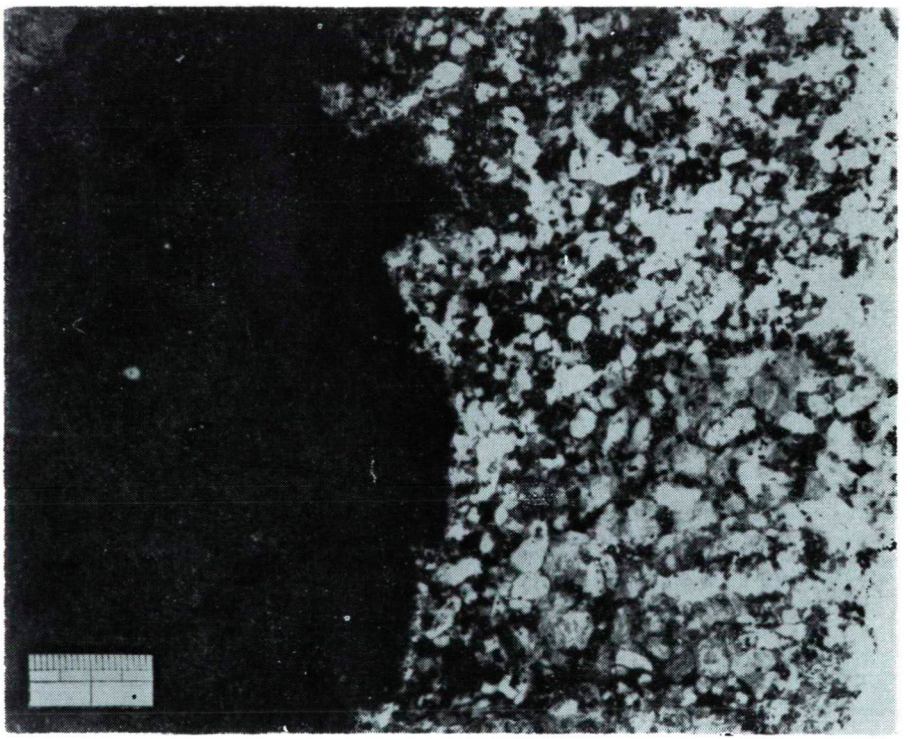

Abb. 1. Buchtige Grenze zwischen dem Diorit und dem granitoiden Ganggestein. Im Diorit etwa 1 cm breite dunkle Saumzone; im Ganggranit zahlreiche Reliktbestände der femischen Bestandteile des Diorits.

Mitunter ist zu sehen, wie die Verdrängung entlang feiner Risse etwas weiter in den Diorit vorgedrungen ist. An der Grenze hat sich im Diorit ein etwa 1 Zentimeter breiter dunkler Saum ausgebildet.

Im Gang sind stellenweise Relikte des Diorits vorhanden. Die Übergangszone ist durch porphyrisches Gefüge gekennzeichnet, während in der Gangmitte grobkörniger Granit auftritt. Das Ganggestein ist stellenweise reich an Mafitresten (*Abb. 1* rechts oben) und unterscheidet sich dann merklich von den gewöhnlichen

Granitgängen. Die Verdrängung des Diorits ist an dessen Kluftgefüge gebunden und somit jünger als die Anlage der prototektonischen Klüfte [CHROBOK, 1964]. Die vom Kluftnetz vordringende Umwandlung führt gelegentlich zu einer ballenförmigen Zerlegung des Diorits. Auch dann weisen die vom granitoiden Material umgebenen Dioritschollen eine cm-mächtige dunkle Saumzone auf.

Zweifellos können in einem weiteren Umwandlungsstadium chorismatische Gefüge, die den Eindruck einer Schollenassimilation bzw. Eruptivbrekzie erwecken, entstehen. Derartige Verhältnisse treffen wir an der Granit-Dioritgrenze im Holtemmetal kurz unterhalb der Steinernen Renne an. In diesem Aufschlußgebiet am SE-Hang des Holtemmetals „schwimmen" gerundete Diorit-„Einschlüsse" im Granit. Offenbar befinden wir uns in einem etwas tieferem Anschnittniveau. Wir können nicht eindeutig entscheiden, ob metasomatische oder intrusive Vorgänge wirksam waren. Vielleicht läßt sich durch petrographisch-geochemische Untersuchungen und durch ein gründliches Studium der Gefügeentwicklung in sicheren Metasomatiten eine Klärung darüber herbeiführen, ob ein Intrusivverband vorliegt oder durch vorangeschrittene Verdrängung eine granitische Zusammensetzung erreicht wurde. Wir müssen von vornherein damit rechnen, daß metasomatische Prozesse und Schollenassimilation ähnliche Gefügebilder hervorbringen. Die hier angeschnittenen Möglichkeiten erschweren die von ERDMANNSDÖRFFER [1951] vorgeschlagene Trennung zwischen „Intrusivgraniten" und „in-situ-Graniten" erheblich.

Dünnschliffbild und Variation des Mineralbestand s

Für die Bestimmung der quantitativ-mineralogischen Zusammensetzung und für Dünnschliffuntersuchungen wurden die megaskopisch abgrenzbaren Zonen bzw. die Übergangsbereiche eines Verdrängungsganges mit der Trennschleifmaschine MINOSECAR FR-Z des VEB Rathenower Optische Werke herausgeschnitten und Schliffserien angefertigt. Im Anschluß daran erfolgte die Ermittlung des Modalbestands mit dem Punktzählgerät ELTINOR der gleichen Firma. Untersuchungen am Diorit des Brockenmassiv-Ostrandzone und an Granitvarietäten des Brockenmassivs wurden zum Vergleich ebenfalls vorgenommen.

Die Veränderungen im Mineralbestand sind in einer graphischen Darstellung veranschaulicht (*Abb. 2*). Dabei wurde zwischen folgenden Gesteinstypen bzw. — varietäten unterschieden:

1 Diorit-Normalvarietät vom Ostrand des Brockenmassivs
2 Diorit neben dem Verdrängungsgang
3 Dunkle Saumzone im Diorit neben dem Verdrängungsgang
4 Metablastischer Diorit unmittelbar neben der Saumzone
5 Metablastischer Diorit in etwas größerer Entfernung
6 Granitoider Gang „granit" mit Gefüge- und Mineralrelikten
7 Granit aus der Mitte des Verdrängungsganges
8 Mittelwert und Variationsbreite von Brockengranitvarietäten.

In einer Serie von Gesteinsdünnschliffen ließen sich folgende Beobachtungen anstellen:

Der fein- bis mittelkörnige *Normaldiorit* des Brockenmassiv-Ostrandzone besteht aus Plagioklas (zonar 65—15% An), monoklinem und rhombischem Pyroxen, Biotit und Hornblende. In fast allen Proben sind Quarz und Kalifeldspat in geringer Menge enthalten. Akzessorische Bestandteile sind Apatit, wenig Zirkon und Erz. Als sekundäre Bildungen treten vor allem Epidot, Chlorit und Serpentin auf. Im Dioritsteinbruch im Braune-Wassertal ist eine Amphibolitisierung der femischen Komponenten auffällig. Das Gefüge bildet eine Kristallisationsfolge mit Plagioklas, Bronzit und Diopsid als Erstausscheidungen und Biotit/Hornblende, Quarz und Kalifeldspat als jüngeren Gemengteilen ab, wobei die Quarz-Kalifeldspatbereiche nicht selten fleckenartig im Gestein verteilt sind.

Schlierigkeit, starke Korngrößenvariation, Einschlußführung und chemische Variabilität, wie sie den durch Transformation oder Assimilation entstandenen Dioriten eigen sind, fehlen weitgehend. Die petrogenetischen Prozesse, die für die Bildung solcher intermediärer Gesteine in Frage kommen, haben MEHNERT und BÜSCH [1966] zusammengestellt und insbesondere den Prozeß der Dioritbildung durch Remobilisation an geeigneten Aufschlüssen gut untersucht. Für die Diorite des Brockenmassivs dürfte als Bildungsweise eine magmatische Differentiation Gabbro → Diorit oder die Intrusion einer dioritischen Schmelze, die in der Kruste durch anatektische Vorgänge aus Altbestand geeigneter Zusammensetzung hervorging, anzunehmen sein.

Der Modalbestand verweist den überwiegenden Teil des Gesteins in die Gruppe der Quarzdiorite bzw. Tonalite. Es existieren lokal auch gabbroide Typen mit entsprechend höherem Anorthitgehalt des Plagioklases (bis max. 80% An).

Der *Diorit neben dem Verdrängungsgang* zeichnet sich durch einen etwas höheren Gehalt an Mafiten und einem geringeren Quarzgehalt aus, während die Plagioklasmenge derjenigen des Normaltyps entspricht. Insbesondere hat der Biotitgehalt zugenommen, was sich im Dünnschliff durch xenoblastische Biotittafeln, welche nicht selten Plagioklasleisten umschließen, bemerkbar macht.

In der *dunklen Saumzone im Diorit neben dem Verdrängungsgang* hat sich der Gehalt an mafischen Komponenten weiter erhöht. Auffälligerweise ist hier auch etwas mehr Quarz anzutreffen, wogegen die Plagioklasmenge verringert erscheint. Charakteristisch für diese schmale Zone ist die Bildung kleiner Diopsidkörner, die sich besonders in den Plagioklasleisten ansiedeln. Während der feinkörnige Diopsid ganz frisch erscheint, ist der Biotit größtenteils chloritisiert. In unmittelbarer Nähe der Verdrängungsfront und auf schmalen Rissen haben sich Hornblendeaggregate ausgebildet. Die Anorthitgehalte in den unzersetzten Bereichen der Plagioklasleisten sind die gleichen, wie im Normaldiorit (⌀ 45% An). Es ist augenfällig, daß sich in dieser dunklen Saumzone bei der Granitisierung des Diorits mobilisierte Elemente (Ca, Mg, Fe) angereichert haben. Der überwiegende Teil dieser Mobilisate wird jedoch entlang des Druckgefälles migriert sein. Diese Annahme müssen wir machen, weil Betrachtungen zur Stoffbilanz zu dem Ergebnis führen, daß nur ein Bruchteil der bei der Gesteinsumbildung mobilisierten Elemente in dieser Saumzone fixiert sein kann.

Im *metablastischen Diorit unmittelbar neben der Saumzone* macht sich eine sprunghafte Quarzzunahme bemerkbar, und zwar zugunsten der melanokraten Gemengteile. Quarz korrodiert die femischen Bestandteile (Diopsid/Bronzit) und stellenweise auch Plagioklas.

Akzessorischer Apatit und opake Bestandteile werden von den klein- bis mittelkörnigen Quarzen übernommen. In dieser Zone erfolgt eine deutliche Kornvergröberung, doch sind nicht selten inselförmige Reliktpartien der Saumzone zu beobachten. Im großen

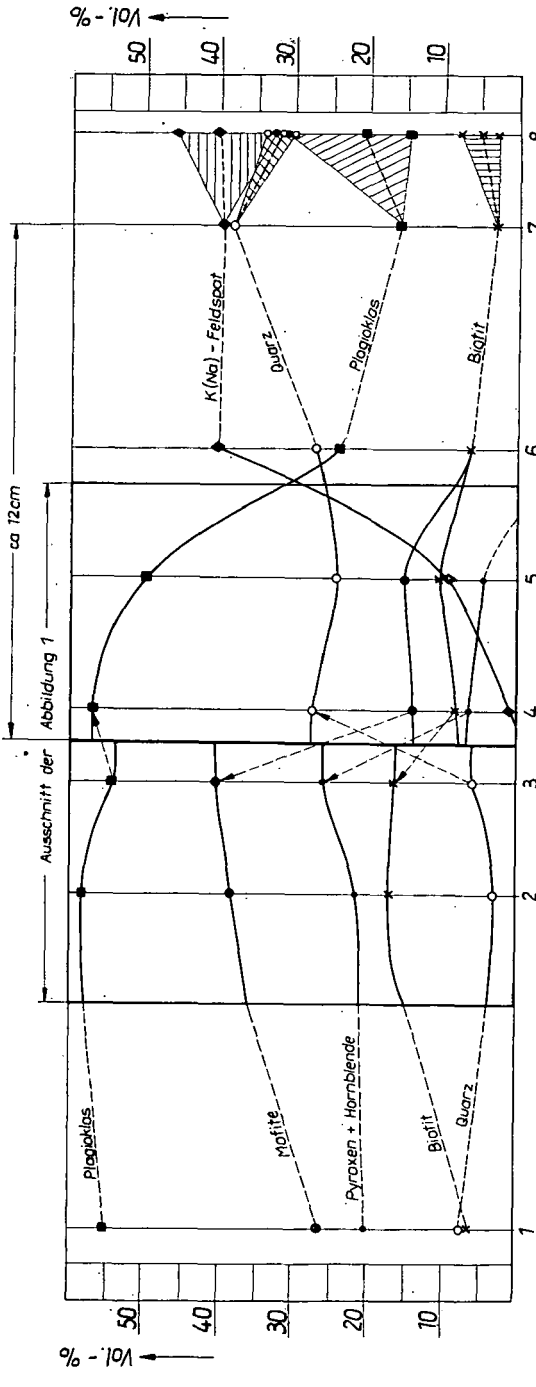

Abb. 2. Variation im Mineralbestand der einzelnen Zonen und — zum Vergleich — Modus des Diorits und der Brockengranitvarietäten.

und ganzen ist das Gefüge poikiloblastisch, indem in den größeren Quarzen und den vereinzelt auftretenden Kalifeldspaten leisten- bis tafelförmiger Plagioklas und reliktische Mafite enthalten sind. Größere Plagioklaskörner werden von Quarz korrodiert und zerlegt, wobei gelegentlich auch schriftgranitähnliche Verwachsungen zu beobachten sind. In einigen Schliffen sind Hornblendeaggregate vorhanden. Die Hornblende ist, im Unterschied zum Biotit und Augit, völlig frisch.

Der *metablastische Diorit in etwas größerer Entfernung* ist im wesentlichen durch eine Zunahme des Kalifeldspates gekennzeichnet. Die cm-großen Kalifeldspatblasten umschließen reliktischen Plagioklas, frische Hornblendekörner, chloritisierten Biotit und akzessorische Kornarten (Apatit und Opakbestand). Neben völlig und teilweise zersetzten klein- bis mittelkörnigen Plagioklaskörnern treten frische Plagioklase mit Anorthitgehalten zwischen 44 und 52% An auf. Das Gefügebild ist sehr wechselhaft. Während manche Bereiche noch das Gefüge des Normaldiorits aufweisen, herrschen im allgemeinen ausgesprochen metablastische Partien mit großen Quarz- und Kalifeldspatkörnern vor. Die mafitischen Komponenten sind, wie sich bereits im Anschliffbild erkennen läßt, fleckenförmig zusammengedrängt. Trotz der starken kristalloblastischen Überprägung und des lebhaften Wechsels von Mineralbestand und Gefüge beweisen typische Mineral- und Gefügerelikte die ursprüngliche Natur dieser Gangzone. Als Mineralneubildung dieses metablastischen Diorits tritt akzessorisch Orthit in Erscheinung.

In einer Entfernung von ca. 6 Zentimetern entspricht die mineralogische Zusammensetzung des Gesteins schließlich dem durchschnittlichen Modus des Brockengranits. Die reliktischen Bereiche treten immer stärker zurück. Die Mafitflecken werden abgebaut, und es bleiben an diesen Stellen Aggregate opaker Akzessorien zurück.

Der *Granit aus der Mitte des Verdrängungsganges*, der auf der Abbildung 1 nicht mehr erfaßt ist, besteht im wesentlichen aus xenomorphen Kalifeldspatkörnern, ebensolchen Quarzen und zumeist völlig zersetzten Plagioklasen. Femische Minerale sind nicht vertreten. Im Schliffbereich finden sich jedoch Erzpartikel und Chlorit stellenweise angehäuft, die als Umwandlungsreste der Mafite gedeutet werden müssen. Ihre Anordnung läßt vermuten, daß auch die ausgesprochen granitischen Partien der Gänge durch vollständige Verdrängung des ursprünglichen Diorits entstanden sind, jedoch läßt sich diese Annahme nicht beweisen. Auch im Ganggranit ist xenomorpher, fetzenartiger Orthit enthalten. Eine weitere Mineralneubildung stellt Granat dar, der in mm-großen Körnern auftritt. Die Granatkörner umschließen Quarz und Kalifeldspat und stellen offenbar eine relativ junge Bildung mit blastischer Wachstumstendenz dar. Bei idiomorpher Korngestalt an der Grenze Granat/Kalifeldspat enthalten die rundlichen Granatkörner mit dem benachbarten Kalifeldspat gleichorientierte Einschlüsse. Der Granat ist entlang feiner Risse chloritisiert.

Die *Abbildung 2* läßt erkennen, daß der Ganggranit recht gut mit der modalen Zusammensetzung der verschiedenen Brockengranit-varietäten übereinstimmt. Lediglich der Quarzgehalt ist etwas höher als im Brockengranit. Im Unterschied zu den Granitvarietäten des Brockenmassivs ist *frischer* Biotit im granitischen Ganggestein nicht enthalten; der im Modus erfaßte Biotit (7) entspricht Chlorit-Erzanhäufungen, die ihrer Form nach zu urteilen aus Biotit hervorgegangen sind.

Chemismus und Stoffbilanz

Um die stofflichen Veränderungen zu erfassen, wurden die einzelnen Zonen des Verdrängungsganges chemisch untersucht. Der Analyse liegt eine Kombination von kolorimetrischen (SiO_2, Fe_2O_3 P_2O_5), flammenphotometrischen (Na_2O, K_2O), emissionsspektralanalytischen (MnO, TiO_2, CaO, MgO) und komplexometrischen (CaO, MgO, Al_2O_3) Methoden zugrunde. In einer tabellarischen Übersicht sind die angewandten Verfahren und die benutzten Geräte zusammengestellt. Untersucht wurden auf diese Weise der dem Verdrängungsgang benachbarte Diorit, die dunkle Saumzone, das an diese Zone grenzende Gestein und schließlich das granitoide Material aus der Gangmitte. Die Resultate der chemischen Untersuchung sind in Tabelle 1 zusammengefaßt.

Bei einem Vergleich der Analysenwerte fällt auf, daß zwischen den Gesteinstypen 2 und 3 nur geringfügige chemische Unterschiede bestehen. Der SiO_2-Wert ist etwas größer, wie das nach der Modalanalyse zu erwarten war, Der erhöhte Mafitgehalt (s. *Abb. 2*) kommt in den chemischen Bestimmungen nicht zum Ausdruck, indessen ist eine gute Abtrennung der schmalen Saumzone für die chemische Analyse recht schwierig. Merkliche chemische Unterschiede ergaben sich erwartungsgemäß für das Ganggestein. Die im Typ 4 im Dünnschliff beobachteten Quarz- und Kalifeldspatgehalte bedingen entsprechende SiO_2- und K_2O-Werte; die sprung-

	Aufschluß	Methode	Literatur	Gerät
SiO_2	NaOH	spektralkolorimetrische Bestimmung als Molybdänblau, Reduktion mit Metol	J. P. RILEY [1958]	Spektralkolorimeter SPEKOL VEB Carl Zeiss
Gesamt Fe als Fe_2O_3	HF/ $HClO_4$	spektralkolorimetrische Bestimmung mit 2,2′ — Dipyridyl		
P_2O_5		spektralkolorimetrische Bestimmung, Molybdänblau-Reaktion mit Ascorbinsäure als Reduktionsmittel		
K_2O Na_2O		flammenphotometrische Bestimmung nach $(NH_4)_2CO_3$-Fällung	M. WEIBEL [1961]	Flammenphotometer Modell III VEB Carl Zeiss Jena
TiO_2 MnO CaO< 1,5% MgO< 1,5%		Emissionsspektralanalyse, Proben mit Kohlepulver (1:2) vermischt, Vergleichselement: Palladium	L. H. AHRENS [1954]	UV-Spektrograph Q24, VEB Carl Zeiss Jena
CaO> 1,5%	Na_2CO_3	Titration mit ÄDTA, Mischindikator: Murexid/Fluorexon, Zugabe von Triäthanol- u. Hydroxylaminhydrochlorid	E. WOHLMANN [1961]	
MgO> 1,5%		Titration von Mg+Ca mit ÄDTA, Indikator: Thymolphthalexon, Zugabe von Triäthanol-u. Hydroxylaminhydrochlorid		
Al_2O_3		Titration mit ÄDTA, Indikatorsystem: PAN + Kupferkomplexonat	H. FLASCHKA & H. ABDINE [1956]	
Glühverlust		Gewichtsverlust bei 1000°		
H_2O		Gewichtsverlust bei 110°		

hafte Abnahme der mafitischen Gemengteile andererseits reduzierte Fe_2O_3-, MgO- und CaO-Gehalte.

Bei einem Vergleich der Analysen der Typen 4 und 7 stellt es sich heraus, daß die Zone neben dem Diorit ein ausgesprochenes Übergangsstadium darstellt.

Tabelle 1

Chemische Zusammensetzung des Diorits und des granitoiden Verdrängungsganges (Nummern nach Abbildung 4)

Gesteinstyp	2	3	4	7
SiO_2	52,9	53,3	66,8	76,4
TiO_2	0,92	0,80	0,88	0,27
Al_2O_3	16,3	16,0	14,8	12,9
Fe_2O_3[1)]	9,19	9,20	4,74	1,01
MnO	0,16	0,16	0,072	0,025
MgO	5,71	5,59	1,80	0,28
CaO	8,87	8,86	4,58	0,49
Na_2O	2,67	2,96	2,92	1,67
K_2O	0,91	0,72	1,88	5,70
P_2O_5	0,13	0,09	0,20	0,05
Glühverlust	1,94	2,47	1,55	0,98
H_2O	0,22	0,26	0,10	0,06
Summe	99,9	100,4	100,3	99,8

[1)] Gesamteisen

Die Veränderungen im Chemismus lassen sich gut überblicken, wenn aus den Analysenwerten die BARTHsche Standardzelle errechnet wird (Tabelle 2). Zum Vergleich sind in diese Tabelle die Kationenzahlen des Diorits der Brockenmassiv-Ostrandzone und des Brockengranits einbezogen. Wegen der geringfügigen Unterschiede wurde Typ 3 nicht mit aufgenommen. Ohne die in der Tabelle 2 enthaltenen Zahlenwerte im einzelnen zu besprechen, sei darauf hingewiesen, daß die Kalzium- und Magnesiumzahlen für den Diorittyp unmittelbar neben dem granitoiden Gang größer sind als im normalen Diorit. Die Siliziumzahl ist — in Übereinstimmung mit dem Modus — niedriger. Im Übergangsmaterial kommt es vor allem zu einer sprunghaften Abnahme von Kalzium, Magnesium und Eisen und zu einer Zunahme von Kalium und Silizium. Der granitoide Gesteinstyp aus der Gangmitte ist im Chemismus dem Brockengranit bereits weitgehend angeglichen. Wenn wir von geringfügigen Differenzen absehen, gibt es nur bei den Natrium-, Kalzium- und

Tabelle 2

BARTH'sche Standardzelle der Gesteine

Kation:	K^+	Na^+	Ca^{2+}	Mg^{2+}	Fe^{3+}	Al^{3+}	Si^{4+}	Ti^{4+}	P^{5+}	O	OH^-
Gestein											
D	1,3	4,8	7,8	6,3	6,7	15,6	52,7	0,2	0,2	149,7	10,3
2	1,2	5,2	8,9	7,9	6,4	17,8	49,4	0,6	0,1	154,0	6,0
4	2,0	5,0	4,3	2,4	3,1	15,1	58,1	0,6	0,2	150,7	9,3
7	6,2	3,0	0,5	0,4	0,7	13,0	65,3	0,2	0,1	154,2	5,8
G	6,1	5,2	1,2	0,4	1,7	13,8	63,4	0,1	0,1	155,6	4,4

D = Diorit der Brockenmassiv Ostrandzone
G = Brockengranit
2,4,7 = Nummern nach Abbildung 4

Eisenwerten merkliche Unterschiede. Bei gleichem Kaliumgehalt führt der Ganggranit weniger Natrium als im Brockengranit durchschnittlich enthalten ist. Auch der Kalziumwert liegt, entsprechend dem geringen Plagioklasgehalt, niedriger. Im Brockengranit ist schließlich mehr Eisen enthalten als im Ganggranit.

Aus dem skizzierten Befund läßt sich die Schlußfolgerung ziehen, daß die metasomatische Umbildung des Diorits von Lösungen bewirkt wurde, die besonders reich an Kalium und Kieselsäure waren. Vor der Verdrängungsfront angereichert bzw. weggeführt wurden im wesentlichen die Elemente Kalzium, Magnesium und Eisen. Formal läßt sich dieser Vorgang durch folgende Stoffbilanz ausdrücken:

Zufuhr:	4,9 K^+	Wegfuhr:	1,8 Na^+
	12,7 Si^{4+}		7,3 Ca^{2+}
	17,6 Metall-Atome		5,9 Mg^{2+}
			6,0 Fe^{3+}
			2,6 Al^{3+}
			0,1 P^{5+}
			4,5 $(OH)^-$
			23,7 Metall-Atome
		und	4,5 (OH)-Ionen

Nach den hauptsächlich zugeführten Stoffen können wir die Bildung der granitoiden Verdrängungsgänge als Spezialfall einer Kieselsäure-Kaliummetasomatose betrachten. Er wurde bereits früher vom Verfasser in eine schematische Zusammenstellung der metasomatischen Prozesse im Brockenmassiv und in dessen Kontaktaureole aufgenommen, jedoch nicht näher beschrieben [SEIM, 1963]. Auch für die Verdrängungsgänge dürfen wir annehmen, daß ihre Entstehung von granitmagmatischen, an SiO_2 und K_2O angereicherten Restlösungen bewirkt wurde, die entlang der Klüfte in den Dioritkörper eindrangen. Für einen solchen Vorgang sprechen zwei weitere Beobachtungen.

In dem Ganggranit sind einige akzessorische Minerale allem Anschein nach angereichert, deren Entstehung auch an anderer Stelle mit einer erhöhten Konzentration postmagmatischer Lösungen an entsprechenden Elementen erklärt wird [z. B. BROMLEY, 1964, ZIMMERLE, 1963]. Sorgfältige Bestimmungen von BAUMGARTEN [1965] ergaben, daß in metablastischen „Granodioriten" mit einer Zirkonzufuhr von etwa 450 g/t zu rechnen ist. Während der Zirkon des „Normaldiorits" einen Integralkoeffizient von 0,6 aufweist, ergibt sich für die metablastischen Gesteine ein Wert von 1,8. Von ZIMMERLE [1963] beschriebene Zirkon- und Monazitanreicherungen am Endokontakt einer Granitintrusion erklären sich ebenfalls aus einer Konzentration der für die Bildung dieser Minerale erforderlichen Elemente in der Restschmelze.

Geochemische Untersuchungen können weiteres Material für die Unterscheidung zwischen magmatischen und metasomatischen Gangbildungen erbringen. TAYLOR [1964] weist auf bestimmte Gesetzmäßigkeiten hin, indem er schreibt: „In these veins are derived from a residual granitic melt, they should be enriched in elements such as Rb, Cs, and Tl. If the melt was rich in volatiles, and this is probably a necessary assumption if the host rock ist to be penetrated by such material to any distance, then high concentrations of elements such as the rare earths, Zr, Hf, Nb, Ta etc., may be anticipated." Die zweite Beobachtung betrifft die Entwicklung granodioritischer Gesteinstypen an der Grenze Diorit-Granit, auf die im folgenden Abschnitt näher eingegangen wird.

3. BEZIEHUNGEN ZUR METASOMATISCHEN ÜBERPRÄGUNG DES DIORITS

Die beschriebenen Gänge sind nur eine Form der metasomatischen Umbildung des Diorits. Sie sind offenbar an den Kontakt des Diorits zu den pelitischen und quarzitischen Sedimentiten gebunden. Im Grenzbereich Diorit-Granit treten demgegenüber mehr schlierige granitische Bereiche im Diorit, die früher als Intrusion des Brockengranitmagmas aufgefaßt und zur Altersbestimmung der Intrusionen herangezogen wurden, auf. Bereits ältere Bearbeiter waren sich indessen der Problematik dieser, mit dem Diorit durch Übergänge verbundenen Gesteinsbereiche bewußt. Die gelegentlich postulierte gleichzeitige Intrusion von Diorit und Granit bezeugt das. Die Rolle metasomatischer Prozesse im Endstadium der magmatischen Kristallisation und deren Auswirkung auf Rahmengesteine, speziell die „Verdrängung der ausgeschiedenen Kristalle durch aggressiven Kalifeldspat und danach oder daneben ebensolchen Quarz" [ERDMANNSDÖRFFER, 1948] wurde eben erst später erkannt.

Nicht selten sind innerhalb des Diorits kalifeldspat- und quarzblastische Bereiche aufzufinden, die ohne scharfe Grenze zum normalen Diorit überleiten. Gefügebeobachtungen lassen keinen Zweifel daran aufkommen, daß es sich, im Unterschied zu Kalifeldspat-Quarz = Zwickelfüllungen, um metablastische Typen handelt. Aus den Dioriten bis Quarzdioriten des Brockenmassivs gehen granodioritische bis granitische Gesteine hervor, deren Entwicklungsrichtung in der *Abbildung 3* — Quarz-Kalifeldspat-Plagioklasdreieck — markiert ist. Die Endtypen haben gewöhnlich einen höheren Quarzgehalt als die Granite des Brockenmassivs, deren Zusammensetzung im gleichen Dreieck dargestellt wurde. Nur wenige Proben zeichnen sich, genau wie die Randbereiche des Verdrängungsganges, durch eine Quarzzunahme bei fehlender Kalifeldspateinsprossung aus. In diesen quarzreichen Dioriten sind die Mafite mehr oder weniger zersetzt und korrodiert.[1]

Nur ausnahmsweise haben die metablastischen Diorite eine modale Zusammensetzung, die den Brockengraniten entspricht. Das unterscheidet sie von den granitoiden Verdrängungsgängen (Punkte 6 und 7). Entweder ist bei diesen die Metasomatose bis zum Granitstadium vorangeschritten, oder wir haben es in der Übergangszone mit ihren Mineral- und Gefügerelikten mit einem metasomatischen Gestein und in der Gangmitte mit einer Intrusion von Granit zu tun. Ohne Beweise beibringen zu können, scheint uns die erste Annahme verständlicher. Auch die mafitischen Erz-Chloritanhäufungen des grobkörnigen Ganggranits erinnern sehr an die besser rekonstruierbaren Mafitrelikte in der porphyroblastischen Übergangszone. Die Annahme einer „selektiven Verdrängung", wie sie MICHEELSEN [1960] für präkambrische Pegmatite von Bornholm wahrscheinlich machen kann, dürfte hier kaum gerechtfertigt sein. Aus dem Quarz-Feldspat-Mafit-Dreieck, in dem die Streubreite des Diorits, des metablastischen Diorits und des Granits abgegreztn sind, läßt sich entnehmen, daß die Quarzzunahme im wesentlichen auf Kosten der dunklen Gemengteile erfolgte, während die Feldspatsumme annähernd konstant bleibt. Der Granit des untersuchten Gangs liegt am Rande des Brockengranitfeldes und zeichnet sich durch einen geringfügig höheren Quarzgehalt aus (*Abb. 3*, Punkt 7).

[1] Die Felderabgrenzung im Quarz-Kalifeldspat-Plagioklasdreieck erfolgte nach dem Vorschlag von STRECKEISEN [1964].

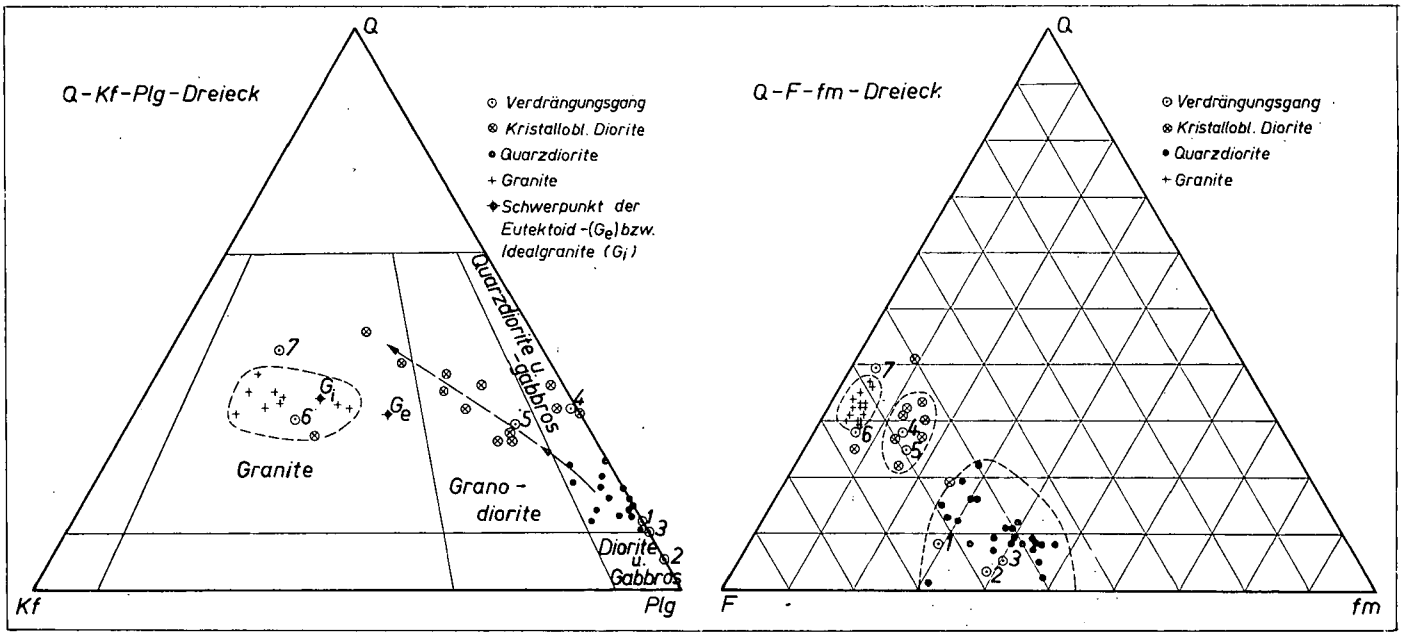

Abb. 3. Darstellung des Modalbestandes der Gesteinstypen einschließlich der kristalloblastischen Diorite aus dem Grenzbereich Granit—Diorit im Quarz—K(Na)-Feldspat-Plagioklas—Dreieck und im Dreieck Quarz-felsische-femische Minerale.

Eine blastische Überprägung dioritischer Gesteine kann unter anderen Bedingungen auch zu Gesteinen mit niedrigem Quarz- und hohem Kalifeldspatgehalt führen. Auf diese Weise entstanden gelegentlich Syenite, wie LANGERFELD [1962] durch eingehende Untersuchung entsprechender Gesteinstypen im Schwarzwald zeigen konnte. In der Kontaktzone des Brockengranits wurde u.a. ein Diabas durch Kalifeldspatblastese zu einem (Meta-)Alkalitrachyt umgebildet. Von einem ägirinaugitischen Syenit, der in Gestalt kleiner steiler Gänge in einem Teschenit unweit von Budnany/ČSSR vorkommt, schreibt FIALA [1965]: „Der Syenit entsteht metasomatisch durch Verdrängung des Teschenits, wie auch Reliktstrukturen zweifellos beweisen." Wenn wir in Rechnung stellen, daß solche Gesteine das Resultat von Stoffaustauschprozessen darstellen, berühren wir damit nicht zuletzt ein Problem der petrographischen Nomenklatur. Wenn wir die Nomenklatur der Magmatite auf solche Bildungen beziehen, dann geschieht das in der Absicht, Mineralbestand (und Gefüge) in einfacher Weise zu charakterisieren. Richtiger wäre es, von granitoiden, syenitoiden, alkalitrachytoiden usw. Metasomatiten zu sprechen; vorausgesetzt natürlich, daß die Bildungsweise erkennbar ist. Auch WIESENEDER [1966] stellte die Metasomatite, die sich vorwiegend im Spätstadium plutonischer und im Verlauf metamorpher Prozesse bilden und wohl zumeist keine große Ausdehnung aufweisen, kürzlich zu den Hauptgruppen der Gesteine. Ihre sichere Abgrenzung von Magmatiten wird indessen nicht selten problematisch sein.

ZUSAMMENFASSUNG

In einem kontaktnahen Dioritsteinbruch des Brockenmassivs (Ostrandzone) treten granitoide Ganggesteine auf. Geländeuntersuchungen führen in Verbindung mit mikroskopischen Beobachtungen zu dem Ergebnis, daß es sich bei diesen Bildungen um *Verdrängungsgänge* handelt, wie sie wohl zuerst von GOODSPEED beschrieben wurden. Die Variationen im Mineralbestand und Chemismus der einzelnen Zonen des Verdrängungsganges wurden ermittelt. In einem gesonderten Abschnitt wird auf die Beziehungen zwischen den Granitgängen im Diorit und den metablastisch überprägten Dioriten, wie sie in Granitkontaktnähe nicht selten auftreten, einge gangen.

LITERATUR

AHRENS, L. H. [1954]: Quantitative spectrochemical analysis of silicates. — Pergamon Press, London.

BAUMGARTEN, E. [1965]: Petrographische Untersuchungen des Diorits der Brockenmassiv-Ostrandzone. — Unveröffentliche Diplomarbeit, Rostock.

DOWES, D. R. [1953]: The transformation of tillite by migmatization at Mount Fitton, South Australia. — Quart. Journ. Geol. Soc. London *109*, 455—481.

BROMLEY, A. V. [1964]: Allanite in the Tan-y-Grisiau microgranite, Merionethshire, North Wales. — American Mineralogist, Menasha *49*, 1747—1752.

BÜSCH, W. und MEHNERT, K. R. [1966]: Dioritbildung durch Remobilisation. — Tscherm. Min. Petr. Mitt., *XI*, 246—265.

BURKE, K. [1959]: Replacement veins in the Dahomeyan of Ghana. — Geol. Mag., *96*, 353—360.

CHINNER, G. A., SANDO, M. und WHITE, A. J. R. [1956]: On the supposed transformation of tillite to granite at Mount Fitton, South Australia. — Geol. Mag., *93*, 18—24.

CHROBOK, S. M. [1964]: Geologische Untersuchungen im Brockenmassiv. — Wiss. Zeitschr. Humboldt-Universität z. Berlin, *13*, 126.

EFIMOV, A. A. und IVANOVA, L. P. [1963]: Über einige metasomatische Erscheinungen, die die Bildung von Pyroxenitgängen in Duniten bedingen. — Dokl. Akad. Nauk. SSSR, *148*, 427—430.

ERDMANNSDÖRFFER, O. H. [1950]: Aus dem Grenzgebiet Magmatisch-Metamorph. — Z. deutsch. Geol. Ges., 204—2212.
— [1951]: Die Entwicklung und jetzige Stellung des Granitproblems. — Heidelb. Beitr. Min. Petr., *2*, 334—377.
FIALA, F. [1965]: Lokalität 13, Straßeneinschnitt von Budnany. — Exkursionsführer zur Konferenz: Paläovulkanite der Böhmischen Masse, Prag.
FLASCHKA, H. und ABDINE, H. [1956]: Zur kompexometrischen Titration von Eisen und Aluminium und der Summe beider, — Zeitschr. anal. Chem. *152*, 77—85.
GOODSPEED, G. E. [1940] Dilation and Replacement Dikes. — Journ. of. Geol. *48*, 175—195.
HÄRME, M. und LEITALA, M. [1955]: An example of granitization. — Bull. Comm. Geol. Finlande, *168*, 97—99.
JANARDAN, RAO Y. [1959]: Replacement dikes in the migmatites of Yellandlapad. — Curr. Sci. India, *28*, 242—243.
LANGERFELD, H. [1961]: Über Syenitbildung durch Palingenese und Kalifeldspat-Metablastesis im mittleren Schwarzwald. — Jb. geol. Landesamt Baden—Württemberg, *5*, 19—51.
MEHNERT, K. R. [1959]: Der gegenwärtige Stand des Granitproblems. — Fortschr. Mineral., *37/2*, 117—206.
MICHEELSEN, H. I. [1960]: Pegmatites in the Pre-Cambrian of Bornholm, Denmark. — Rep. Twenty-First-Session Norden, Part *XVIII*, 128—136, Copenhagen.
PALIVCOVA, M. [1959]: Die Beziehungen zwischen Gesteinsgängen und Vererzung. — N. Jb. f. Min. Monatshefte, 110—120.
REITAN, P. H. [1960]: The genetic significance of two kinds of basified zones near small pegmatite venis. — Rep. Twenty-First-Seession Norden, Part *XVIII*, 102—107, Copenhagen.
RILEY, J. P. [1958]: The rapid analysis of silicate rocks and minerals. — Anal. Chim. Act. *19*, 413—458.
SEIM, R. [1960]: Über kontaktmetasomatische Prozesse an einem Diorit-Granitkontakt. — Geologie, *9*, 513—520.
— [1963]: Petrographische Untersuchungen an kontaktmetasomatischen Gesteinen vom Ostrand des Brockenmassivs. — Geologie, Beiheft *37*, Berlin.
SMITHSON, S. B. [1965]: Oriented plagioclase grains in K-feldspar porphyroblasts. — Contr. Geol. Laramie *4*, 63—68.
STRECKEISEN, A. [1960]: Zur Klassifikation der Eruptivgesteine. — N. Jb. Min., Monatshefte, 125—222.
TAYLOR, S. R.: The application of trace element data to problems in petrology.
WEIBEL, M. [1961]: Die Schnellmethoden der Gesteinsanalyse. — Schweiz. Mineral. und Petrogr. Mitt. *41*, 285—294.
WIESENEDER, H. [1966]: Zum Gesteinsbegriff. — Tscherm. Min. und Petr. Mitt. *XI*, 203—208.
WINKLER, H. G. F. und v. PLATEN, H. [1957, 1958, 1960]: Experimentelle Gesteinsmetamorphose I bis IV. — Geochim. et Cosmochim. Acta, *13*, 42—69. *15*, 91—112. *18*, 294—316.
WOHLMANN, E. [1961]: Schnellverfahren zur Analyse einfacher Silikate. — Zeitschr. f. angew. Geol., *7*, 534—539.
ZIMMERLE, W. [1963]: Eine Anreicherung von Zirkon und Monazit in der Kontaktzone des Rattlesnake-Granits, Südkalifornien. — N. Jb. Mineral. Abh., *100*, 164—184.

PROF. DR. ROLF SEIM
DR. JÜRGEN EIDAM
Sektion Geologische Wissenschaften
Ernst-Moritz-Arndt-Universität
Friedrich-Ludwig-Jahn-Str. 17a
22 Greifswald
Deutsche Demokratische Republik

GEOLOGICAL, MINERALOGICAL AND PETROGRAPHICAL EXAMINATIONS IN THE COURSE OF EXPLORATIONS FOR BINDING RAW MATERIALS IN THE NEIGHBOURHOOD OF VÁC

GY. VITÁLIS and MRS. J. HEGYI-PAKÓ
Central Research and Design Institute for Silicate Industry, Budapest

INTRODUCTION

During the cement raw material explorations, — for the Cement and Lime Works Duna —, in the neighbourhood of Vác, detailed geological prospecting was made by our Institute on the limestone area Nagyszál and the clay area of Gombás *(Fig. 1.)*. 24 core drillings of about 3550 metres in the Nagyszál limestone district and 2660 metres of 56 core drillings in the Gombás clay area were made. The connected laboratory investigation of materials served first of all the purpose of qualification for cement and lime industrial use, beside the knowledge of the mineral and petrographical structure of the area.

THE LIMESTONE EXPLORATION AREA OF NAGYSZÁL

Geological conditions. The underlaying rock of usable raw materials in the area is the Triassic dolomite of Carnian age, to be found also on the SE border of the exploration area in a little hill on the surface. The drilling No XV—1 situated on the east side of the area, penetrated nearly 100 m, the drilling No XVI—3 67,7 m of thickness into the dolomite with calcareous dolomite interbeddings. Dachstein limestone layers of Norian age, formerly considered homogeneous, are to be found in the overlaying of the dolomite series, with clayey limestone, dolomitic limestone, calcareous dolomite, even subordinately dolomite interbeddings. These ware penetrated in some places, with drillings, 200 m thick *(Fig. 2)*. The dolomitic interbeddings of the limestone formations are partly of syngenetic, partly of late hydrothermal origin.

The karstic cavities of limestone stratas are filled with red and brown Pleistocene clay, — with debris of limestone and sandstone —, silty clay, and sandy clay. In some karstic holes of Norian limestones, in the depth of 20, 30, 70, even 105 m below surface, as filling „Hárshegy" sandstone of subgressive origin, Oligocene age, conglomerate and breccia can be observed too. Taking these into account, in the karstic symptoms of the limestone we can separate with certainity a period before Lower-Oligocene and a Post-Oligocene period.

The limestone series area is covered, in connection with the fractured structure, with „Hárshegy" sandstone and conglomerate layers of various 0—60 m thickness, depending upon the individual blocks.

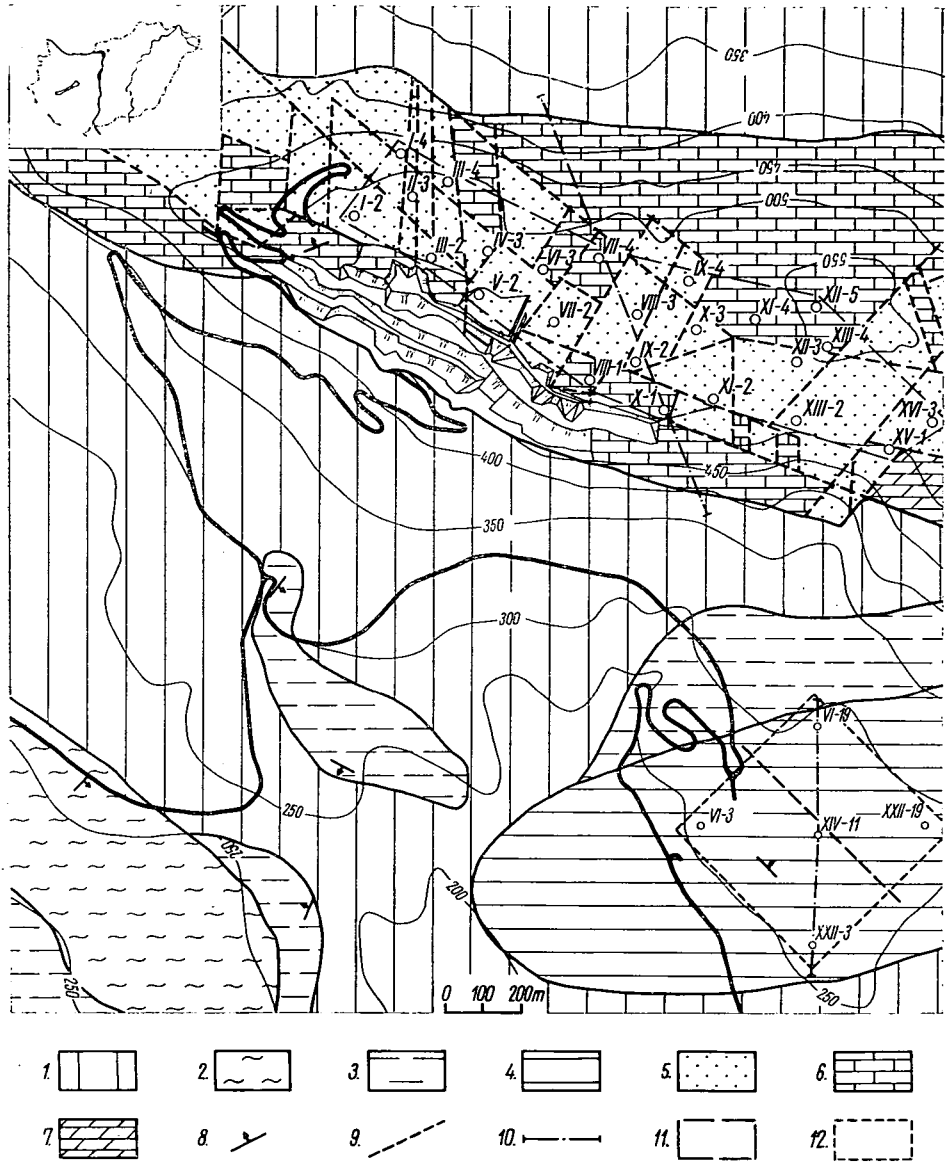

Fig. 1. Geological sketch map of raw material exploration in the surrounding areas of Vác. (After L. JUGOVICS and F. SZENTES with supplement.)
1. Sandy clay, loess, talus (Pleistocene). *2.* Sand, clay-marl (Helvetian). *3.* Clayey sand, sand, sandstone (Kattian). *4.* Marly aleurite (Rupelian). *5.* „Hárshegy" sandstone and conglomerate (Lattorfian). *6.* Dachstein limestone (Norian). *7.* Dolomite (Karn). *8.* Dip. *9.* Fault. *10.* Line of profile. *11.* Limestone exploration area Nagyszál. *12.* Clay exploration area Gombás.

We determined exactly the cavities in the limestone, the depth of fractured layers, clayey sections, depth of sandstone interbeddings — with drillings and electrical loggings with the methods: gamma-ray, gamma-gamma-ray and gamma-ray neutron. The method of this is shown on a part of the drilling log No IV—3 *(Fig.4)*.

1—3 cm thick calcite veins were observed in the filling of larger joints in the limestone stratas seen in operating quarry. The calcite veins refer to former thermal spring activity. During which the hydrothermal metasomatose, caused by thermal springs, — on the greatest part of the area —, dolomitized the limestone in various degrees.

Geological structure. The uplifted horst of the Nagyszál mountains along WNW-ESE longitudinal fractures, is dissected on the whole by transversal faults with directions of NE-SW and N-S *(Fig. 1)*. Average of dip angle of faults is 65°. The limestone strata of the exploration area Nagyszál dips averagely 30°, in the direction NNW, — on base of measurements made in the quarry. The smallest dip angle is 20°, the greatest 45° *(Fig. 2)*.

According to the investigations of chemical and mineralogical composition, the comparative distribution of rock sorts, penetrated in the 24 exploration holes of the area Nagyszál, till the depth of 420 m, are the following:

Sort of rock	Percent
Clay, silt and rock debris (Pleistocene)	5,10
Sandstone and conglomerate (Lower-Oligocene)	11,30
Limestone (Upper Triassic)	52,97
Limestone, clayey and clayey soiled (Upper Triassic)	5,84
Limestone with dolomite (Upper Triassic)	10,65
Calcareous dolomite (Upper Triassic)	10,05
Dolomite (Upper Triassic)	4,09

Table 1 contains the average and extreme values of the rocks chemical composition. The presence of the sandy, clayey, dolomitic stain to be seen from this, was shown by the thermal (derivatographic) and X-ray diffractogram investigations too.

On *Fig. 3/a* a derivatogram of a Dachstein limestone sample is shown, from the bore hole VIII—3, depth 105,0 m, situated in the middle part of the area. Beside the endotherm calcite peak, near to 950 or 900° C of the DTG and DTA curves, no other curve or peak can be observed referring to other crystalline component.

The value of 98, 96% $CaCO_3$, calculated from the analysis of the sample, corresponds very well with the 99,14% calcite content computed from the TG curve. *Fig. 3/b* is the derivatogram of the dolomitic limestone from the depth 146,0 m of the bore hole No VIII—3. A steep endotherm peak is to be seen with a 770° C temperature maximum, before the calcite peak near to 900° C, characteristic for the decomposition of magnesium-carbonate of dolomites. The CaO content of the sample is 46,57, the MgO content 7,47%. Dolomite content, calculated from the TG curve is 35%. On *Fig. 3/c* a derivatogram of a dolomite is to be seen, from the depth 136,0 m of bore hole VIII—3. The first endothermic peak here, originating from decomposition of $MgCO_3$ is by far greater than the former. CaO content of the sample is 32,62%, MgO content is 19,12%. The dolomite content calculated from the TG curve is 87%.

According to thermal and X-ray investigations, contaminating material of the Norian Dachstein limestone in the area is dolomite, quartz, clay mineral and feldspar.

Table 1

Average and extreme values of chemical analyses*

	Loss on ignition	SiO_2	Al_2O_3	Fe_2O_3	CaO	MgO	Na_2O	K_2O	SO_3	$CaCO_3$
	Per cent by weight									
Limestone (Upper Triassic)										
Minimum	41,68	0,09	0,01	0,01	51,36	0,09	0,02	0,01	0,01	91,68
Maximum	44,34	3,61	1,28	0,57	55,97	2,20	0,50	0,22	0,05	99,91
Average	43,08	0,74	0,23	0,12	55,05	0,50	0,21	0,11	0,02	98,26
Clayey and clayey coloured limestone (Upper Triassic)										
Minimum	13,48	6,48	0,65	0,41	15,92	0,10	0,17	0,16	0,01	28,42
Maximum	38,77	65,63	8,36	6,67	49,61	1,41	1,08	0,80	0,08	88,55
Average	29,54	26,31	4,46	2,04	36,07	0,56	0,51	0,44	0,04	67,95
Dolomitic limestone (Upper Triassic)										
Minimum	37,10	0,32	0,01	0,01	42,73	2,39	0,02	0,01	0,01	—
Maximum	45,90	12,11	0,88	14,74	53,54	11,60	0,49	0,19	0,70	—
Average	43,13	1,37	0,23	1,55	47,27	6,07	0,25	0,11	0,02	—
Calcareous dolomite (Upper Triassic)										
Minimum	41,91	0,10	0,07	0,07	33,17	10,74	0,12	0,05	0,01	—
Maximum	47,11	5,21	1,10	2,32	42,75	19,69	1,07	1,90	0,07	—
Average	45,84	0,67	0,30	0,44	35,98	16,52	0,38	0,21	0,02	—
Dolomite (Upper Triassic)										
Minimum	31,78	0,32	0,09	0,12	20,37	13,56	0,44	0,14	0,02	—
Maximum	46,39	15,15	7,41	10,37	32,16	20,94	0,68	0,43	0,02	—
Average	41,40	7,25	2,04	3,21	27,99	17,62	0,56	0,25	0,02	—
Marly aleurite (Middle Oligocene)										
Minimum	4,28	28,78	2,47	0,82	2,09	0,10	0,13	0,02	0,01	3,73
Maximum	30,73	78,23	18,19	7,02	25,00	10,58	2,15	2,56	3,98	44,63
Average	13,14	51,82	13,73	5,17	9,56	2,41	0,58	1,80	0,71	17,75
Rock floured clayey silt (Pleistocene)										
Minimum	7,89	49,43	10,50	3,63	6,15	2,04	0,54	1,41	0,02	10,98
Maximum	15,18	63,10	14,60	5,88	14,28	3,52	1,02	2,55	2,18	25,49
Average	11,78	54,28	12,97	4,82	9,25	2,92	0,80	2,12	0,30	16,61

* Remarks: Maximum and minimum values in the Table, are not everywhere datas of the same rock samples.

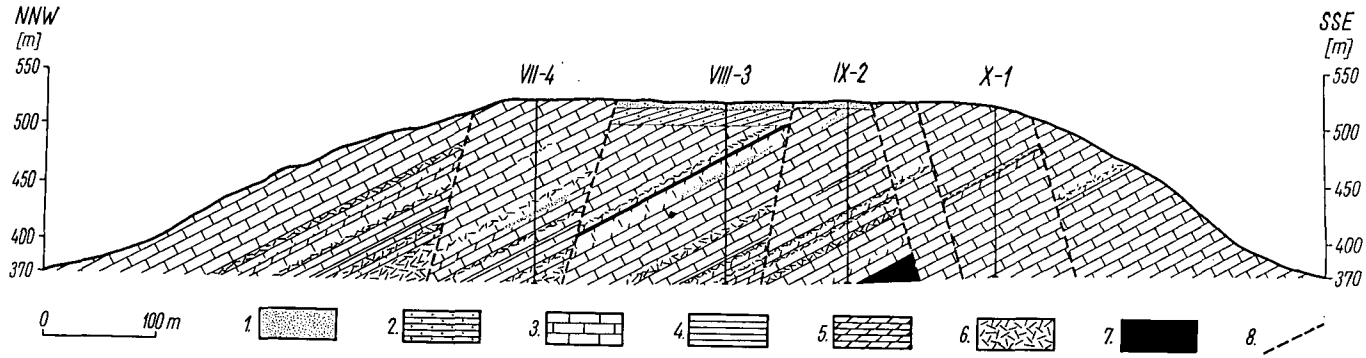

Fig. 2. Geological profile of limestone exploration area Nagyszál. *1.* Clay, silt, sand, small gravel (Pleistocene) covering surface and filling cavities. *2.* Sandstone and conglomerate (Lower Oligocene). *3.* Dachstein limestone. *4.* Clay and clayey coloured limestone. *5.* Dolomitic limestone. *6.* Calcareous dolomite. *7.* Dolomite (Upper Triassic). *8.* Fault.

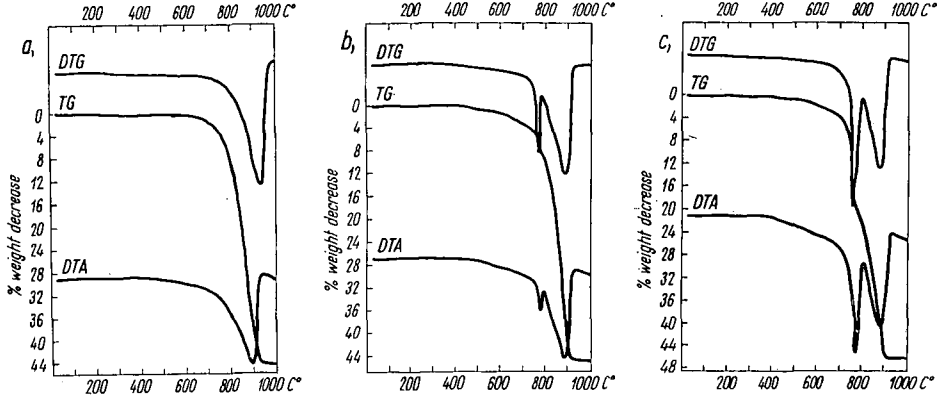

Fig. 3. Thermal curves of Upper Triassic Dachstein limestone (a), dolomitic limestone (b) and dolomite (c) from No VIII-3 boring, Nagyszál.

In the course of our investigations we looked for a connection between the technological characteristics and the results of geophysical examinations made in the bore holes. We show on *Fig. 4* the geophysical and exploitability profile of the interval between 30—130 m from well No IV—3, indicating fluid losses too, observed

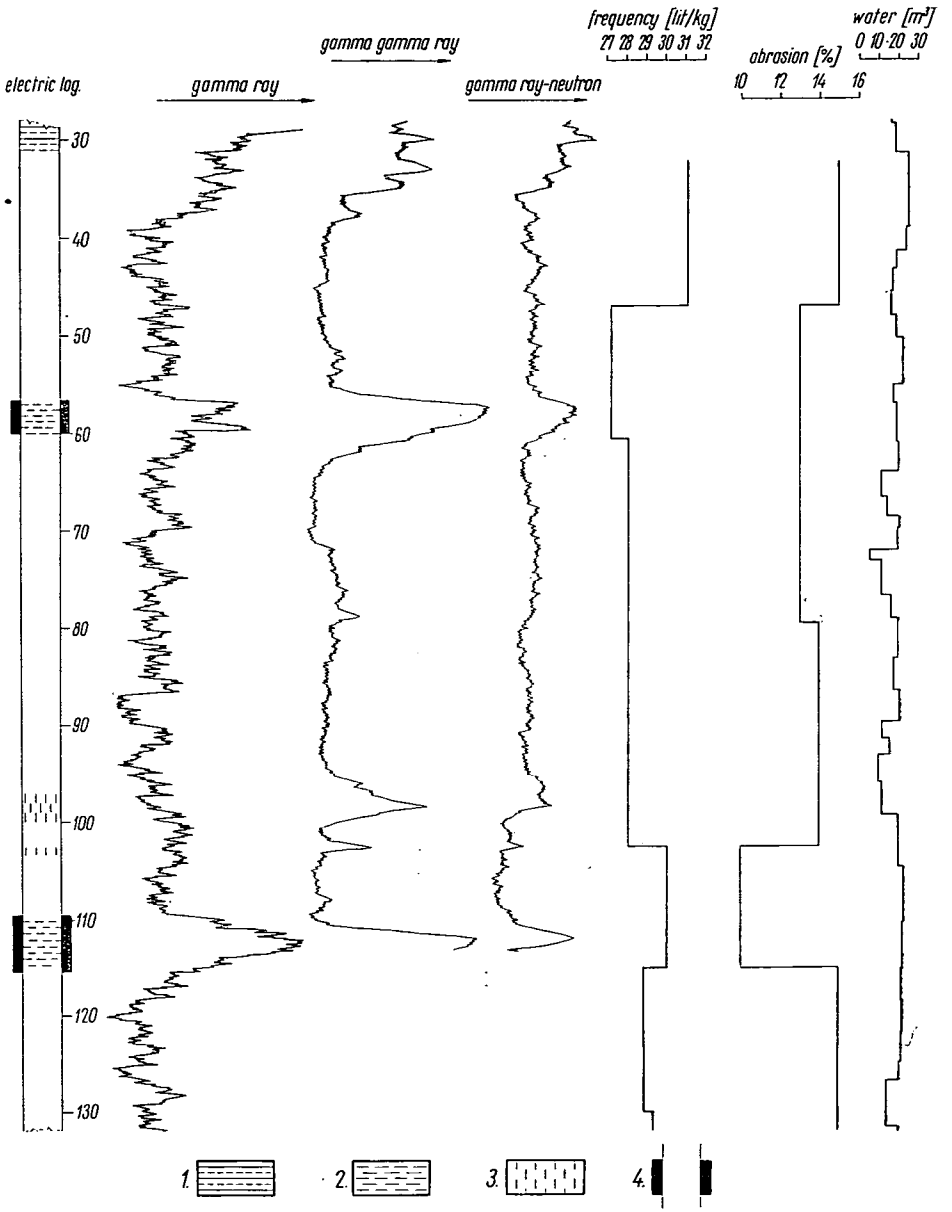

Fig. 4. Radioactive and exploitability profile from depth interval 30—130 m of bore hole No IV-3. Nagyszál, — with drilling fluid losses. *1.* Sandstone. *2.* Clay interbedding. *3.* Fissures. *4.* Cavern.

during drilling. After the evidence of radioactive measurings made in the holes, we marked the cavernous, clay stained and broken intervals. The average samples taken for technological examinations, — in the given section —, are from the depth intervals of 32,2—46,9; 46,9—60,5; 60,5—79,5; 79,5—102,6; 102,6—115,0 and 115,0—130,0 metres.

It became evident, that the values of frequency and wear out are generally in connection with radiological profiles. So for example the increase and wear out values show a decrease of raw material quality in the depth between 60—110 m, with caverns, clayey impurity. Data referring to the quantity of used drilling water, or loss of water, are mostly in connection with karstic features and the changing of rock quality.

THE CLAY EXPLORATION AREA OF GOMBÁS

Geological conditions. The base of usable raw material in the area is „Hárshegy" sandstone and conglomerate, Lower Oligocene, tectonically broken up chessboard like.

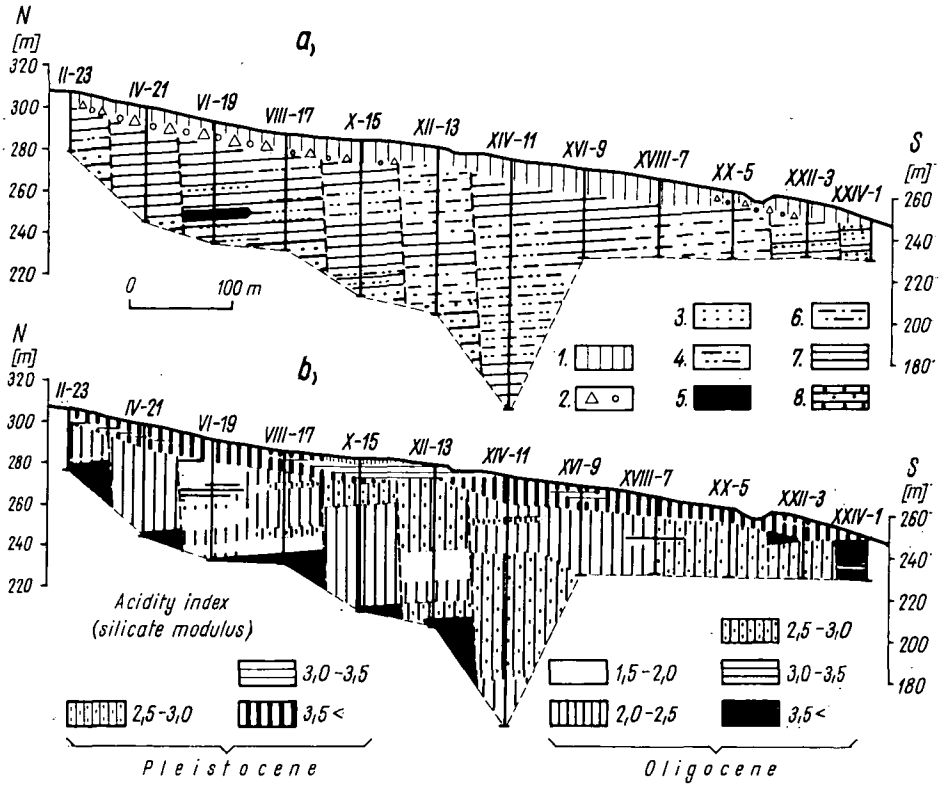

Fig. 5. Geological (a) and Silicate Module (b) profiles of clay exploration area Gombás. *1.* Clay formation coverstrata. *2.* Gravel and talus (Pleistocene). *3.* Fine and small grained loose sandstone, sand. *4.* Fine sanded marly aleurite. *5.* Aleurite with sandstone streaks. *6.* Partly fine sanded marly aleurite. *7.* Marly aleurite (Middle Oligocene); *8.* Sandstone and conglomerate (Lower Oligocene).

The raw material to be used for the cement industry is composed from marly aleurite, in some places with thin fine grained sandstone and sand stratas, which belong to the formation of „Kiscell clay", Upper-Oligocene.

An Upper-Oligocene sand-sandstone strata of great thickness, contacts with the former, along joints.

Pleistocene clay, silty clay, sandy clay, boulders and gravel transferred from talus (0—16 m thick) composes the layer upon Oligocene. The situation of clayey and gravely stratas to each and to the Oligocene stratas is conform.

Geological and exploitability relations of the Gombás area are shown on *Fig. 5*, with a geological (a) and a silicate module (b) profile.

Geological structure. The directions of fractures observed in the explored area correspond with the course of fractures drafted upon datas of drillings. It is similar with the structural directions of the Rupelian, Kattian and Helvetian formations in the area. The marly aleurite stratas, — on the SW side of the NW-SE course main fault, middle part of the region —, are everywhere more than 100 m thick. The underlying sandstone and conglomerate strata is, in the NE part of the exploration area, because of faults, near the surface, proceeding toward NE, the thickness of usuable raw material decreases.

A trace of former thermal spring activity, connected with tectonic movements, can be observed in the marly aleurite strata too. The hydrothermal alterations, because of the water sealing quality of marly aleurite, are only to be observed near the bottom sandstone stratas. They are present in drillings generally with a thickness of 0,1—0,7 m.

The average and extreme values of *chemical analyses* made on the rock samples of drilling in the area, are included in Table 1.

The typical thermograms of Middle-Oligocene marly aleurite are shown in *Fig. 6*.

According to the thermogram shown on *Fig. 6/a*, the sample taken from 15,0 m contains calcite, a small quantity of clay mineral and, on base of X-ray diffraction investigations quartz and feldspar too. The great exothermic peak around 400° C, on the DTA curve of *Fig. 6/b* is characteristic for pyrite. On the DTA curve of the hydrothermally decomposed marly aleurite, — shown on *Fig. 6/c* —, the pointed

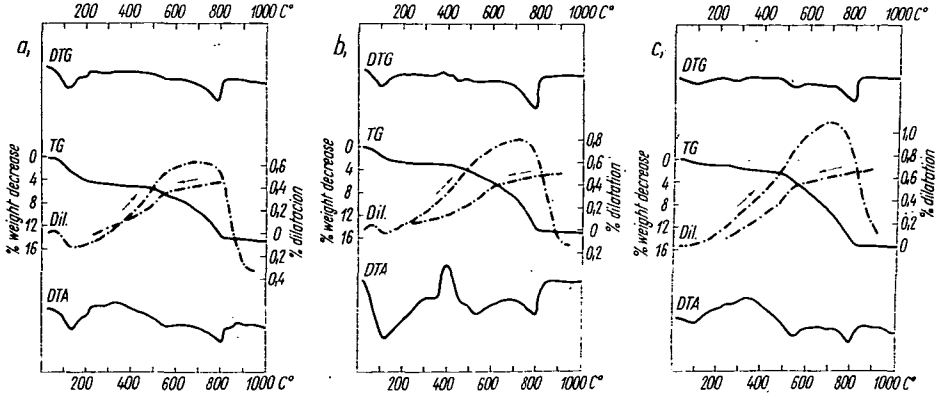

Fig. 6. Thermal curve of Middle Oligocene marly aleurite (a), pyritic marly aleurite (b), and marly aleurite decomposed hydrothermally (c) from bore hole No XXII-19, Gombás.

exothermic peak, characteristic for pyrite, vanished, instead of it an exothermic peak can be seen. This difference between DTA curves of pyritic fresh and hydrothermally altered rock samples can be observed in case of other samples too. All three types of clay-minerals (kaolinite, illite, montmorillonite) can be shown in drilling samples clay-mineral character is in no case definite, thermograms on DTA and DTG curves of the clay-minerals components are presumably badly crystallized or of mixed structure.

We made grain size distribution curves with hydrometrisation from typical materials of the area. These investigations were made in two states of conditions (normal or maximally peptized with Na_2CO_3). We publish the cover curves of grain size distribution belonging to two conditions, on *Fig. 7.* In accordance with the

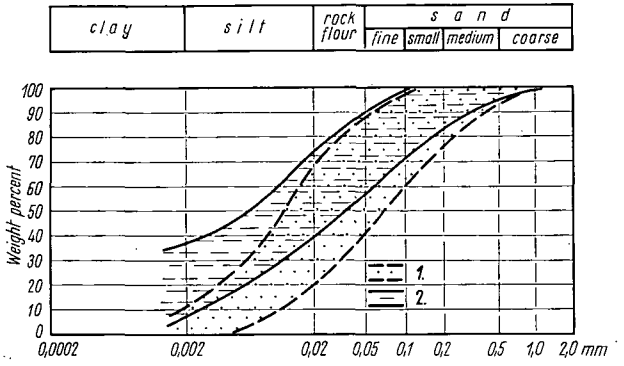

Fig. 7. Grain size composition cover curves of the Middle Oligocene marly aleurite exploited in area Gombás.
1. Normal state. *2.* Peptized state.

curves, the „Kiscell-clay", mapped and known by this name in literature, is really no clay, but as the thermal examinations and grain size distribution curves prove, marly aleurite, according to the fractions of bounded silty rock flour, rock floured silt, and subordinately rock floured clayey silt. With the remark marly, we tried to emphasize the carbonate content and binding of clay.

REFERENCES

BÁRDOSSY, GY. [1961]: Üledékes kőzeteink nevezéktanának kérdései. — Problems of the nomenclature of sedimentary rocks. — Földtani Közlöny, *XCI*, 44—64.

HEGYI, J. [1968]: A Vác—Gombás-i agyagminták hidrotermális elváltozásainak derivatográfiás vizsgálata. — Derivatographische Untersuchung der hydrothermalen Veränderung der Tonproben bei Vác—Gombás. — Hidrológiai Tájékoztató, 70—72.

JUGOVICS, L. [1962]: A Dunai Cement- és Mészmű nyersanyag készletének agyag és mészkő tömegének minőségi és mennyiségi megkutatása. — Manuscript, Magyar Állami Földtani Intézet, Budapest.

KRIVÁN, P. [1959]: Mezozóos karsztosodási és karsztlefedési szakaszok, alsóbartoni sziklásparti jelenségek a Budai hegységben. A szubgresszió fogalma. — Phases de karstification et de karst couvert mésozoiques, phénomènes de falaise du Bartonien inf. dans la Montagne de Buda. La notion de subgression. — Földtani Közlöny, *LXXXIX*, 393—401.

KUBACSKA, A. [1925]: Adatok a Nagyszál környékének geológiájához. — Daten zur Geologie der Umgebung des Nagyszál. — Földtani Közlöny. *LV*, 150—161, 327—332.

LÁNG, S. [1967]: A Cserhát természeti földrajza. — Földrajzi monográfiák VII. Akadémiai Kiadó, Budapest.

Noszky, J. Sr. [1941]: A dunabalparti hegyrögök környezetének geológiai viszonyai. — Földt. Int. Évi Jelentései az 1936—1938. évekről I. Budapest, 473—501.
Noszky, J. Sr. [1940]: A Cserhát hegység földtani viszonyai. — Die Geologie des Cserhát—Gebirges. *Magyar tájak földtani leírása III.* Budapest.
Oravecz, J. [1963]: A Dunántúli Középhegység felsőtriász képződményeinek rétegtani- és fácieskérdései. — Questions stratigraphiques et faciales des formations triasiques supérieures de la Montagne Centrale de Transdanubie. — Földtani Közlöny. *XCIII*, 63—73.
Sebestyén, K., Morvai, L. [1967]: Hasadékvizsgálatok mészköves fúrólyukszakaszokon. — Földtani Kutatás, X. 1. 41—46.
Vadász, E. [1910—1911]: A Duna-balparti idősebb rögök őslénytani és földtani viszonyai. — Die paläontologischen und geologischen Verhältnisse der älteren Schollen am linken Donauufer. Földt. Int. Évkönyve. *XVIII*, 99—171, 115—193.
Vitális, Gy., Hegyi, J. [1967]: Zárójelentés a Dunai Cement- és Mészmű mészkő és agyag nyersanyag kutatásáról. — Manuscript. Dept. of Silicate-Chemistry of the SZIKKTI, Budapest.

Dr. György Vitális
Mrs. J. Hegyi Pakó
Central Research and Design
Institute for Silicate Industry
Bihari u. 6.
Budapest X, Hungary

CONTENTS

Investigations on the Electrode Potential of Sulfide Ores. *M. Agócs* 61
On the Phosphorus-Bearing Mineral of the Manganese Oxide Ore Deposits of Eplény and Úrkút. *Gy. Grasselly* 73
Adsorption Properties of Some Manganese Oxides. *Gy. Grasselly* and *M. Hetényi* 85
Potassium Metasomatism in the Neighbourhood of Mátraszentistván. *J. Mezősi* 99
Tectonic Control of Sedimentation in the Upper Pannonian Section of a Borehole at Macs, Great Hungarian Plain, Hungary. *B. Molnár* 109
On the Relationship between the Degree of Manganese Oxide-Hydrate Precipitates and the Conditions of their Precipitation. *E. Molnár* 121
Some Contributions to the Knowledge of Zeolites. *É. Pécsi-Donáth* 127
Über granitische Verdrängungsgänge im Diorit der Brockenmassiv-Ostrandzone (Harz). *R. Seim* und *J. Eidam* 143
Geological, Mineralogical and Petrographical Examinations in the Course of Explorations for Binding Raw Materials in the Neighbourhood of Vác. *Gy. Vitális* and *J. Hegyi-Pakó* 157

Felelős kiadó: Dr. Koch Sándor
Megjelent 625 példányban 9,8 (A/5) ív terjedelemben
Kézirat a nyomdába érkezett: 1968. szept. hó
Készült: monó-szedéssel, íves magasnyomással az MSZ 5601-59 és az 5603-55 szabványok szerint.
68-6050 — Szegedi Nyomda